1988

Developing Laminar Natural Convective Flow In Inclined Square Ducts--a Preliminary Investigation

Michael L. Papple

NOTICE

The quality of this microform is heavily dependent upon the quality of the original thesis submitted for microfilming. Every effort has been made to ensure the highest quality of reproduction possible.

If pages are missing, contact the university which granted the degree.

Some pages may have indistinct print especially if the original pages were typed with a poor typewriter ribbon or if the university sent us an inferior photocopy.

Previously copyrighted materials (journal articles, published tests, etc.) are not filmed.

Reproduction in full or in part of this microform is governed by the Canadian Copyright Act, R.S.O. 1970, c. C-30.

AVIS

La qualité de cette microforme dépend grandement de la qualité de la thèse soumise au microfilmage. Nous avons tout fait pour assurer une qualité supérieure de reproduction.

S'il manque des pages, veuillez communiquer avec l'université qui a conféré le grade.

La qualité d'impression de certaines pages peut laisser à désirer, surtout si les pages originales ont été dactylographiées à l'aide d'un ruban usé ou si l'université nous a fait parvenir une photocopie de qualité inférieure.

Les documents qui font déjà l'objet d'un droit d'auteur (articles de revue, tests publiés, etc.) ne sont pas microfilmés.

La reproduction, même partielle, de cette microforme est soumise à la Loi canadienne sur le droit d'auteur, SRC 1970, c. C-30.

DEVELOPING LAMINAR NATURAL CONVECTIVE FLOW IN INCLINED SQUARE DUCTS -A PRELIMINARY INVESTIGATION

by

Michael L.C. Papple

Faculty of Engineering Science

Department of Mechanical Engineering

Submitted in partial fulfillment

of the requirements for the degree of

Doctor of Philosophy

Faculty of Graduate Studies

The University of Western Ontario

London, Ontario

January, 1988

ISBN 0-315-40786-7

ABSTRACT

Steady, laminar, developing natural convective flow in vertical and inclined open-ended ducts was studied by the author using a Mach-Zehnder interferometer. Square ducts were considered. The ducts were isothermal, and heated to a temperature above that of the ambient fluid (air).

This study was unique in two respects; almost no information is available at present on natural convective flow in inclined ducts, and to the best of the authors' knowledge this is the first heat transfer study to employ an interferometer with the test beam traversing the heated model in a direction which was not horizontal.

Test beam averaged Nusselt numbers, and average Nusselt numbers are presented for the ducts under investigation. The most significant effects of inclining the ducts are to cause two rolls to form in the developing length of the duct, and to reduce the heat transfer rates on the upper region and increase those on the lower region of the tube and duct surface.

In addition to these experimental results, numerical solutions for fully developed flow in inclined ducts were presented. Two thermal boundary conditions were considered; isothermal as well as a duct with one side heated and the opposite side cooled. The solution for fully developed flow in inclined isothermal ducts are identical to that of vertical isothermal ducts provided the Rayleigh number contains the cosine of the angle of inclination.

ACKNOWLEDGEMENTS

I wish to thank my advisor, Professor J.D. Tarasuk for his advice and constructive criticism throughout the course of this project.

I also wish to express my appreciation to my fellow graduate students, both past and present. Their willingness to discuss a wide range of interesting topics, which include convection, was very helpful.

TABLE OF CONTENTS

* * *

LIST OF FIGURES

LIST OF TABLES

NOMENCLATURE

a	tube radius or square duct half width
C	constant
g	acceleration due to gravity ($9.806 m/s^2$)
H	dimensionless net heat transfer
K	discretization factor
K_{gd}	Gladstone-Dale constant – ($1.504 \times 10^{-4} m^3/kg$, dry air)
l	duct length
L	dimensionless duct length, $L = l/a$
h	fluid local refractive index
Nu	average Nusselt number
Nu_x	test beam averaged Nusselt number
Nu_y	test beam averaged Nusselt number
p_o	fluid pressure (Pa)
p	fluid hydrostatic pressure (Pa)
p_∞	ambient pressure (Pa)
P	dimensionless pressure deffect
Pe	grid Peclet number
Pr	fluid Prandtl number
R	ideal gas constant
Ra	duct Rayleigh number
	$Ra = \frac{g \cos(\delta) \beta (T_s - T_\infty) a^4 Pr}{\nu^2 l}$
Ra_{cr}	duct cross-plane Rayleigh number
	$Ra_{cr} = \frac{g \sin(\delta) \beta (T_s - T_\infty) a^3 Pr}{\nu^2}$ isothermal ducts
	$Ra_{cr} = \frac{g \sin(\delta) \beta (T_1 - T_2) (2a)^3 Pr}{\nu^2}$ differentially heated
T	fluid absolute temperature
$\overline{T}$	average surface temperature $\overline{T} = \frac{1}{2}(T_1 + T_2)$
u	fluid velocity in x direction
U	dimensionless fluid velocity
v	fluid velocity in y direction
V	dimensionless fluid velocity
w	fluid velocity in z (axial) direction
W	dimensionless fluid velocity
x	coordinate along duct surface
X	dimensionless coordinate, $X = x/a$
y	coordinate normal to duct surface
Y	dimensionless coordinate, $Y = y/a$
z	coordinate along test beam
Z	dimensionless coordinate, $Z = z/a$
α	fluid thermal diffusivity (m^2/s)
β	fluid volume coefficient of expansion
δ	duct angle of inclination from the vertical
ε	fringe shift with respect to the surface
ε_c	fringe shift from surface to core
ε_{c^*}	fringe shift from T_∞ to T_s

θ dimensionless temperature

$$\theta = \frac{\bar{T} - T_\infty}{T_s - T_\infty}$$

$$\theta = 2\frac{\bar{T} - \bar{T}}{T_1 - T_2}$$ (antisymmetric or differentially heated square duct)

ψ dimensionless cross-plane stream function

$$U = \frac{\partial \psi}{\partial Y} \quad V = -\frac{\partial \psi}{\partial X}$$

λ laser wavelength (6.328×10^{-7}m)

ρ fluid density (Kg/m^3)

ν fluid viscosity (m^2/s)

ω dimensionless cross-plane vorticity

$$\omega = \frac{\partial U}{\partial Y} - \frac{\partial V}{\partial X}$$

ζ temperature ratio for differentially heated duct

$$\zeta = \frac{\bar{T} - T_\infty}{T_1 - T_2}$$

m denotes average along test beam

s denotes surface

∞ denotes ambient

CHAPTER 1

GENERAL REVIEW

1.1 Introduction and Statement of Problem

Interferometric heat transfer studies normally involve a model which is oriented horizontally, and whose cross-section does not vary along its length. The model surface temperatures are constant in the direction of the model axis. The interferometer test beam traverses the model along its axis. The fluid velocity and temperature fields within or outside this model can be considered two dimensional, and the influence of end effects are considered part of the experimental error.

In studies carried out by the author, the models were vertical or inclined, and as a result the temperature and velocity fields were three dimensional. The interferometer test beam traversed the model in this vertical or inclined direction. The flow in the ducts under investigation was developing, and as a result the temperature field was not uniform in the test beam direction. Since an interferometer integrates the fluid refractive index in the direction the test beam traverses, the Nusselt numbers obtained were averaged along the test beam.

A technique was developed for measuring these test beam averaged heat transfer rates. Results were obtained for steady, laminar developing natural convective flow in vertical and inclined open-ended square ducts. These duct surfaces were isothermal, and heated to a temperature above that of the ambient fluid (air).

This study was unique in two respects; almost no information is available at present on natural convective flow in inclined ducts, and to the best of the author's knowledge this is the first heat transfer study to employ an interferometer with the test beam traversing the heated model in a direction which was not horizontal. Vertical or inclined ducts have never been studied previously using an interferometer.

A numerical study was also carried out to demonstrate a finite-difference technique for obtaining solutions for developing flow in inclined square ducts. Solutions for fully developed flow in inclined square ducts were obtained, and are presented in chapter 2. For these numerical solutions, the duct side surfaces were heated to different temperatures in order to test the numerical algorithm, as well as to provide new results for ducts with this new thermal boundary condition.

1.2 Review of Previous Interferometric Studies of Three-Dimensional Refractive Index Fields

Few studies have been carried out in the past where three dimensional flows were studied using interferometers. In 1970 Franke [1] presented a paper on free convection from heated vertical flat plates. The flow was three dimensional since the plate surface temperatures varied linearly in the horizontal direction. He presented results for the temperature field, averaged along the test beam, as well as the Nusselt numbers, averaged along the test beam. To obtain the mean temperature field he used a linearized form of

the equation relating the interferometer fringe shift field to the integral of the refractive index field along the test beam.

More recently, in 1980 Yousef [2,3,4] examined developing mixed convective flow in horizontal isothermal tubes, and in 1981 McKeen [5] studied developing mixed convective flow in horizontal concentric annuli. The flow through their models was parallel to the interferometer test beam, as is the case in the present study. Their experimental models are similar to the one used by the author in that an exit section was employed to deflect the warm air leaving the model, out of the test beam. This is discussed further in section 4.2.

1.3 Natural Convective Duct Flows

For natural convective flow in a vertical, isothermal, open-ended duct, the fluid within the duct is heated and its density is less than that of the fluid outside the duct. An axial flow is induced through the duct as a result of this density difference. The cool fluid entering the duct is in contact with the heated duct surface, and thermal and momentum boundary layers form. Under the influence of viscous forces, the axial velocity profile changes from an essentially uniform profile at the duct entrance to a parabolic type of profile.

For inclined ducts, in addition to this developing flow two rolls are present; in the cross-plane the fluid next to each side is heated and therefore rises. The fluid then falls from the upper to the lower surfaces of the duct. The fluid thus travels in a spiral

motion as it rises within the duct, as indicated in figure 1.1 . This cross-plane fluid motion influences the temperature field and the local heat transfer rates. This phenomena occurs for ducts of any cross-section such as circular tubes or square ducts.

As the fluid rises within the duct its bulk temperature approaches that of the duct surface. The local heat transfer rates asymptotically approach zero. The fluid cross-plane motion diminishes until the fluid velocity is uni-directional and consists only of an axial component, or the duct exit is reached.

1.4 Review of Natural Convective Flow in Tubes

Vertical circular tubes have been studied extensively by a number of authors [6-13]. Elenbaas [6] obtained a correlation for the heat transfer by matching the analytical solution for fully developed flow with his experimental results in the developing region. In [7-10], finite-difference techniques were used in obtaining numerical solutions for developing flow in circular tubes. They had simplified the governing equations by assuming the flow was parabolic in the axial direction. Churchill [12] and Aihara [13] have compiled review papers for natural convection in vertical ducts.

1.5 Review of Natural Convective Flow in Square Ducts

For vertical isothermal square ducts, Elenbaas [6] obtained a correlation for the heat transfer by matching the analytical solution for fully developed flow with his experimental results in

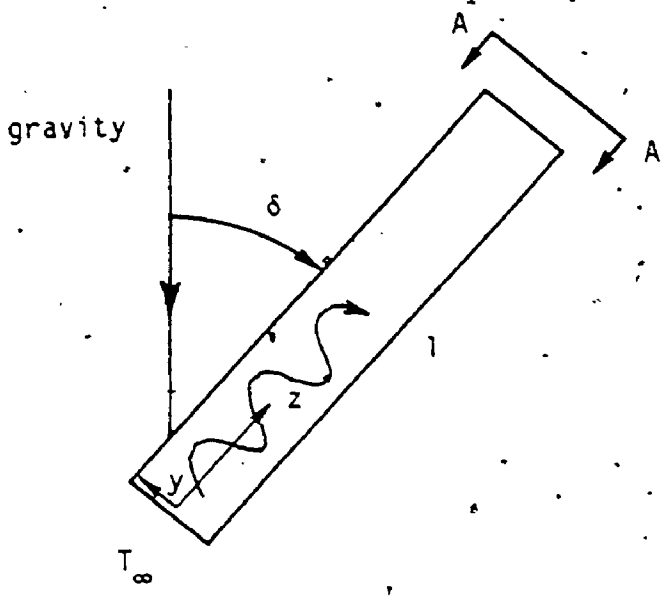

1.1a) side view

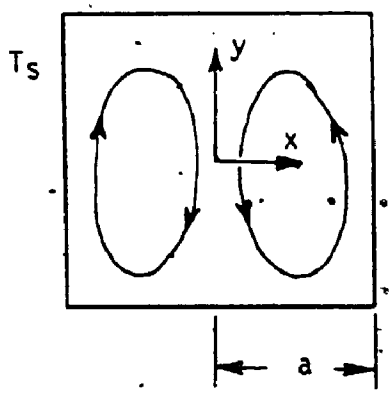

1.1b) view A-A

Figure 1.1 Developing Flow in an Inclined Isothermal Square Duct.

the developing region in the same manner as his correlation for tubes. This correlation is given by:

$$Nu = \frac{Ra}{14.225}\left[\,1 - e^{-14.225\,(\frac{0.5}{Ra})^{0.75}}\,\right]$$

Ramakrishna [14,15] obtained a finite-difference solution for developing flow in vertical isothermal square ducts. The governing equations were taken to be parabolic in the axial direction. His average heat transfer results in the fully developed regime (Ra<1) are 11% lower than the corresponding solution of Elenbaas [6].

Ramakrishna divides the flow for vertical square ducts into the following regimes: fully developed or nearly fully developed for Ra<1, developing for 1<Ra<500 and a boundary-layer type of flow for Ra>500.

Although the problem of combined free and forced convection in inclined tubes and square ducts has been studied, there is no information available at present for free convection in inclined isothermal tubes and ducts. One study [16] was conducted in 1962 on developing natural convective flow in inclined tubes, however a uniform heat flux thermal boundary condition was considered. An energy balance technique was employed to obtain average heat transfer rates.

1.6 Scope of Thesis

Numerical and experimental studies are presented in this thesis. In the following chapter, the numerical study is detailed. The governing equations specifying three dimensional duct flows are derived. The simplifications to these equations in the limit of

fully developed flow are indicated. Solutions for fully developed flow in inclined isothermal square ducts, as well as square ducts with the side surfaces heated to different temperatures are presented. The numerical technique developed here can be applied to three dimensional developing duct flows.

The steady, laminar developing natural convective flow in vertical and inclined open-ended isothermal square ducts was studied by the author using a Mach-Zehnder interferometer. This study was unique in two respects; almost no information is available at present on natural convective flow in inclined ducts, and to the best of the author's knowledge this is the first heat transfer study to employ an interferometer with the test beam traversing the heated model in a direction which was not horizontal.

The technique employed to analyze the interference fringes and obtain Nusselt numbers is described first in this thesis, beginning in chapter 3. The interferometric arrangement used by the author to study an inclined isothermal square duct model is then described. Finally, results for the test beam averaged Nusselt numbers, and average Nusselt numbers are presented in chapter 5.

CHAPTER 2

NUMERICAL SOLUTIONS FOR FULLY DEVELOPED FLOW

2.1 Introduction

The steady, laminar, fully developed natural convective flow in inclined square ducts was studied numerically using a finite difference technique. The ambient fluid was taken to be a gas, with a Prandtl number of 0.7.

The material presented in this chapter was part of a study to examine developing natural convective flow in inclined ducts. The average Nusselt numbers for this developing flow was measured using a Mach-Zehnder interferometer (see chapters 3-5). It was considered desirable to supplement these experimental results with numerical results for the limit of fully developed flow.

This material was also preliminary to a more extensive numerical study of developing natural convective flow in inclined ducts. The numerical technique employed here was selected with that goal in mind. The important parameters were also established for this flow.

For the present study, two temperature boundary conditions were considered. For the first case, all four duct walls were heated to the same temperature T_s with the ambient temperature being T_∞. For the second case, the side walls were heated to temperatures T_1 and T_2 while the other two sides were taken to be adiabatic.

2.2 Governing Equations for Developing Flow in Square Ducts

The partial differential equations which govern natural

convection within a square duct are continuity, three momentum (Navier-Stokes) equations and an energy equation [17]. In this thesis, the flow was incompressible with the exception of the buoyancy terms in the Navier-Stokes equations (Boussinesq approximation). The fluid properties were taken to be constant, and steady-state forms of the equations were employed. These governing equations in cartesian coordinates are given by:

1) the continuity equation

$$\frac{\partial u}{\partial x}+\frac{\partial v}{\partial y}+\frac{\partial w}{\partial z}=0 \tag{2.1}$$

2) the Navier-Stokes equations

$$u\frac{\partial u}{\partial x}+v\frac{\partial u}{\partial y}+w\frac{\partial u}{\partial z} = -\frac{1}{\rho}\frac{\partial (p-p_o)}{\partial x} +\nu\left[\frac{\partial^2 u}{\partial x^2}+\frac{\partial^2 u}{\partial y^2}+\frac{\partial^2 u}{\partial z^2}\right] \tag{2.2}$$

$$u\frac{\partial v}{\partial x}+v\frac{\partial v}{\partial y}+w\frac{\partial v}{\partial z} = -\frac{1}{\rho}\frac{\partial (p-p_o)}{\partial y} +g\sin(\delta)\,\beta\,(T-T_\infty)+\nu\left[\frac{\partial^2 v}{\partial x^2}+\frac{\partial^2 v}{\partial y^2}+\frac{\partial^2 v}{\partial z^2}\right] \tag{2.3}$$

$$u\frac{\partial w}{\partial x}+v\frac{\partial w}{\partial y}+w\frac{\partial w}{\partial z} = -\frac{1}{\rho}\frac{\partial (p-p_o)}{\partial z} +g\cos(\delta)\,\beta\,(T-T_\infty)+\nu\left[\frac{\partial^2 w}{\partial x^2}+\frac{\partial^2 w}{\partial y^2}+\frac{\partial^2 w}{\partial z^2}\right] \tag{2.4}$$

3) the energy equation

$$\rho C_p\left(u\frac{\partial T}{\partial x}+v\frac{\partial T}{\partial y}+w\frac{\partial T}{\partial z}\right) = u\frac{\partial (p-p_o)}{\partial x}+v\frac{\partial (p-p_o)}{\partial y}+w\frac{\partial (p-p_o)}{\partial z} +\mu\Phi+k\left[\frac{\partial^2 T}{\partial x^2}+\frac{\partial^2 T}{\partial y^2}+\frac{\partial^2 T}{\partial z^2}\right] \tag{2.5}$$

Two terms in the energy equation were neglected, the work done by pressure term $\left(u\frac{\partial (p-p_o)}{\partial x}+v\frac{\partial (p-p_o)}{\partial y}+w\frac{\partial (p-p_o)}{\partial z}\right)$ and the viscous dissipation term $(\mu\Phi)$. For the velocities normally encountered in natural convection the pressure does not vary strongly in the flow and the work done by pressure term, and the viscous dissipation term are negligible compared to the other terms in the energy equation.

2.3 Governing Equations for Isothermal Square Ducts

The equations in the previous section were non-dimensionalized for isothermal square ducts by introducing the following dimensionless parameters.

$$Ra = \frac{g \cos(\delta)\, \beta\, (T_s - T_\infty)\, a^4\, Pr}{\nu^2\, l}$$

$$Ra_{cr} = \frac{g \sin(\delta)\, \beta\, (T_s - T_\infty)\, a^3\, Pr}{\nu^2}$$

$$Pr = \frac{\nu}{\alpha}$$

$$X = \frac{x}{a} \qquad Y = \frac{y}{a} \qquad Z = \frac{z}{l\, Ra}$$

$$U = \frac{u\, a}{\alpha} \qquad V = \frac{v\, a}{\alpha} \qquad = \frac{w\, a^2}{\alpha\, l\, Ra}$$

$$\theta = \frac{T - T_\infty}{T_s - T_\infty} \qquad P = \frac{(p - p_0)\, a^4}{\rho\, \alpha^2\, l^2\, Ra^2} \qquad (2.6)$$

The governing equations for developing flow become:

$$\frac{\partial U}{\partial X} + \frac{\partial V}{\partial Y} + \frac{\partial W}{\partial Z} = 0 \qquad (2.7)$$

$$U\frac{\partial U}{\partial X} + V\frac{\partial U}{\partial Y} + W\frac{\partial U}{\partial Z} = -\frac{\partial P}{\partial X}\left(\frac{Ra\, l}{a}\right)^2 + Pr\left[\frac{\partial^2 U}{\partial X^2} + \frac{\partial^2 U}{\partial Y^2} + \frac{\partial^2 U}{\partial Z^2}\left(\frac{a}{Ra\, l}\right)^2\right] \qquad (2.8)$$

$$U\frac{\partial V}{\partial X} + V\frac{\partial V}{\partial Y} + W\frac{\partial V}{\partial Z} = -\frac{\partial P}{\partial Y}\left(\frac{Ra\, l}{a}\right)^2 + \theta\, Pr\, Ra_{cr} + Pr\left[\frac{\partial^2 V}{\partial X^2} + \frac{\partial^2 V}{\partial Y^2} + \frac{\partial^2 V}{\partial Z^2}\left(\frac{a}{Ra\, l}\right)^2\right] \qquad (2.9)$$

$$U\frac{\partial W}{\partial X} + V\frac{\partial W}{\partial Y} + W\frac{\partial W}{\partial Z} = -\frac{\partial P}{\partial Z} + \theta\, Pr + Pr\left[\frac{\partial^2 W}{\partial X^2} + \frac{\partial^2 W}{\partial Y^2} + \frac{\partial^2 W}{\partial Z^2}\left(\frac{a}{Ra\, l}\right)^2\right] \qquad (2.10)$$

$$U\frac{\partial \theta}{\partial X} + V\frac{\partial \theta}{\partial Y} + W\frac{\partial \theta}{\partial Z} = \frac{\partial^2 \theta}{\partial X^2} + \frac{\partial^2 \theta}{\partial Y^2} + \frac{\partial^2 \theta}{\partial Z^2}\left(\frac{a}{Ra\, l}\right)^2 \qquad (2.11)$$

The parameters which specify the flow are the fluid Prandtl number Pr, the Rayleigh number Ra (a measure of flow development), and the cross-plane Rayleigh number Ra_{cr} (a measure of the strength of the cross-plane motion).

A fourth parameter is required if axial-diffusion is not neglected. This parameter is given by $\frac{a}{Ra\, l}$. Axial-diffusion is strongest near the duct entrance.

Appropriate boundary conditions for developing flow in isothermal square ducts are:

1) at the duct entrance (Z=0),

$$W = W_0 \qquad \text{(uniform velocity profile)}$$

$$U = V = 0$$

$$P = -\frac{W_0^2}{2}$$

$$\theta = 0 \qquad \text{(ambient temperature)}$$

2) on the duct surface (X=±1, or Y=±1),

$$U = V = W = 0$$

$$\theta = 1$$

3) at the duct exit,

$$P = 0 \qquad (2.12)$$

In this thesis, a dimensionless vorticity was introduced to eliminate the continuity equation, as well as the pressure gradient terms in the X momentum and Y momentum equations.

$$\omega = \frac{\partial U}{\partial Y} - \frac{\partial V}{\partial X} . \qquad (2.13)$$

A cross-plane vorticity transport equation was then obtained by differentiating the X momentum equation (2.8) with respect to Y, differentiating the Y momentum equation (2.9) with respect to X, and subtracting these two equations. The resulting cross-plane vorticity equation is given by:

$$U\frac{\partial \omega}{\partial X} + V\frac{\partial \omega}{\partial Y} + W\frac{\partial \omega}{\partial Z} + \omega\left(\frac{\partial U}{\partial X} + \frac{\partial V}{\partial Y}\right)$$
$$+\left(\frac{\partial U}{\partial Z}\frac{\partial W}{\partial Y} - \frac{\partial V}{\partial Z}\frac{\partial W}{\partial X}\right) + \frac{\partial \theta}{\partial X} Pr \frac{Ra_{cr}}{8}$$
$$= Pr\left[\frac{\partial^2 \omega}{\partial X^2} + \frac{\partial^2 \omega}{\partial Y^2} + \frac{\partial^2 \omega}{\partial Z^2}\left(\frac{a}{Ra\ 1}\right)^2\right] \qquad (2.14)$$

Two additional equations are required, in addition to (2.14).

To obtain the first of these equations, differentiate the vorticity with respect to Y.

$$\frac{\partial \omega}{\partial Y} = \frac{\partial^2 U}{\partial Y^2} - \frac{\partial^2 V}{\partial X\, \partial Y}$$

$$\text{but } \frac{\partial V}{\partial Y} = -\frac{\partial U}{\partial X} - \frac{\partial W}{\partial Z} \quad \text{(from continuity)}$$

$$\text{therefore } \frac{\partial \omega}{\partial Y} = \frac{\partial^2 U}{\partial X^2} + \frac{\partial^2 U}{\partial Y^2} + \frac{\partial^2 W}{\partial X\, \partial Z}$$

$$\text{or } \frac{\partial^2 U}{\partial X^2} + \frac{\partial^2 U}{\partial Y^2} = -\frac{\partial^2 W}{\partial X\, \partial Z} + \frac{\partial \omega}{\partial Y} \qquad (2.15)$$

The second equation was obtained in a similar manner by differentiating the vorticity with respect to X.

$$\frac{\partial^2 V}{\partial X^2} + \frac{\partial^2 V}{\partial Y^2} = -\frac{\partial^2 W}{\partial Y\, \partial Z} - \frac{\partial \omega}{\partial X} \qquad (2.16)$$

Equation (2.15) is the X Poisson equation and equation (2.16) is the Y Poisson equation.

The governing equations for developing flow in isothermal square ducts are thus given by the vorticity transport equation (2.14), the X Poisson equation (2.15), the Y Poisson equation (2.16), the Z momentum equation (2.10) and the energy equation (2.11). Appropriate boundary conditions are:

1) at the duct entrance (Z=0),

$W = W_0$ (uniform velocity profile)

$U = V = \omega = 0$

$P = -\frac{W_0^2}{2}$

$\theta = 0$ (ambient temperature)

2) on the duct surface (X=±1, or Y=±1),

$U = V = W = 0$

$\theta = 1$

$\omega = -\frac{\partial V}{\partial X}$ (X=±1)

$\omega = \frac{\partial U}{\partial Y}$ (Y=±1)

3) at the duct exit,

$$P = 0 \tag{2.17}$$

In the limit of fully developed flow for isothermal square ducts, the fluid temperature approaches that of the duct surface. The local heat transfer rates approach zero. The cross-plane velocities U and V are everywhere equal to zero. The pressure defect P is uniform within the duct. The fluid motion in the axial direction is due to buoyancy rather than any pressure gradients. Each of the governing equations become trivial except for the axial momentum equation. It is only necessary to solve the following equation for the axial velocity W.

$$1 + \frac{\partial^2 W}{\partial X^2} + \frac{\partial^2 W}{\partial Y^2} = 0 \tag{2.18}$$

The boundary conditions are:

on the duct surface ($X=\pm 1$, or $Y=\pm 1$),

$$W = 0 \tag{2.19}$$

The solution to this equation is universal since, in dimensionless form, the equation does not contain any parameters such as Ra, Ra_{cr}, δ or Pr. Practically speaking, this solution applies for $Ra<1.$ in which case the average Nusselt number is within 1% of that predicted for fully developed flow.

2.4 Method of Solution for Isothermal Square Ducts

Equation (2.18) is in the form of Poisson's equation, and its solution was straightforward. This equation was solved on a uniform grid over the entire region $-1<X<1$ and $-1<Y<1$. Central difference approximations for the derivatives were employed. An alternating direction implicit method was used, with the resulting tri-diagonal

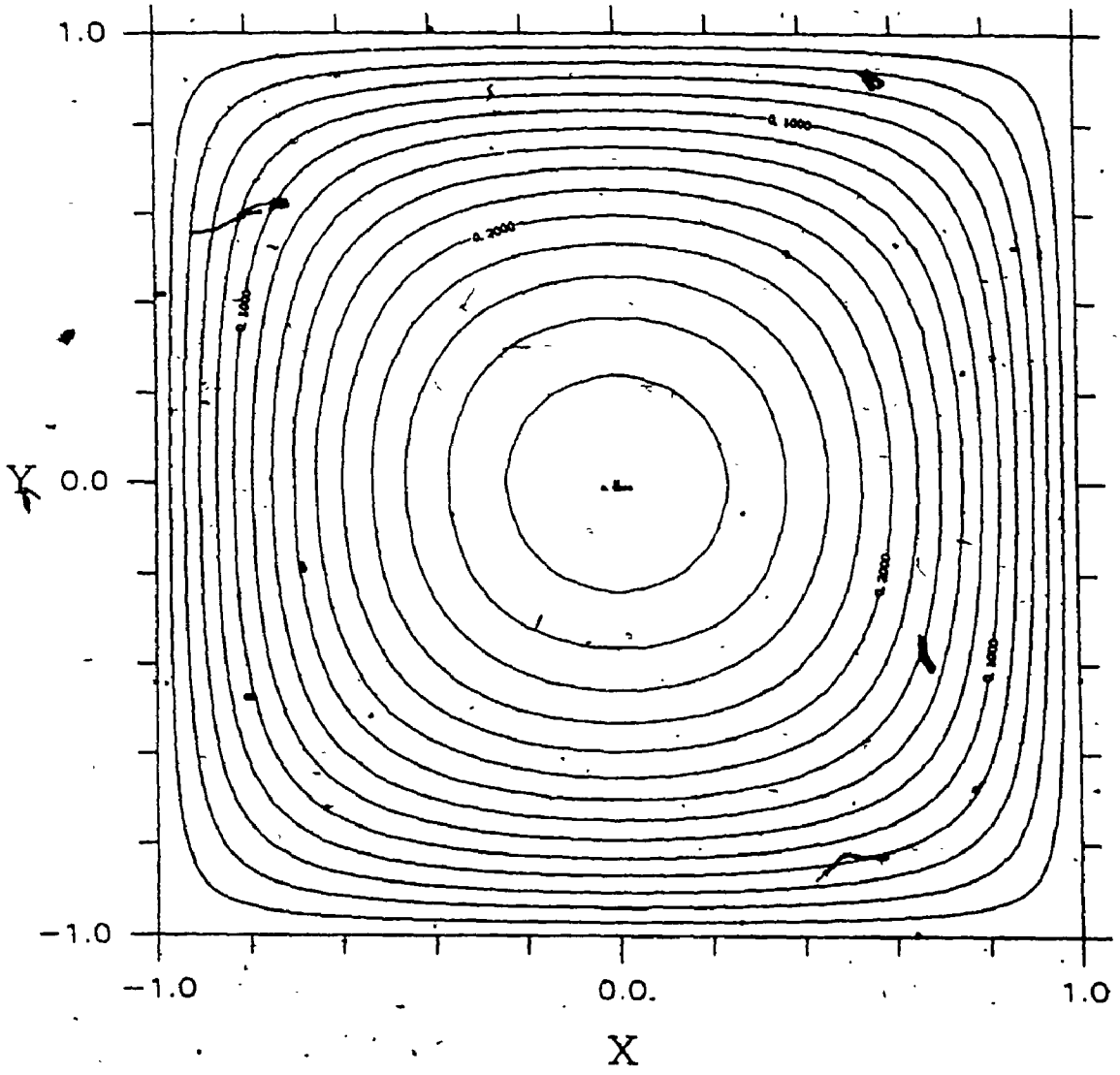

Figure 2.1 Fully Developed Axial Velocity Field W for an Isothermal Square Duct. (contour interval $\Delta W=0.02$).

system of equations solved using a Thomas algorithm. The solutions for successive iterations were over-relaxed to accelerate convergence. The axial velocity W was solved on grids with 40×40 and 80×80 steps.

2.5 Results for Isothermal Square Ducts

The solution of the axial velocity field W for fully developed flow in an inclined isothermal square duct is shown in figure 2.1. The axial velocity has a nearly parabolic shape, with a value of zero at the duct surface and a maximum value (W=0.295) at the centre. The solution for fully developed flow exhibits symmetry even though the duct is inclined to the vertical. Since the fluid inside the duct is at the same temperature as the duct surface, there are no density variations in the duct to cause any asymmetry.

The average velocity was calculated by integrating the axial velocity over the duct cross-section.

$$W = \tfrac{1}{4} \int_{-1}^{1}\int_{-1}^{1} W \, dX \, dY$$

$$= 0.1405 \qquad (2.20)$$

Although the local heat transfer rates approach zero in the limit of fully developed flow, an average heat transfer rate can be calculated by evaluating the thermal energy convected from the duct at its exit, and subtracting the thermal energy convected in at the entrance. The total heat transfer is given by:

$$h = h_m \, 8 \, a \, l \, (T_s - T_\infty)$$

$$= \rho \, C_p \int_{-a}^{a}\int_{-a}^{a} w(T_s - T_\infty) \, dx \, dy$$

The average Nusselt number is defined as

$$Nu = \frac{h_m\, a}{k} \tag{2.21}$$

where h_m is the average heat transfer coefficient. In dimensionless form,

$$H = \frac{8Nu}{Ra} = \int_{-1}^{1}\int_{-1}^{1} W\,\theta\, dX\, dY$$
$$= 0.5620 \tag{2.22}$$

The values reported in this section for maximum velocity, average velocity and average heat transfer were obtained using the 80×80 grid. These results are considered accurate since the solutions for the 40×40 grid were only 0.15% lower than the solutions for the 80×80 grid.

These results agree closely with those of Elenbass [6] for fully developed natural convective flow in vertical, isothermal square ducts. In the notation used here, his average velocity was 0.14060, just 0.07% higher than the value reported here for the 80×80 grid.

It should also be noted that the solutions for fully developed natural convective flow in isothermal ducts are identical to those for forced or mixed fully developed flow provided each variable is non-dimensionalized in the appropriate manner. Cook and Rahman [18] reported a Fourier series solution for the axial velocity field which converges rapidly. Their solution was intended for forced flow, however it is equally valid for natural convective flow.

The boundary conditions, and the governing equation are the same for each of these flows. The axial velocity solution is universal in that it is valid for forced, mixed and natural flows.

2.6 Governing Equations for Differentially Heated Square Ducts

A diagram of an inclined duct with the differentially heated thermal boundary condition is shown in figure 2.2 . For this duct, one side surface is heated to the temperature T_1, the opposite side surface is maintained at the temperature T_2, and the upper and lower surfaces were adiabatic. At present, there is no information available in literature for natural convective flow in inclined, differentially heated ducts.

Equations (2.1) to(2.5)in section 2.2 were non-dimensionalized for these square ducts by introducing the following dimensionless parameters.

$$Ra = \frac{g \cos(\delta)\, \beta\, (T_s - T_\infty)\, a^4\, Pr}{\nu^2\, l}$$

$$Ra_{cr} = \frac{g \sin(\delta)\, \beta\, (T_1 - T_2)\, (2a)^3\, Pr}{\nu^2}$$

$$Pr = \frac{\nu}{\alpha}$$

$$X = \frac{x}{a} \qquad Y = \frac{y}{a} \qquad Z = \frac{z}{l\, Ra}$$

$$U = \frac{u\, a}{\alpha} \qquad V = \frac{v\, a}{\alpha} \qquad W = \frac{w\, a^2}{\alpha\, l\, Ra}$$

$$\theta = 2\,\frac{T - \bar{T}}{T_1 - T_2} \qquad \zeta = \frac{\bar{T} - T_\infty}{T_1 - T_2} \qquad P = \frac{(p - p_0)\, a^4}{\rho\, \alpha^2\, l^2\, Ra^2} \qquad (2.23)$$

Note that these parameters are not defined in quite the same manner as those for isothermal ducts. A new parameter ζ was introduced to relate the ambient temperature T_∞ to the surface temperatures T_1 and T_2. The cross-plane Rayleigh number Ra_{cr} was defined using the characteristic dimension '2a' rather than 'a'. The governing equations for developing flow become:

$$\frac{\partial U}{\partial X} + \frac{\partial V}{\partial Y} + \frac{\partial W}{\partial Z} = 0 \qquad (2.24)$$

$$U\frac{\partial U}{\partial X} + V\frac{\partial U}{\partial Y} + W\frac{\partial U}{\partial Z} = -\frac{\partial P}{\partial X}\left(\frac{Ra\, l}{a}\right)^2 + Pr\left[\frac{\partial^2 U}{\partial X^2} + \frac{\partial^2 U}{\partial Y^2} + \frac{\partial^2 U}{\partial Z^2}\left(\frac{a}{Ra\, l}\right)^2\right] \qquad (2.25)$$

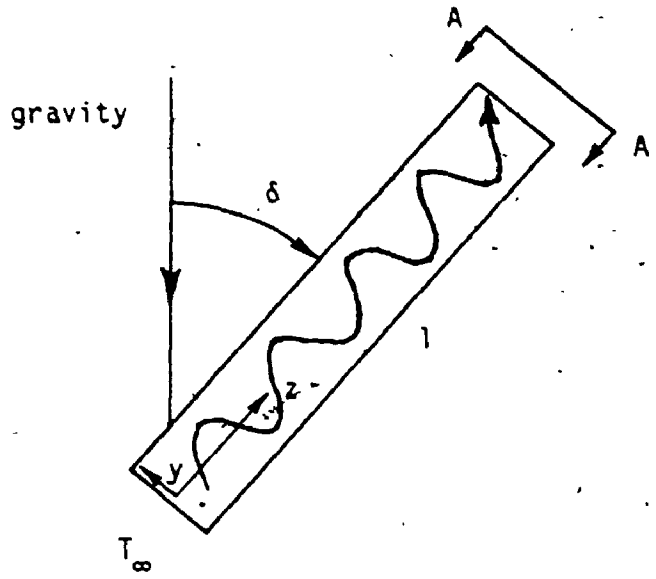

2.2a) side view

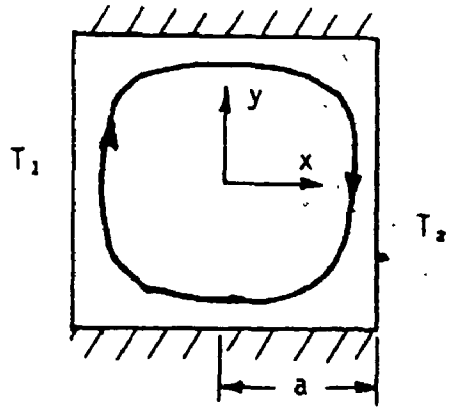

2.2b) view A-A

Figure 2.2 Differentially Heated Square Duct

$$U\frac{\partial V}{\partial X} + V\frac{\partial V}{\partial Y} + W\frac{\partial V}{\partial Z} = -\frac{\partial P}{\partial Y}\left(\frac{Ra\ 1}{a}\right)^2 + Pr\,\frac{Racr}{16} + Pr\left[\frac{\partial^2 V}{\partial X^2} + \frac{\partial^2 V}{\partial Y^2} + \frac{\partial^2 V}{\partial Z^2}\left(\frac{a}{Ra\ 1}\right)^2\right] \quad (2.26)$$

$$U\frac{\partial W}{\partial X} + V\frac{\partial W}{\partial Y} + W\frac{\partial W}{\partial Z} = -\frac{\partial P}{\partial Z} + Pr\left[\frac{\theta}{2\zeta} + 1\right] + Pr\left[\frac{\partial^2 W}{\partial X^2} + \frac{\partial^2 W}{\partial Y^2} + \frac{\partial^2 W}{\partial Z^2}\left(\frac{a}{Ra\ 1}\right)^2\right] \quad (2.27)$$

$$U\frac{\partial \theta}{\partial X} + V\frac{\partial \theta}{\partial Y} + W\frac{\partial \theta}{\partial Z} = \frac{\partial^2 \theta}{\partial X^2} + \frac{\partial^2 \theta}{\partial Y^2} + \frac{\partial^2 \theta}{\partial Z^2}\left(\frac{a}{Ra\ 1}\right)^2 \quad (2.28)$$

Appropriate boundary conditions for developing flow in differentially heated square ducts are:

1) at the duct entrance (Z=0),

$W = W_0$ (uniform velocity profile)

$U = V = 0$

$P = -\frac{W_0^2}{2}$

$\theta = 2\frac{T_\infty - \bar{T}}{T_1 - T_2}$ (ambient temperature)

2) on the duct surface,

$U = V = W = 0$ (X=±1, or Y=±1)

$\theta = 1.0$ (X=-1)

$\theta = -1.0$ (X= 1)

$\frac{\partial \theta}{\partial Y} = 0.0$ (Y=±1)

3) at the duct exit,

$P = 0$ (2.29)

A dimensionless vorticity was introduced to eliminate the continuity equation, as well as the pressure gradient terms in the X momentum and Y momentum equations.

$$\omega = \frac{\partial U}{\partial Y} - \frac{\partial V}{\partial X} \quad (2.30)$$

The resulting cross-plane vorticity transport equation is given by:

$$U\frac{\partial\omega}{\partial X} + V\frac{\partial\omega}{\partial Y} + W\frac{\partial\omega}{\partial Z} + \omega\left(\frac{\partial U}{\partial X} + \frac{\partial V}{\partial Y}\right)$$
$$+\left(\frac{\partial U}{\partial Z}\frac{\partial W}{\partial Y} - \frac{\partial V}{\partial Z}\frac{\partial W}{\partial X}\right) + \frac{\partial\theta}{\partial X}\,Pr\,\frac{Racr}{16}$$
$$= Pr\left[\frac{\partial^2\omega}{\partial X^2} + \frac{\partial^2\omega}{\partial Y^2} + \frac{\partial^2\omega}{\partial Z^2}\left(\frac{a}{Ra\ 1}\right)^2\right] \qquad (2.31)$$

The Poisson equations for differentially heated square ducts are identical to those for isothermal ducts. These are given by:

$$\frac{\partial^2 U}{\partial X^2} + \frac{\partial^2 U}{\partial Y^2} = -\frac{\partial^2 W}{\partial X\,\partial Z} + \frac{\partial\omega}{\partial Y} \qquad (2.32)$$

$$\frac{\partial^2 V}{\partial X^2} + \frac{\partial^2 V}{\partial Y^2} = -\frac{\partial^2 W}{\partial Y\,\partial Z} - \frac{\partial\omega}{\partial X} \qquad (2.33)$$

The governing equations for developing flow in differentially heated square ducts are thus given by the vorticity transport equation (2.31), the X Poisson equation (2.32), the Y Poisson equation (2.33), the Z momentum equation (2.27) and the energy equation (2.28). Appropriate boundary conditions are:

1) at the duct entrance (Z=0),

$W = W_0$ (uniform velocity profile)

$U = V = \omega = 0$

$P = -\frac{W_0^2}{2}$

$\theta = 2\,\frac{T_\infty - \bar{T}}{T_1 - T_2}$ (ambient temperature)

2) on the duct surface,

$U = V = W = 0$ $\quad (X=\pm1,\ \text{or}\ Y=\pm1)$

$\theta = 1.0$ $\quad (X=-1)$

$\theta = -1.0$ $\quad (X=1)$

$\frac{\partial\theta}{\partial Y} = 0.0$ $\quad (Y=\pm1)$

$\omega = -\frac{\partial V}{\partial X}$ $\quad (X=\pm1)$

$\omega = \frac{\partial U}{\partial Y}$ $\quad (Y=\pm1)$

3) at the duct exit,

$P = 0$ $\qquad (2.34)$

2.7 Fully Developed Flow in Differentially Heated Ducts

In the limit of fully developed flow in differentially heated square ducts, the governing equations simplify. Terms in the governing equations containing derivatives with respect to Z approach zero. The vorticity transport equation is given by:

$$U\frac{\partial\omega}{\partial X} + V\frac{\partial\omega}{\partial Y} + \frac{\partial\theta}{\partial X} Pr \frac{Racr}{16} = Pr\left[\frac{\partial^2\omega}{\partial X^2} + \frac{\partial^2\omega}{\partial Y^2}\right] \qquad (2.35)$$

Rather than solving the two Poisson equations (2.32) and 2.33) directly for U and V, a slightly different approach was utilized. A cross-plane stream function ψ was introduced where

$$U = \frac{\partial\psi}{\partial Y} \quad V = -\frac{\partial\psi}{\partial X} \qquad (2.36)$$

When these are substituted in the vorticity definition (2.30) the Poisson equation (2.37) results.

$$\omega = \frac{\partial^2\psi}{\partial X^2} + \frac{\partial^2\psi}{\partial Y^2} \qquad (2.37)$$

The energy and Z momentum equations become

$$U\frac{\partial\theta}{\partial X} + V\frac{\partial\theta}{\partial Y} = \frac{\partial^2\theta}{\partial X^2} + \frac{\partial^2\theta}{\partial Y^2} \qquad (2.38)$$

$$U\frac{\partial W}{\partial X} + V\frac{\partial W}{\partial Y} = Pr\left[\frac{\theta}{2\zeta} + 1\right] + Pr\left[\frac{\partial^2 W}{\partial X^2} + \frac{\partial^2 W}{\partial Y^2}\right] \qquad (2.39)$$

in the limit of fully developed flow. Note for natural convective flows the pressure gradient in the axial direction $\frac{\partial P}{\partial Z}$ approaches zero. Any flow in the axial direction is due to buoyancy.

The boundary conditions for fully developed flow are given by

on the duct surface,

$$U = V = W = \psi = 0 \quad (X=\pm1, \text{ or } Y=\pm1)$$

$$\theta = 1.0 \quad (X=-1)$$

$$\theta = -1.0 \quad (X=1)$$

$$\frac{\partial\theta}{\partial Y} = 0.0 \quad (Y=\pm1)$$

$$\omega = \frac{\partial^2\psi}{\partial X^2} \quad (X=\pm1)$$

$$\omega = \frac{\partial^2\psi}{\partial Y^2} \quad (Y=\pm1) \qquad (2.40)$$

2.7.1 Anti-Symmetrically Heated Ducts

An anti-symmetrically heated duct is a special case of a differentially heated duct. For this duct, the fluid temperature lies midway between the two surface temperatures. The temperature ratio has a value $\zeta=0$. Since this term is in the denominator of the Z momentum equation (2.39), it is necessary to redefine several variables for this particular case. These new definitions are given by:

$$Z = \frac{z}{a\ Ra}$$

$$W = \frac{w\ a}{Ra}$$

$$\text{where } Ra = \frac{g\ \cos(\delta)\ \beta\ (T_1-T_2)\ a^3\ Pr}{\nu^2} \tag{2.41}$$

The Z momentum equation in the limit of fully developed flow becomes:

$$U\frac{\partial W}{\partial X} + V\frac{\partial W}{\partial Y} = \frac{\theta}{2} Pr + Pr\left[\frac{\partial^2 W}{\partial X^2} + \frac{\partial^2 W}{\partial Y^2}\right] \tag{2.42}$$

The other governing equations and all the boundary conditions remain unchanged from the differentially heated duct.

2.8 Method of Solution for Differentially Heated Square Ducts -

The method of solution for fully developed flow in differentially heated square ducts is discussed in this section. Four particular aspects are considered; the discretization of the governing equations and boundary conditions, how the source terms were treated in these discretized governing equations, how the resulting tri-diagonal matrices were solved, and finally, the procedure for updating each variable.

2.8.1 Discretization of Governing Equations

The applicable governing equations were discretized in such a way that they would yield an almost exact solution to the one-dimensional convection-diffusion problem. The resulting equations retain some diagonal dominance even for strong convective effects. This approach was first described by Spalding [19] in 1972. To derive this discretization method, begin by considering the steady, one-dimensional convection-diffusion equation (2.43).

$$\rho u \frac{\partial \phi}{\partial x} = \Gamma \frac{\partial^2 \phi}{\partial x^2} \qquad (2.43)$$

The variable ϕ can represent any field such as temperature, velocity or vorticity, and Γ would then represent the thermal conductivity or viscosity. The values ρ, Γ and u were taken to be constant over the region of interest.

Consider the region lying between the points x^W and x^E in figure 2.3a. The above equation can be integrated analytically over this region, and the resulting exact solution is given by:

$$\frac{\phi - \phi^W}{\phi^E - \phi^W} = \frac{e^{Pe_x\left(\frac{x - x^W}{x^E - x^W}\right)} - 1}{e^{Pe_x} - 1}$$

where the Peclet number Pe_x is defined as

$$Pe_x = \frac{\rho u \delta x}{\Gamma} \qquad (2.45)$$

$$\text{where } \delta x = x^E - x^W \qquad (2.46)$$

The Peclet number is a dimensionless indicator of the convective strength of the flow. For Pe=0 there is only diffusion. The superscripts E and W indicate the values of ϕ at the locations x^E and x^W. If we are interested in the solution for ϕ at the location

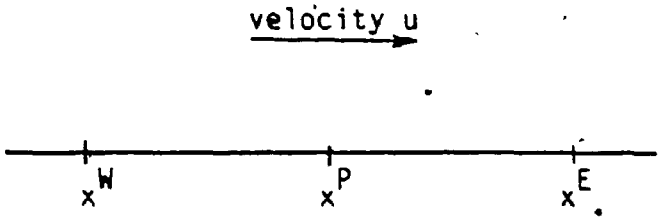

2.3a) one-dimensional grid

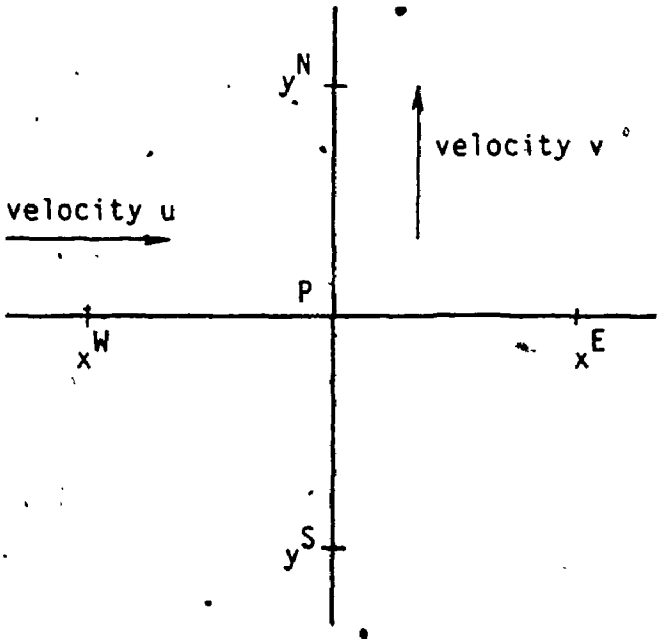

2.3b) two dimensional grid

Figure 2.3: Discretization Grids

x^P lying midway between x^E and x^W, this is given by:

$$\frac{\phi^P - \phi^W}{\phi^E - \phi^W} = K_x \tag{2.47}$$

$$\text{where } K_x = \frac{e^{Pex/2} - 1}{e^{Pex} - 1} \tag{2.48}$$

To find the solution at the midpoint x^P, calculate the discretization factor K_x, and use this factor to calculate ϕ^P. In effect, we wish to solve

$$(K_x - 1)\phi^W + \phi^P - K_x \phi^E = 0 \tag{2.49}$$

for ϕ^P, with K_x, ϕ^E and ϕ^W known.

A similar equation would result if a more familar technique, such as central differencing, were to be used to discretize (2.43). In this case we have

$$\rho u \frac{\phi^E - \phi^W}{\delta x} = \frac{\phi^W - 2\phi^P + \phi^E}{(\delta x/2)^2} \tag{2.50}$$

$$\text{or } \frac{(K_x - 1)}{(\delta x)^2}\phi^W + \frac{1}{(\delta x)^2}\phi^P - \frac{K_x}{(\delta x)^2}\phi^E = 0 \tag{2.51}$$

For the case of central differencing, the discretization factor K_x is now defined as:

$$K_x = \frac{4 - Pex}{8} \tag{2.52}$$

Equation (2.49) is identical to (2.51) if each coefficient is divided by $(\delta x)^2$.

We can now consider a more general form of the convection-diffusion equation.

$$\rho\left(u\frac{\partial\phi}{\partial x} + v\frac{\partial\phi}{\partial y}\right) = \Gamma\left(\frac{\partial^2\phi}{\partial x^2} + \frac{\partial^2\phi}{\partial y^2}\right) + S \tag{2.53}$$

The term S represents a source term in the governing equation. By writing this equation in terms of discretization factors on the grid shown in figure 2.3b, the following equation would result.

$$\begin{aligned} &- \frac{K_y}{(\delta y)^2}\phi^N \\ &+ \frac{(K_x - 1)}{(\delta x)^2}\phi^W + \left(\frac{1}{(\delta x)^2} + \frac{1}{(\delta y)^2}\right)\phi^P - \frac{K_x}{(\delta x)^2}\phi^E \\ &+ \frac{(K_y - 1)}{(\delta y)^2}\phi^S = S^P/8 \end{aligned} \tag{2.54}$$

If the grid spacing is $\Delta x=\frac{\delta x}{2}$ and $\Delta y=\frac{\delta y}{2}$, the discretized equation reduces to

$$\begin{aligned} & -\frac{K_y}{(\Delta y)^2}\phi^N \\ +\frac{(K_x-1)}{(\Delta x)^2}\phi^W & +\left(\frac{1}{(\Delta x)^2}+\frac{1}{(\Delta y)^2}\right)\phi^P - \frac{K_x}{(\Delta x)^2}\phi^E \\ & +\frac{(K_y-1)}{(\Delta y)^2}\phi^S = S^P/2 \end{aligned} \qquad (2.55)$$

The Peclet numbers would be

$$Pe_x = \frac{\rho\, u\, 2\Delta x}{\Gamma} \quad Pe_y = \frac{\rho\, v\, 2\Delta y}{\Gamma} \qquad (2.56)$$

Equation (2.55) can be used to calculate the function ϕ^P at the grid point P, provided the function values ϕ^N, ϕ^S, ϕ^E and ϕ^W at each neighbouring grid point are known. If we consider a region which has been divided into many steps in both the x and y direction, we can write an equation such as (2.55) for each grid point within the region. A set of discretized equations would result, which would be solved iteratively for the solution of ϕ at each grid point.

In general, the discretization factor is a function of the Peclet number, K=f(Pe). The particular form of this function chosen for a numerical study depends on several factors. It is desirable for the discretization method to yield the exact solution in regions where the flow is essentially uni-directional, such as near surfaces where boundary layers are forming. The discretization factor defined in (2.48) satisfies this criteria, however exponentials are time consuming to compute and a simpler function which has the same behaviour is desirable.

Central differencing (2.52) has been used extensively in the past, however this method results in equation (2.54) losing its diagonal dominance for large Peclet number. The coefficient of ϕ^P

becomes similar in magnitude to the coefficients at the neighbouring grid points. Other methods, such as upwind, or a method proposed by Dennis [20] retain some diagonal dominance for large Peclet number. Some of these methods are decribed in this section, along with two new methods.

Two forms of the discretization factor were employed by the author in the present thesis. The first is based on a Taylor's series expansion about Pe=0 of the exact one-dimensional factor.

$$K = \frac{e^{Pe/2} - 1}{e^{Pe} - 1} \approx \frac{1}{2} - \frac{1}{8} Pe + \frac{1}{384} Pe^3 + \ldots \qquad (2.57)$$

This expansion, truncated after these three terms, agrees closely with the exact factor for Peclet numbers in the range $-2.5<Pe<2.5$, and has reasonable behaviour for $-4<Pe<4$. It should be noted the first two terms of this expansion is just the discretization factor for central differencing. This expression was used to obtain solutions for the lower cross-plane Rayleigh numbers where the maximum Peclet numbers were less than 2.5 .

For larger Ra_{cr} (and Pe), a second discretization factor was employed. To derive this factor, expand the numerator and denominator of the exact factor in a Taylor's series.

$$K = \frac{\sum_{n=0}^{\infty} \frac{(Pe/2)^n}{n!} - 1}{\sum_{n=0}^{\infty} \frac{Pe^n}{n!} - 1} = \frac{\frac{1}{2} \sum_{n=1}^{\infty} \frac{Pe^{n-1}}{2^{n-1} n!}}{\sum_{n=1}^{\infty} \frac{Pe^{n-1}}{n!}} \qquad (2.58)$$

Truncating after five terms,

$$K = \frac{\frac{1}{2}\left(1 + \frac{Pe}{4} + \frac{Pe^2}{24} + \frac{Pe^3}{192} + \frac{Pe^4}{1920}\right)}{1 + \frac{Pe}{2} + \frac{Pe^2}{6} + \frac{Pe^3}{24} + \frac{Pe^4}{120}} \qquad (2.59)$$

This expression is accurate for Pe>0. For Pe<0, the following expression should be used.

$$K = 1 - K(-Pe)$$

$$K = 1 - \frac{\frac{1}{2}\left(1 - \frac{Pe}{4} + \frac{Pe^2}{24} - \frac{Pe^3}{192} + \frac{Pe^4}{1920}\right)}{1 - \frac{Pe}{2} + \frac{Pe^2}{6} - \frac{Pe^3}{24} + \frac{Pe^4}{120}} \qquad (2.60)$$

Various discretization methods were rearranged in the form used here. Expressions for the discretization factor have been included in table 2.1, and the discretization factors were plotted versus Peclet number in figure 2.4 .

2.8.2 Discretized Equations for Differentially Heated Ducts

The governing equations for fully developed flow in differentially heated square ducts were non-dimensionalized in the following manner. The cross-plane Rayleigh number is a measure of the strength of the fluid motion in the cross-plane. The Peclet numbers Pe_x and Pe_y are thus Ra_{cr} dependent. For Ra_{cr} up to 10^3, the maximum Peclet numbers in the cross-plane were relatively small and as a result the discretized equations were diagonally dominant and convergence was rapid. The discretized vorticity transport equation becomes:

$$-\frac{K_y}{(\Delta y)^2}\omega^N + \frac{(K_x-1)}{(\Delta x)^2}\omega^W + \left(\frac{1}{(\Delta x)^2} + \frac{1}{(\Delta y)^2}\right)\omega^P - \frac{K_x}{(\Delta x)^2}\omega^E + \frac{(K_y-1)}{(\Delta y)^2}\omega^S = -\frac{\theta^E - \theta^W}{2\,\Delta x}\frac{Racr}{32} \qquad (2.61)$$

Table 2.1 Discretization Factors.

Method	Discretization Factor K	
exact	$\frac{e^{Pe/2}-1}{e^{Pe}-1}$	
central	$\frac{4-Pe}{8}$	
upwind	$1-\frac{2}{4-Pe}$	$Pe<0$
	$\frac{2}{4+Pe}$	$Pe\geq 0$
Dennis	$\frac{1-\frac{Pe}{4}+\frac{Pe^2}{32}}{2+\frac{Pe^2}{16}}$	
present (Taylor's expansion)	$\frac{5}{6}$	$Pe<-4$
	$\frac{1}{2}-\frac{Pe}{8}+\frac{Pe^3}{384}$	$-4\leq Pe\leq 4$
	$\frac{1}{6}$	$Pe>4$
present (numerator and denominator expansion)	$\frac{\frac{1}{2}\left(1+\frac{Pe}{4}+\frac{Pe^2}{24}+\frac{Pe^3}{192}+\frac{Pe^4}{1920}\right)}{1+\frac{Pe}{2}+\frac{Pe^2}{6}+\frac{Pe^3}{24}+\frac{Pe^4}{120}}$	$Pe\geq 0$
	$1-\frac{\frac{1}{2}\left(1-\frac{Pe}{4}+\frac{Pe^2}{24}-\frac{Pe^3}{192}+\frac{Pe^4}{1920}\right)}{1-\frac{Pe}{2}+\frac{Pe^2}{6}-\frac{Pe^3}{24}+\frac{Pe^4}{120}}$	$Pe<0$

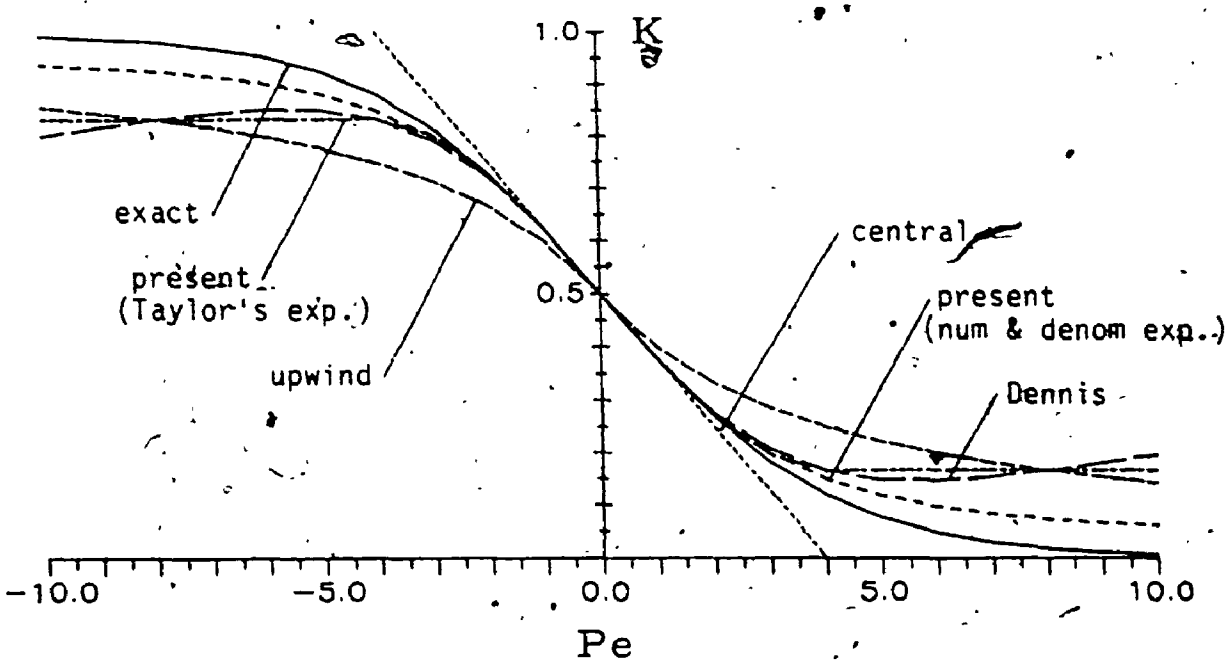

Figure 2.4 Variation of Discretization Factor K with Peclet Number Pe.

The Peclet numbers in terms of dimensionless variables are for the vorticity transport equation

$$Pe_x = \frac{U\ 2\ \Delta X}{Pr} \qquad Pe_y = \frac{V\ 2\ \Delta Y}{Pr} \tag{2.62}$$

The Poisson equation for the cross-plane stream function was discretized using central differences since no convective terms are present.

$$\begin{aligned} & -\frac{0.5}{(\Delta Y)^2}\psi^N \\ -\frac{0.5}{(\Delta X)^2}\psi^W & +\left(\frac{1}{(\Delta X)^2}+\frac{1}{(\Delta Y)^2}\right)\psi^P - \frac{0.5}{(\Delta X)^2}\psi^E \\ & -\frac{0.5}{(\Delta Y)^2}\psi^S = -\frac{\omega^P}{2} \end{aligned} \tag{2.63}$$

The energy equation becomes:

$$\begin{aligned} & -\frac{K_y}{(\Delta Y)^2}\theta^N \\ +\frac{(K_x-1)}{(\Delta X)^2}\theta^W & +\left(\frac{1}{(\Delta X)^2}+\frac{1}{(\Delta Y)^2}\right)\theta^P - \frac{K_x}{(\Delta X)^2}\theta^E \\ & +\frac{(K_y-1)}{(\Delta Y)^2}\theta^S = 0 \end{aligned} \tag{2.64}$$

The Reclet numbers for the energy equation are defined as

$$Pe_x = U\ 2\Delta X \qquad Pe_y = V\ 2\Delta Y \tag{2.65}$$

The Z momentum equation becomes

$$\begin{aligned} & -\frac{K_y}{(\Delta Y)^2}W^N \\ +\frac{(K_x-1)}{(\Delta X)^2}W^W & +\left(\frac{1}{(\Delta X)^2}+\frac{1}{(\Delta Y)^2}\right)W^P - \frac{K_x}{(\Delta X)^2}W^E \\ & +\frac{(K_y-1)}{(\Delta Y)^2}W^S = \tfrac{1}{2}\left[\frac{\theta}{2\zeta}\right] \end{aligned} \tag{2.66}$$

or for the anti-symmetric duct with $\zeta=0$,

$$\begin{aligned} & -\frac{K_y}{(\Delta Y)^2}W^N \\ +\frac{(K_x-1)}{(\Delta X)^2}W^W & +\left(\frac{1}{(\Delta X)^2}+\frac{1}{(\Delta Y)^2}\right)W^P - \frac{K_x}{(\Delta X)^2}W^E \\ & +\frac{(K_y-1)}{(\Delta Y)^2}W^S = \frac{\theta^P}{4} \end{aligned} \tag{2.67}$$

The Peclet numbers for the Z momentum equation are

$$Pe_x = \frac{U\ 2\ \Delta X}{Pr} \qquad Pe_y = \frac{V\ 2\ \Delta Y}{Pr} \tag{2.68}$$

The region of interest, $-1 \le X \le 1$ and $-1 \le Y \le 1$ was divided into a uniform grid. Each grid point is specified by the indices i and j in the X and Y directions, where $-NX \le i \le NX$ and $-NY \le j \le NY$. Two grid sizes were employed here with NX=NY=20 and NX=NY=40, corresponding to 40×40 and 80×80 grid points. Any function ϕ at the grid point i,j is specified as $\phi_{i,j}$.

The derivative boundary conditions for θ and ω must be discretized. The formulations used in the present study for θ were the second order forward or backward first derivatives.

$$\left.\frac{\partial\theta}{\partial Y}\right|_{Y=-1} = \frac{-3\theta_{i,-NY} + 4\theta_{i,-NY+1} - \theta_{i,-NY+2}}{2\,\Delta Y}$$

$$= 0$$

$$\text{or } \theta_{i,-NY} = \frac{4}{3}\theta_{i,-NY+1} - \frac{2}{3}\theta_{i,-NY+2} \qquad (2.69)$$

$$\left.\frac{\partial\theta}{\partial Y}\right|_{Y=1} = \frac{\theta_{i,NY-2} - 4\theta_{i,NY-1} + 3\theta_{i,NY}}{2\,\Delta Y}$$

$$= 0$$

$$\text{or } \theta_{i,NY} = -\frac{1}{3}\theta_{i,NY-2} + \frac{4}{3}\theta_{i,NY-1} \qquad (2.70)$$

The formulations used here for the boundary conditions for ω are the same as those used by Wilkes and Churchill [21]. To derive this expression, consider Taylor's series expansions of the stream function in the vicinity of the wall i=-NX.

$$\psi_{-NX+1,j} = \psi_{-NX,j} + \Delta X \left.\frac{\partial\psi}{\partial X}\right|_{X=-1} + \frac{(\Delta X)^2}{2}\left.\frac{\partial^2\psi}{\partial X^2}\right|_{X=-1} + \frac{(\Delta X)^3}{6}\left.\frac{\partial^3\psi}{\partial X^3}\right|_{X=-1} + \cdots \qquad (2.71)$$

$$\psi_{-NX+2,j} = \psi_{-NX,j} + 2\Delta X \left.\frac{\partial\psi}{\partial X}\right|_{X=-1} + \frac{(2\Delta X)^2}{2}\left.\frac{\partial^2\psi}{\partial X^2}\right|_{X=-1} + \frac{(2\Delta X)^3}{6}\left.\frac{\partial^3\psi}{\partial X^3}\right|_{X=-1} + \cdots \qquad (2.72)$$

The value of the stream function at the surface is $\psi_{-NX,j}=0$. If we multiply (2.71) by 8 and subtract (2.72) we obtain

$$\left.\frac{\partial^2\psi}{\partial X^2}\right|_{X=-1} = \frac{8\,\psi_{-NX+1,j} - \psi_{-NX+2,j}}{2\,(\Delta X)^2}$$

The boundary condition for the vorticity is thus given by

$$\omega_{-NX,j} = \frac{\partial^2 \psi}{\partial X^2}\Big|_{X=-1} = \frac{8\,\psi_{-NX+1,j} - \psi_{-NX+2,j}}{2(\Delta X)^2} \qquad (2.73)$$

Similarly, the vorticity boundary conditions on each of the remaining surfaces are

$$\omega_{NX,j} = \frac{8\,\psi_{NX-1,j} - \psi_{NX-2,j}}{2(\Delta X)^2}$$

$$\omega_{i,-NY} = \frac{8\,\psi_{i,-NY+1} - \psi_{i,-NY+2}}{2(\Delta Y)^2}$$

$$\omega_{i,NY} = \frac{8\,\psi_{i,NY-1} - \psi_{i,NY-2}}{2(\Delta Y)^2}$$

2.8.3 Source Term Linearization

For cross-plane Rayleigh numbers Ra_{cr} greater than 10^3, it was necessary to increase the diagonal dominance of the discretized vorticity transport and energy equations by including an additional term in the coefficient of the function ϕ^P, and balancing this by increasing the magnitude of the source term. This is also referred to as linearizing the source term. With source term linearization, the general second order discretized equation (2.55) becomes:

$$-\frac{K_Y}{(\Delta X)^2}\phi^N + \frac{(K_X-1)}{(\Delta Y)^2}\phi^W + \left[\frac{1+C}{(\Delta X)^2} + \frac{1+C}{(\Delta Y)^2}\right]\phi^P - \frac{K_X}{(\Delta X)^2}\phi^E + \frac{(K_Y-1)}{(\Delta Y)^2}\phi^S = S^P/2 + \left[\frac{C}{(\Delta X)^2} + \frac{C}{(\Delta Y)^2}\right]\phi^P_{old} \qquad (2.74)$$

The function ϕ^P_{old} represents the value of ϕ^P from the previous iteration.

The value C in (2.74) must be determined by trial. If C is small or zero, solutions for large cross-plane Rayleigh number will oscillate as the discretized equations are iterated. If the value

of C is optimal, the equations approach the desired solution after iterating. The effect of this source term linearization is to dampen out the solution oscillations. For C larger than optimal, the desired solution is approached after iterating, however the convergence rates are reduced.

2.8.4 Solution of Discretized Equations

The discretized equations were solved using the ADI, or alternating direction implicit method. The resulting tri-diagonal matrices were solved using the Thomas algorithm. With this algorithm, the values of a function along a particular grid line were updated simultaniously.

For grid lines in the X direction the function values next to the boundary Y=-1 were updated first, followed by the function values on the adjacent grid lines closer to the duct centre. Successive grid lines were considered, until the duct centre was reached. This was repeated for the grid lines near the Y=+1 boundary.

As is characteristic of the ADI method, this procedure was then applied to grid lines in the Y direction, starting with the grid lines next to the X=±1 boundaries.

The function values were updated on grid lines starting at the boundaries and working to the centre, rather than from one side to the opposite side, so the variables would be updated in a symmetrical manner. The convergence rates were then similar everywhere in the duct, and the calculated values of the variables

part way through the iterations having a similar variation as the converged solution.

The particular manner in which the variables in the discretized equations were updated was similar to the unsteady method for obtaining steady state solutions. For updating along grid lines in the X direction, equation (2.74) was written in the following form.

$$\frac{(K_x-1)}{(\Delta X)^2}\phi^W + \left[\frac{1+C}{(\Delta X)^2} + \frac{1+C}{(\Delta Y)^2}\right]\phi^P - \frac{K_x}{(\Delta X)^2}\phi^E = S^P/2 - \frac{(K_y-1)}{(\Delta Y)^2}\phi^S_{old} + \frac{K_y}{(\Delta Y)^2}\phi^N_{old} + \left[\frac{C}{(\Delta X)^2} + \frac{C}{(\Delta Y)^2}\right]\phi^P_{old} \quad (2.75)$$

For updating along grid lines in the Y direction we have:

$$\frac{(K_y-1)}{(\Delta Y)^2}\phi^S + \left[\frac{1+C}{(\Delta X)^2} + \frac{1+C}{(\Delta Y)^2}\right]\phi^P - \frac{K_y}{(\Delta Y)^2}\phi^N = S^P/2 - \frac{(K_x-1)}{(\Delta X)^2}\phi^W_{old} + \frac{K_x}{(\Delta X)^2}\phi^E_{old} + \left[\frac{C}{(\Delta X)^2} + \frac{C}{(\Delta Y)^2}\right]\phi^P_{old} \quad (2.76)$$

Using large values of C is equivalent to under-relaxing the function ϕ to improve convergence.

2.8.5 Procedure for Updating Variables

It is most important to note that for fully developed flow in differentially heated ducts, the vorticity transport equation (2.35), the Poisson equation (2.37), the U and V velocity definition equations (2.36) and the energy equation (2.38) as well as the boundary conditions for ω, ψ, U, V and θ do not contain the axial velocity W. The Z momentum equation is decoupled from the these equations. Final solutions for ω, ψ, U, V and θ were obtained before the Z momentum equation, and the axial velocity W, were considered.

The procedure for calculating these cross-plane variables is given below. A program employing this procedure is shown in Appendix A.

1) Guess initial values for each variable. This initial guess could be $\omega=\psi=U=V=0$ everywhere, with θ varying linearly with X. A better guess might be to use the converged solution for a smaller cross-plane Rayleigh number than the solution desired, or the converged solution for a coarser grid.

2) Calculate new values for the vorticity ω. The discretized equations for the vorticity consist of

$$\frac{(K_X-1)}{(\Delta X)^2}\omega^W + \left[\frac{1+C}{(\Delta X)^2} + \frac{1+C}{(\Delta Y)^2}\right]\omega^P - \frac{K_X}{(\Delta X)^2}\omega^E = -\frac{\theta^E-\theta^W}{2(\Delta X)}\frac{Ra_{cr}}{32} - \frac{(K_Y-1)}{(\Delta Y)^2}\omega^S_{old} + \frac{K_Y}{(\Delta Y)^2}\omega^N_{old} + \left[\frac{C}{(\Delta X)^2} + \frac{C}{(\Delta Y)^2}\right]\omega^P_{old} \quad (2.77)$$

$$\frac{(K_Y-1)}{(\Delta Y)^2}\omega^S + \left[\frac{1+C}{(\Delta X)^2} + \frac{1+C}{(\Delta Y)^2}\right]\omega^P - \frac{K_Y}{(\Delta Y)^2}\omega^N = -\frac{\theta^E-\theta^W}{2(\Delta X)}\frac{Ra_{cr}}{32} - \frac{(K_X-1)}{(\Delta X)^2}\omega^W_{old} + \frac{K_X}{(\Delta X)^2}\omega^E_{old} + \left[\frac{C}{(\Delta X)^2} + \frac{C}{(\Delta Y)^2}\right]\omega^P_{old} \quad (2.78)$$

The coefficients of these equations must be calculated every iteration since the velocities U and V, and thus the Peclet numbers and discretization factors, vary. One updating of ω consists of solving (2.77) along each grid line in the X direction, then immediately solving (2.78) along each grid line in the Y direction.

3) Calculate new values for the cross-plane stream function ψ. Equation (2.63) was solved along grid lines in the X direction, then in the Y direction. This procedure was repeated 6 times. The coefficients of the Poisson equation, other than the source

term, need only be calculated once, since they are constants.

4) Calculate the velocities U and V by differentiating the stream function according to (2.36) . Second order central differences were used to approximate the first derivatives.

5) Calculate new values for the temperature θ. This was done in the same manner as the vorticity ω. The discretized equation for consists of

$$\frac{(K_X-1)}{(\Delta X)^2}\theta^W + \left[\frac{1+C}{(\Delta X)^2} + \frac{1+C}{(\Delta Y)^2}\right]\theta^P - \frac{K_X}{(\Delta X)^2}\theta^E$$
$$= -\frac{(K_Y-1)}{(\Delta Y)^2}\theta^S_{old} + \left[\frac{C}{(\Delta X)^2} + \frac{C}{(\Delta Y)^2}\right]\theta^P_{old} + \frac{K_Y}{(\Delta Y)^2}\theta^N_{old} \quad (2.79)$$

The temperature θ was calculated by solving (2.79) along each grid line in the X direction. The temperature along each adiabatic surface Y=±1 was updated by approximating the first derivative for the temperature with second order backward or forward differences. The temperature θ was updated twice in this manner on the grid.

6) Each of the variables ω, ψ, U, V and θ were updated in steps 2-5. The convergence of the solution was then checked. This was done in two ways; the value of the stream function at the duct centre was compared with the values for previous iterations, and the average Nusselt numbers were compared with those for previous iterations. Both relative and absolute criteria for the difference between successive iterations were employed. Steps 2-6 were repeated until the solutions for ω, ψ, U, V and θ were considered converged. These solutions were considered converged when their error was less than the error due to using a finite number of grid points in the region.

7) Once the solutions for the variables in the cross-plane were obtained, the Z momentum equation was solved to obtain W. This was done by successively solving (2.66) or (2.67) along grid lines in the X and Y directions. This was done until a converged solution for W was obtained. Solutions for W after each iteration were over-relaxed to accelerate convergence. The relaxation factor was typically 1.25 . The value of the maximum axial velocity was used to determine convergence. The residuals of the Z momentum equation were also calculated to determine how accurately the solution for W satisfied the discretized Z momentum equation.

2.9 Proposed Method for Developing Flows

Although solutions for developing flow in inclined isothermal or differentially heated ducts were not obtained by the author, a suitable method was considered and is described as follows:

1) Ignore the effects of axial-diffusion. If terms in the vorticity transport and energy equations containing $\frac{a}{Ra\ l}$ are neglected, the computer time and memory requirements to obtain solutions are reduced considerably. The governing equations become parabolic in nature and solutions can be obtained by marching from the duct entrance to the exit, rather than solving the governing equations everywhere simultaneously. The problem is reduced from a fully three-dimensional set of equations to one with a lesser degree of difficulty. If this assumption is not made, solutions for developing flow in inclined ducts may not be feasible using present computer facilities. Axial diffusion is significant only in

the entrance region, and should have a minimal effect on the local results downstream, and on the average Nusselt number.

2) A vorticity-velocity formulation for the governing equations is recommended. With this formulation, each governing equation is a second order partial differential equation. Numerical algorithms for solving such equations are well established. The first order continuity equation is no longer one of the governing equations.

3) Staggered or non-staggered grids could be used. The non-staggered grids used in this thesis have the advantage of being simpler to program, while staggered grids can have greater accuracy for the same grid fineness. For non-staggered grids, the discretization method employed here for fully developed flow in differentially heated ducts is applicable. For staggered grids, the discretization method of Patankar [22,23], applied to the vorticity-velocity formulation could be used.

2.10 Results for Differentially Heated Square Ducts

It should be noted the governing equations and the appropriate boundary conditions for the case of horizontal, differentially heated square cavities are the same as those described in this chapter for the cross-plane of differentially heated inclined square ducts, in the limit of fully developed axial flow. The horizontal cavity can be considered as the special case of a differentially heated duct inclined 90° to the vertical. Thus the results for ω, ψ, U, V and θ in the present study should agree with those obtained by previous investigators [21,24-30] for horizontal cavities.

The new results presented here are the axial velocity W, the

average axial velocity W_{ave} and the net heat transfer to the fluid H. These last two results, W_{ave} and H are important for design calculations.

All of the results in the present study were calculated for a Prandtl number of 0.7, corresponding to monotomic and diatomic gases such as air. Cross-plane Rayleigh numbers extending over the entire laminar range (up to 10^6) were considered. The particular Rayleigh numbers considered were Ra_{cr}= 0, 10^2, 10^3, 10^4, 10^5 and 10^6.

2.10.1 Cross-Plane Results

In this section, solutions for the cross-plane stream function ψ, the temperature θ, the local Nusselt number Nu(y) and the average Nusselt number are presented and compared with the results of previous investigators for horizontal square cavities.

For low cross-plane Rayleigh numbers the motion in the cross-plane is that of one roll, as indicated by the stream function contours in figures 2.5a-e. The fluid next to the heated surface at X=-1 rises along this surface, then falls along the opposite surface.

As Ra_{cr} is increased this cross-plane motion becomes more pronounced. The minimum values of the stream function are 0, -0.126, -1.18, -5.04, -9.62 and -19.4 for Ra_{cr}= 0, 10^2, 10^3, 10^4, 10^5 and 10^6. These minima occur at the duct centre in each case. The corresponding maximum fluid cross-plane velocities are 0, 0.196, 1.84, 9.80, 33.9 and 113.

This cross-plane fluid motion influences the fully developed temperature field within the duct. For a vertical duct with Ra_{cr}=0,

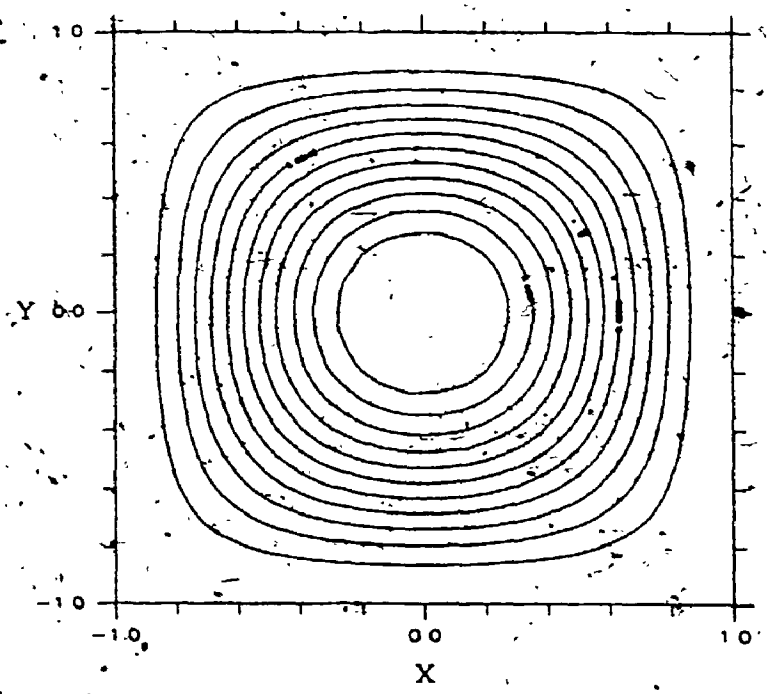

2.5a) $Ra_{cr}=10^2$, $\Delta\psi=0.01$

Figure 2.5 Fully Developed Cross-Plane Stream Function ψ for a Differentially Heated Duct.

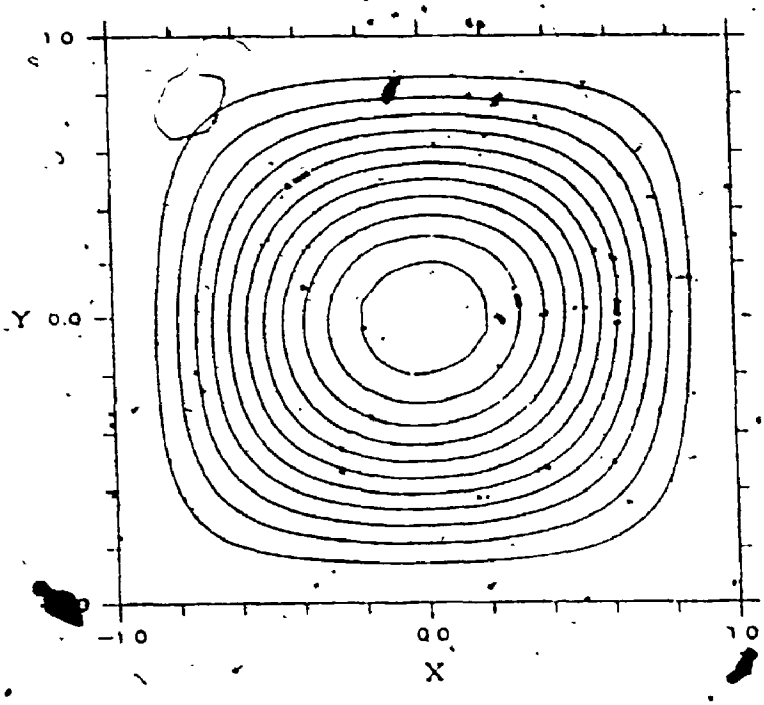

2.5b) $Ra_{cr}=10^3$, $\Delta\psi=0.1$

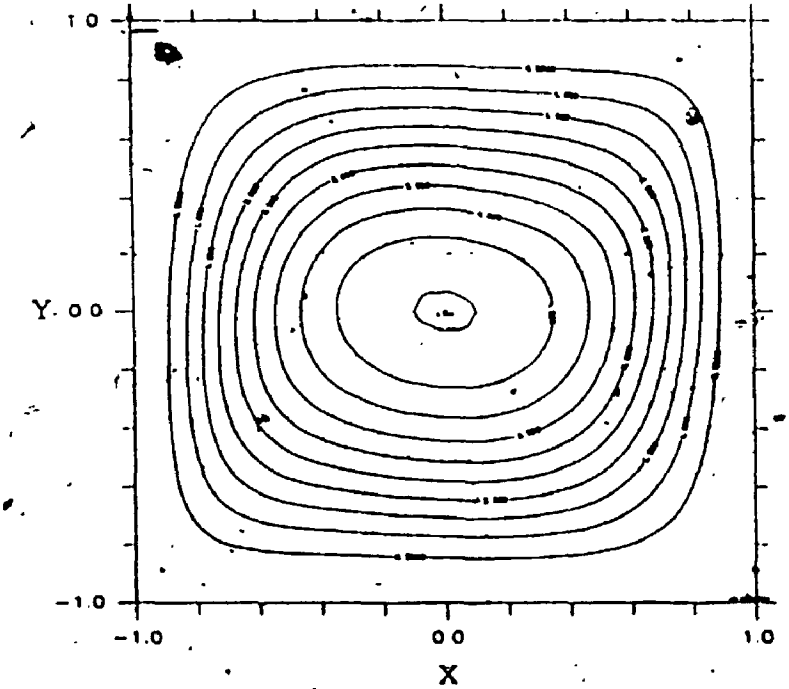

2.5c) $Ra_{cr}=10^4$, $\Delta\psi=0.5$

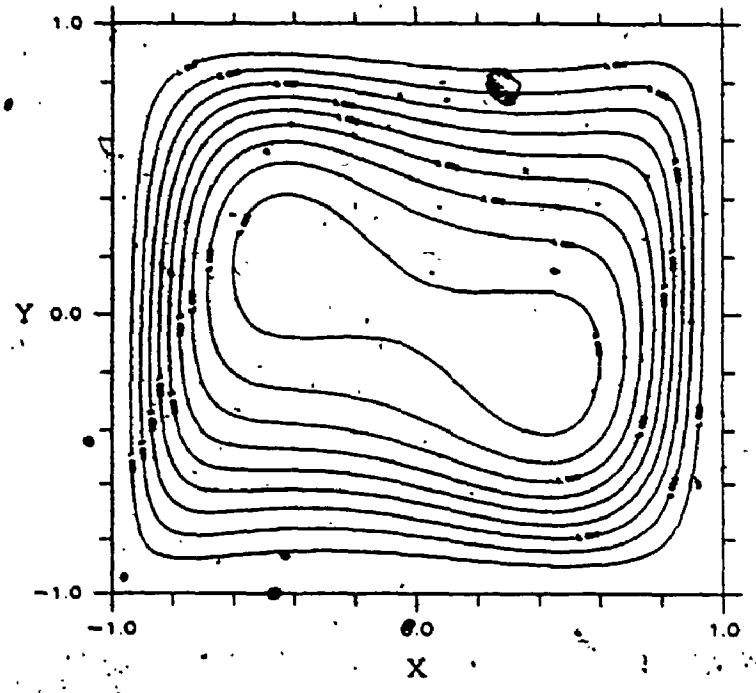

2.5d) $Ra_{cr}=10^5$, $\Delta\psi=1.0$

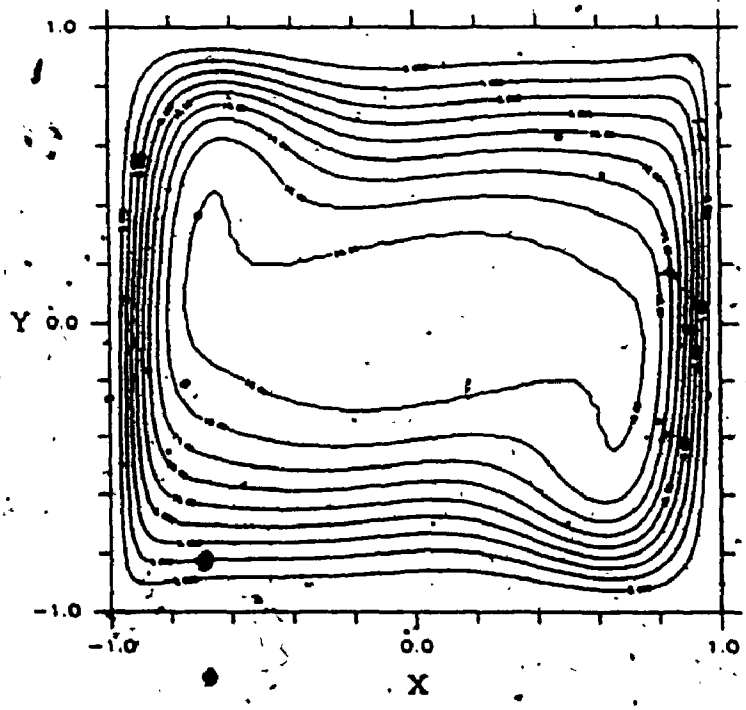

2.5e) $Ra_{cr}=10^6$, $\Delta\psi=2.0$

there is no cross-plane fluid motion and the resulting temperature field is that due to conduction only, as indicated in figure 2.6a . For larger Ra_{cr} (figures 2.6b-f) the temperature field becomes significantly distorted by this convective motion.

In figure 2.7, the local Nusselt number is shown versus location along the duct side. The profiles for $Ra_{cr}=0$ and 10^2 are not shown on this figure since they do not differ significantly from the conduction profile. For larger Ra_{cr}, there is a large variation of local Nusselt number. For $Ra_{cr}=10^6$, the maximum local Nusselt number is 20.6, compared to a conduction Nusselt number of one. Due to a strong cross-plane fluid motion, fluid near the heated surface with a high thermal energy is convected to the opposite side of the duct where it impinges on the cooler surface. Similarly, fluid near the cool surface with a low thermal energy is convected to and impinges on the opposite, heated surface. High heat transfer rates occur where fluid strikes a surface with a different temperature.

The average Nusselt numbers for the duct side surfaces has been plotted versus Ra_{cr} in figure 2.8 . The maximum and minimum local Nusselt Numbers are also shown on this same graph. For Ra_{cr} up to 500, the average Nusselt number does not differ significantly from the value for conduction.

These results are summarized in table 2.2a . The finest grid used, the maximum Peclet number, the maximum U and V velocities as well as the minimum, average and maximum Nusselt numbers are indicated. The maximum Peclet numbers for $Ra_{cr}=10^5$ and 10^6 are 2.42 and 8.07 with a 80x80 grid. At these Peclet numbers, the choice of

Table 2.2a Summary of Cross-Plane Results -Fine Grid

Ra_{cr}	grid	Pemax	Umax	Vmax	Numin	Nuave	Numax
0	40x40	0.0	0.0	0.0	1.0000	1.0000	1.0000
10^2	40x40	0.0279	0.196	0.196	0.9593	1.0013	1.0428
10^3	40x40	0.263	1.81	1.84	0.6904	1.118	1.5074
10^4	80x80	0.699	8.05	9.80	0.5762	2.247	3.5707
10^5	80x80	2.42	21.7	33.9	0.703	4.51	7.84
10^6	80x80	8.07	56.5	113.0	0.624	8.51	20.64

Table 2.2b Summary of Cross-Plane Results -Coarse Grid

Ra_{cr}	grid	Pemax	Umax	Vmax	Numin	Nuave	Numax
0	20x20	0.0	0.0	0.0	1.0000	1.0000	1.0000
10^2	20x20	0.0549	0.192	0.192	0.9551	1.0015	1.0475
10^3	20x20	0.513	1.78	1.80	0.6848	1.120	1.5230
10^4	40x40	1.39	8.05	9.70	0.578	2.251	3.567
10^5	40x40	4.74	21.38	33.17	0.706	4.57	8.09
10^6	40x40	16.6	53.5	116.5	0.32	8.85	30.53

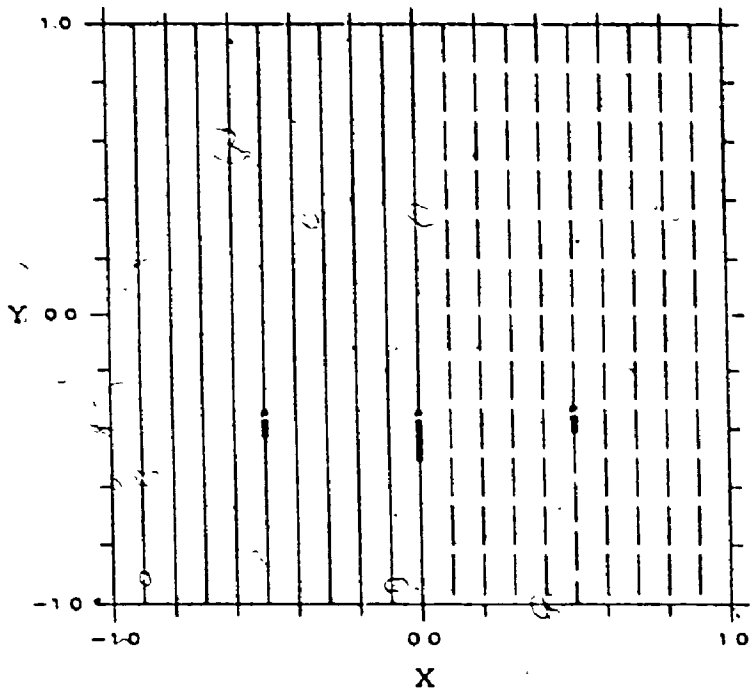

2.6a) Racr=0

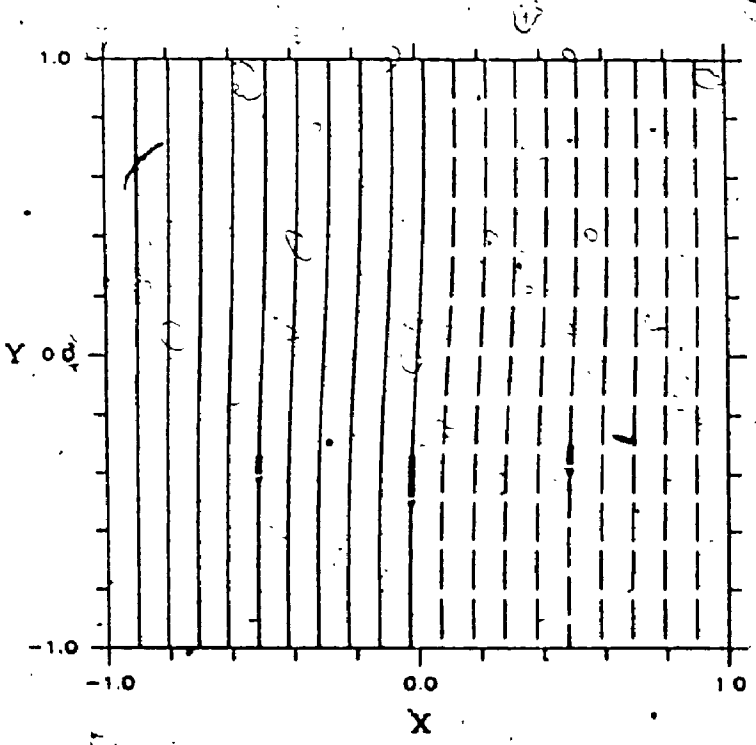

2.6b) Racr=10^2

Figure 2.6 Fully Developed Temperature Field θ for a Differentially Heated Duct. ($\Delta\theta$=0.1)

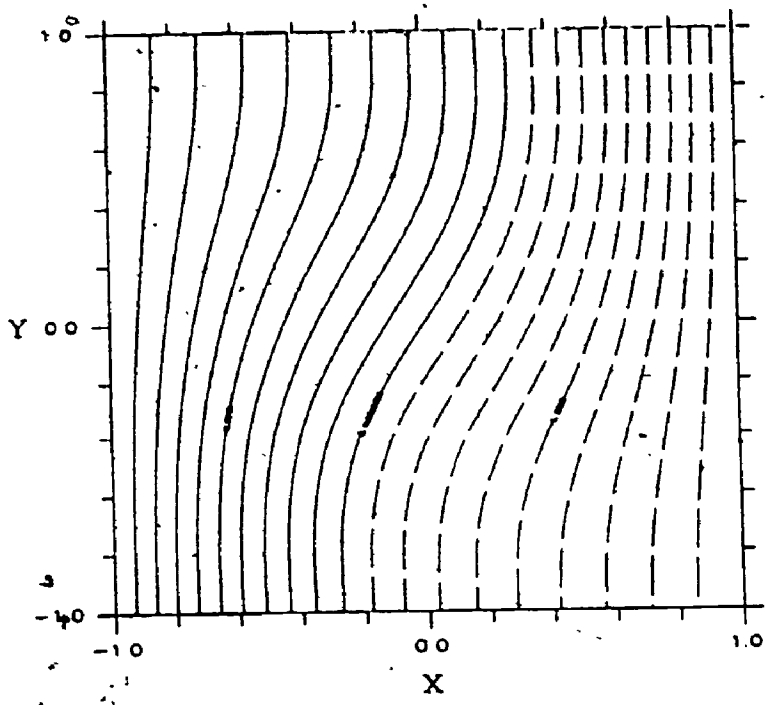

2.6c) $Ra_{cr}=10^3$

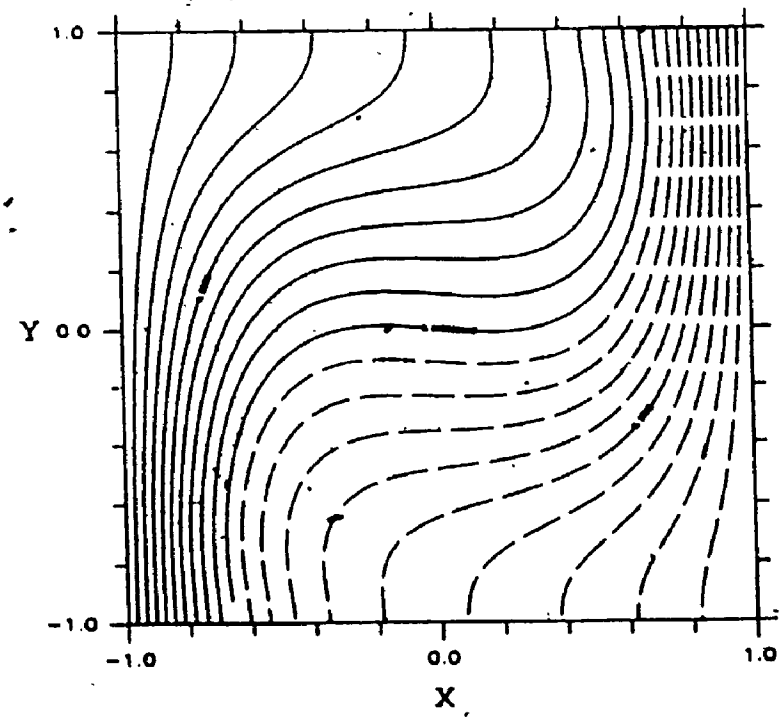

2.6d) $Ra_{cr}=10^4$

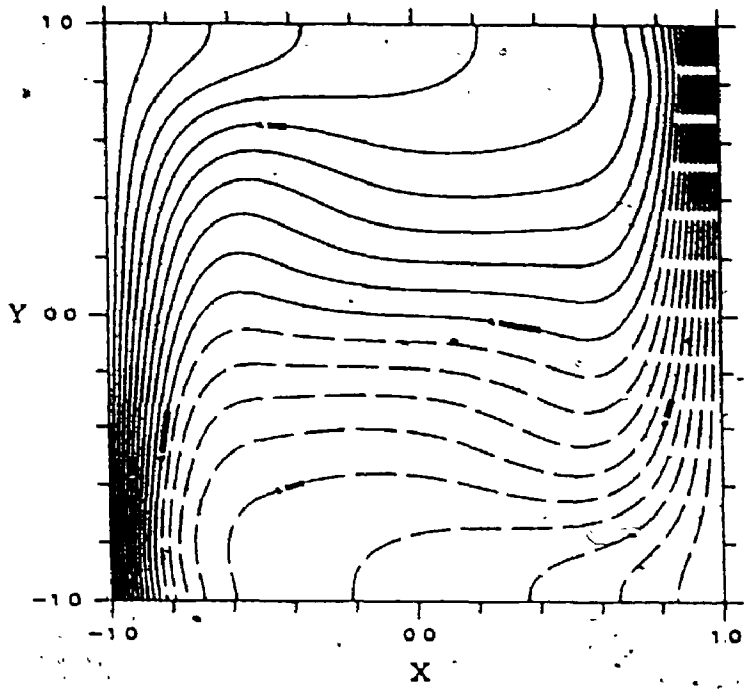

2.6e), $Ra_{cr}=10^5$

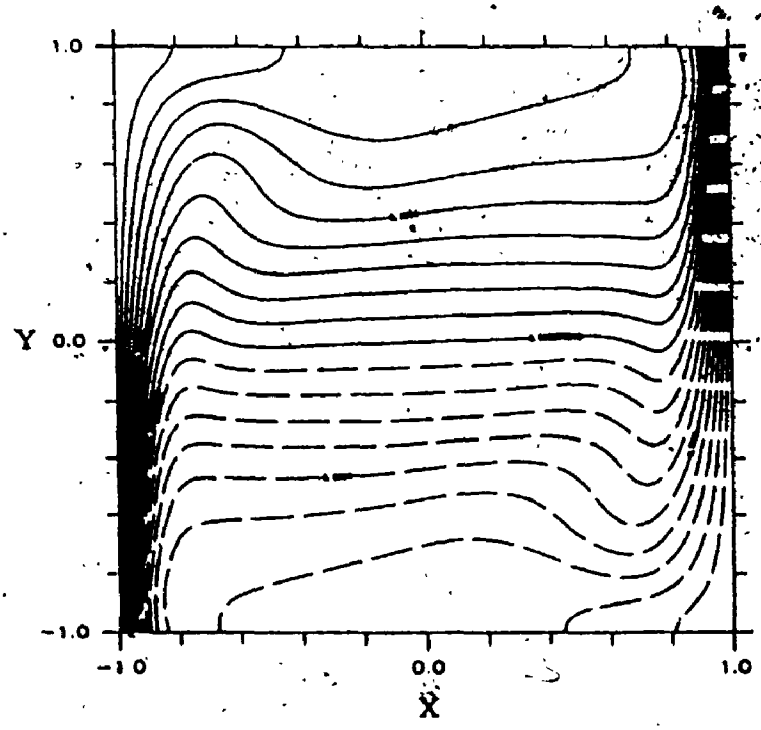

2.6f) $Ra_{cr}=10^6$

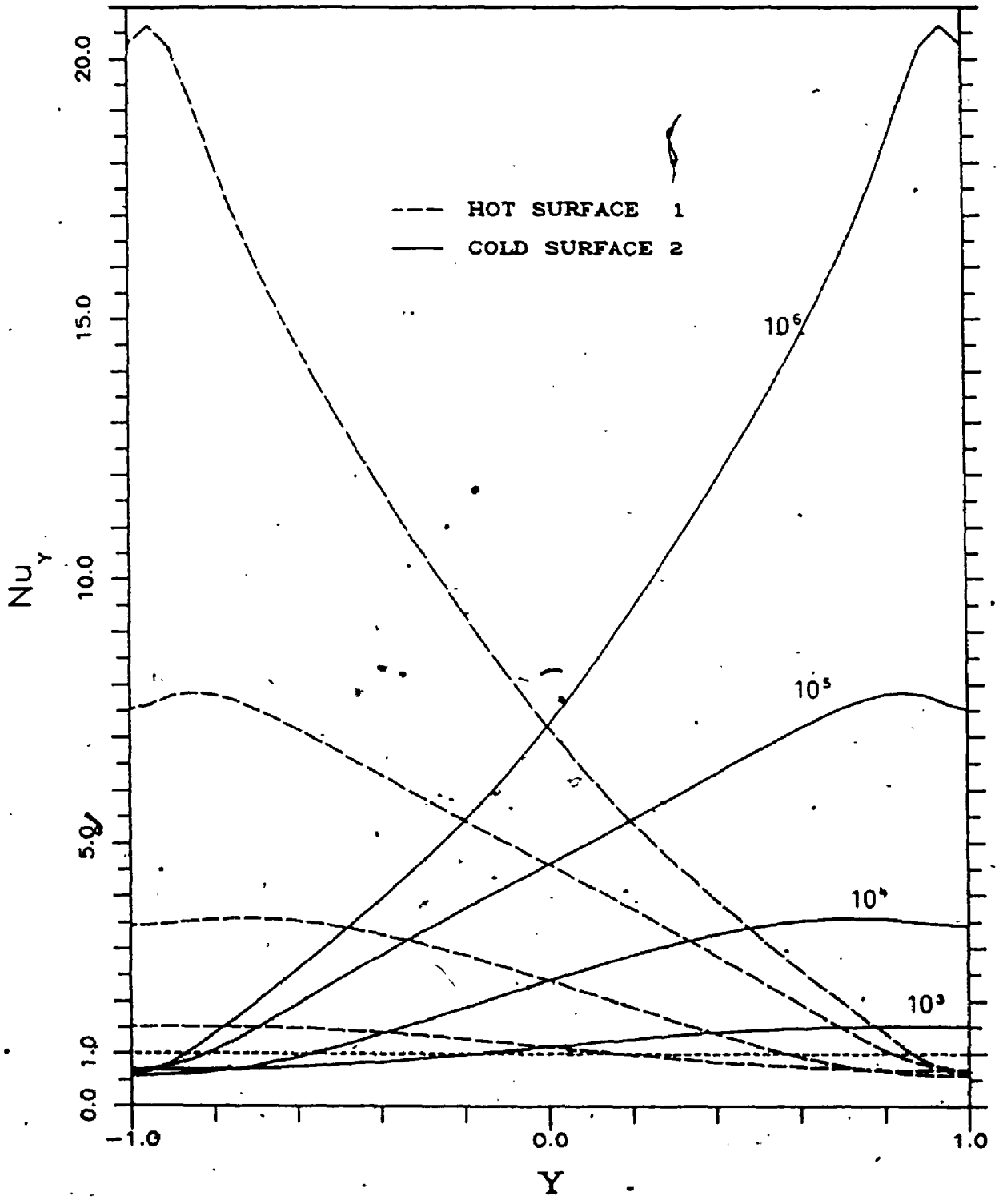

Figure 2.7 Fully Developed Local Heat Transfer Rates versus Location on Duct Side Surface

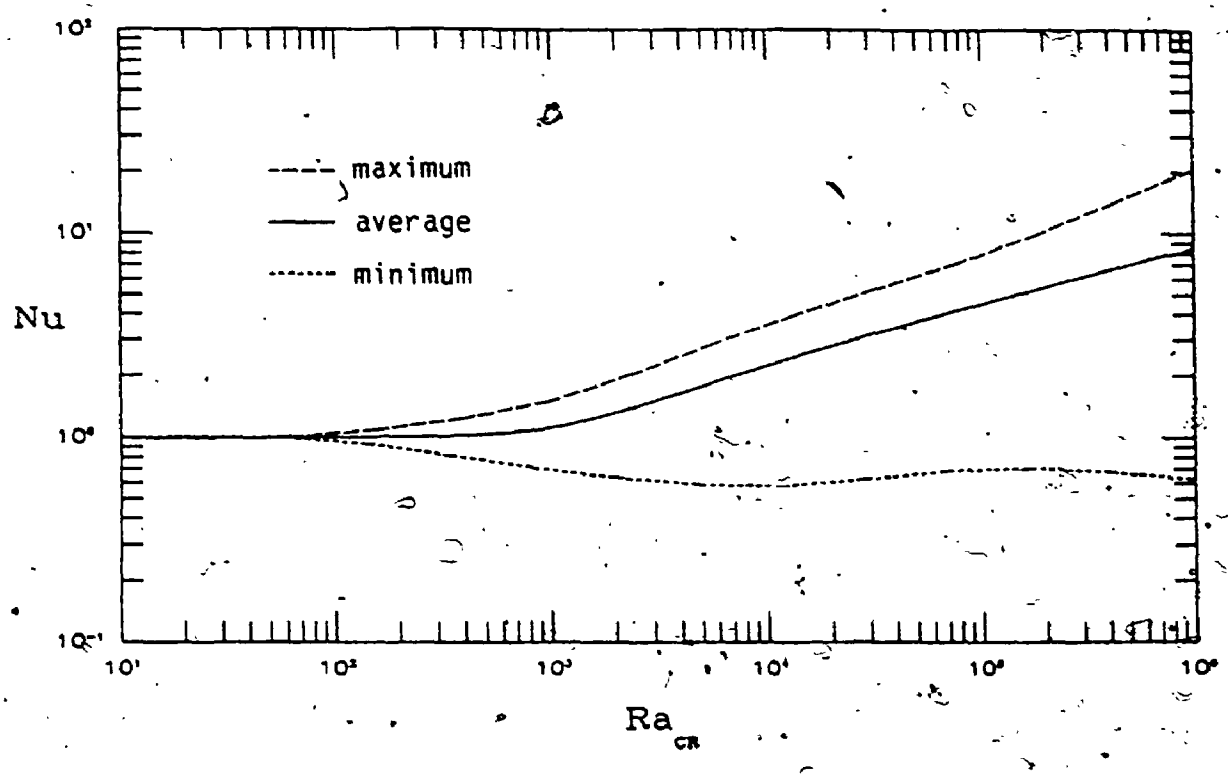

Figure 2.8 Maximum, Average and Minimum Heat Transfer Rates for Duct Side Surfaces.

discretization method can influence the resulting numerical solutions. If finer grids are used, the Peclet numbers are correspondingly reduced, however this is not feasible because of computer memory and execution time limitations.

The accuracy of the numerical solutions for Raleigh numbers of 10^5 and particularly 10^6 is less than the accuracy for the lower Rayleigh numbers because of the coarse grid mesh used. Not only are large Peclet numbers encountered, but the solutions for the variables have strong variations near the two side surfaces of the duct. In order for a discrete numerical method to accurately model this problem, it was necessary to have about five grid points in the X direction in this region to accurately define the flow in the boundary layers next to these surfaces.

The accuracy of the solutions were evaluated in two ways; by comparing solutions on a coarse grid with those on a finer grid, and by comparing the present solutions with those of previous investigators for horizontal square cavities. The solutions on coarser grids are shown in table 2.2b . For Rayleigh numbers up to 10^3 the coarser grid was 20x20, while for the higher Rayleigh numbers, the coarser grid was 40x40.

The coarse and fine grid solutions are in close agreement for Ra_{cr} up to 10^5. For $Ra_{cr}=10^6$, the minimum and maximum Nusselt numbers differ significantly, although the average Nusselt numbers differ only by 3%. For the coarse grid solution with $Ra_{cr}=10^6$, the maximum Peclet number is 16.6 . For such a large Peclet number, the resulting solutions vary depending on the discretization method.

For this coarse grid solution, there are an insufficient number of grid points to accurately resolve the strong variations in the flow and temperature fields near the duct surfaces.

2.10.2 Comparison with Existing Results for Horizontal Cavities

In a review paper by de Vahl Davis and Jones [24], the problem of natural convection in a horizontal, differentially heated cavity was studied. The fluid was taken to be air with Pr=0.71 . A total of 37 papers from various authors were considered, and their results summarized.

In a companion paper, de Vahl Davis [25] presents a bench mark solution for cross-plane Rayleigh numbers from 10^3 to 10^6 where all the results are believed accurate to 1%. A summary of these results are shown in table 2.3 . The solution procedure is similar to that used in this thesis, in that a finite difference, alternating direction implicit method was employed on a uniform mesh. Central

Table 2.3 Bench Mark Solution of de Vahl Davis [25]

Ra_{cr}	grid	Umax	Vmax	Numin	Nuave	Numax
10^3	40x40	1.825	1.849	0.692	1.118	1.505
10^4	40x40	8.089	9.809	0.586	2.243	3.528
10^5	80x80	17.37	34.30	0.729	4.519	7.717
10^6	80x80	32.32	109.7	0.989	8.800	17.925

difference discretization was used. The finest grids are the same as those in this thesis. The results from a series of successively finer grids, together with Richardson's extrapolation were used to obtain the bench mark solution.

The agreement is excellent between this bench mark solution and the results presented in the previous section for the cross-plane results for fully developed flow in inclined, differentially heated ducts. The fine grid solutions in table 2.2a for the average Nusselt number are within 0.2% for Ra_{cr} up to 10^5, and differ by 3.3% for $Ra_{cr}=10^6$. The local values such as the minimum and maximum velocities and Nusselt numbers show a larger difference for the largest Rayleigh number, as indicated in table 2.2a and 2.3 .

A large number of references are available on the topic of differentially heated cavities [21,24-30]. The numerical and experimental results obtained are consistent with the bench mark solution described here.

2.10.3 Axial Flow and Heat Transfer Results

The new numerical results presented in this thesis are the axial velocity W, the average axial velocity W_{ave} and the net heat transfer to the fluid H for fully developed flow. The Prandtl number was 0.7 and the cross-plane Rayleigh numbers considered were $0, 10^2, 10^3, 10^4, 10^5$ and 10^6, consistent with the cross-plane results of section 2.10.1 .

The axial velocity field W is shown in figures 2.9a-f for an antisymmetrically heated duct (temperature ratio $\zeta=0$), The axial

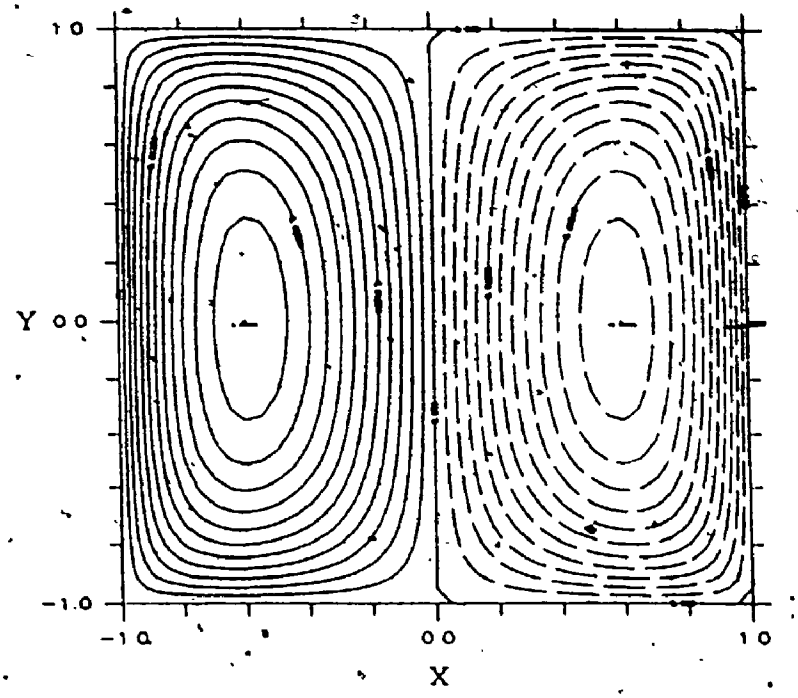

2.9a) $\zeta=0$, $Ra_{cr}=0$

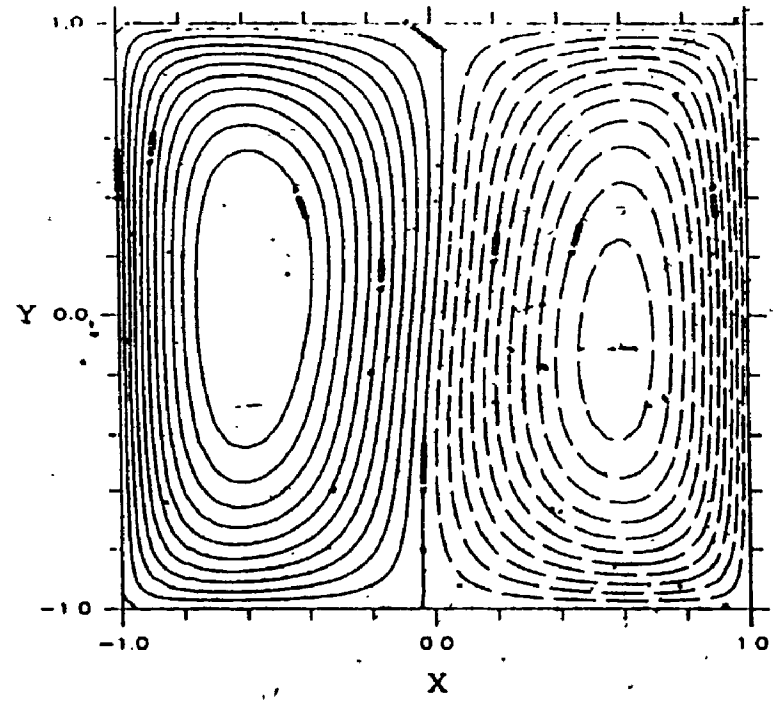

2.9b) $\zeta=0$, $Ra_{cr}=10^2$

Figure 2.9 Fully Developed Axial Velocity Field W for an Antisymmetrically Heated Duct. (contour interval $\Delta W=0.0025$)

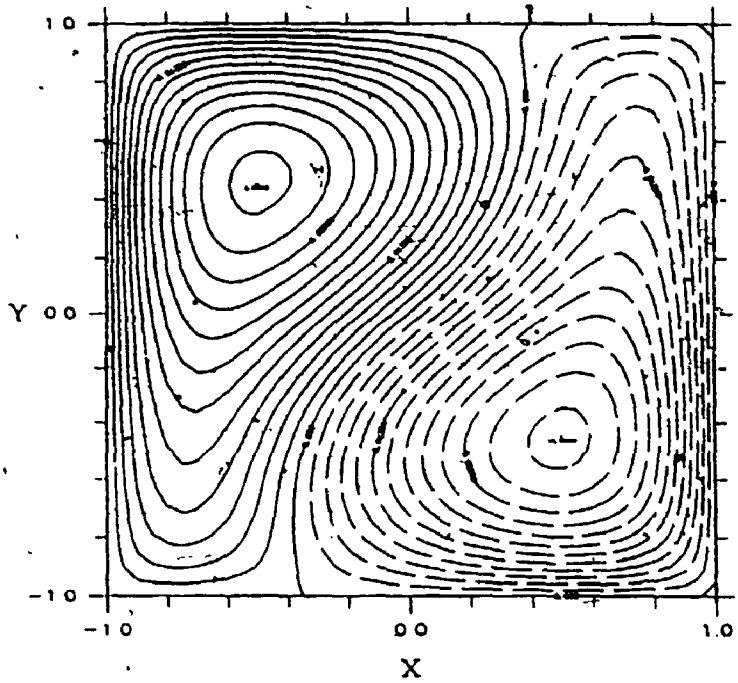

2.9c) $\zeta=0$, $Ra_{cr}=10^3$

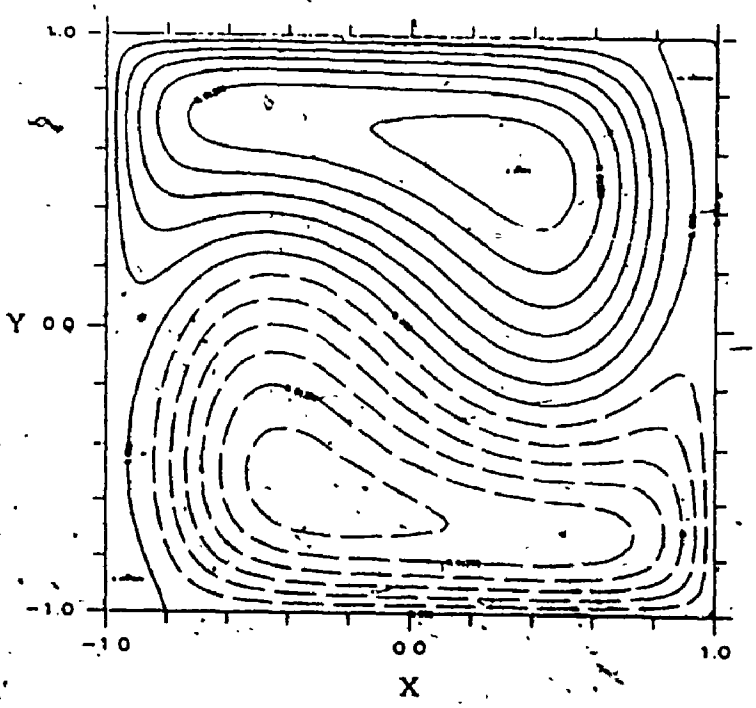

2.9d) $\zeta=0$, $Ra_{cr}=10^4$

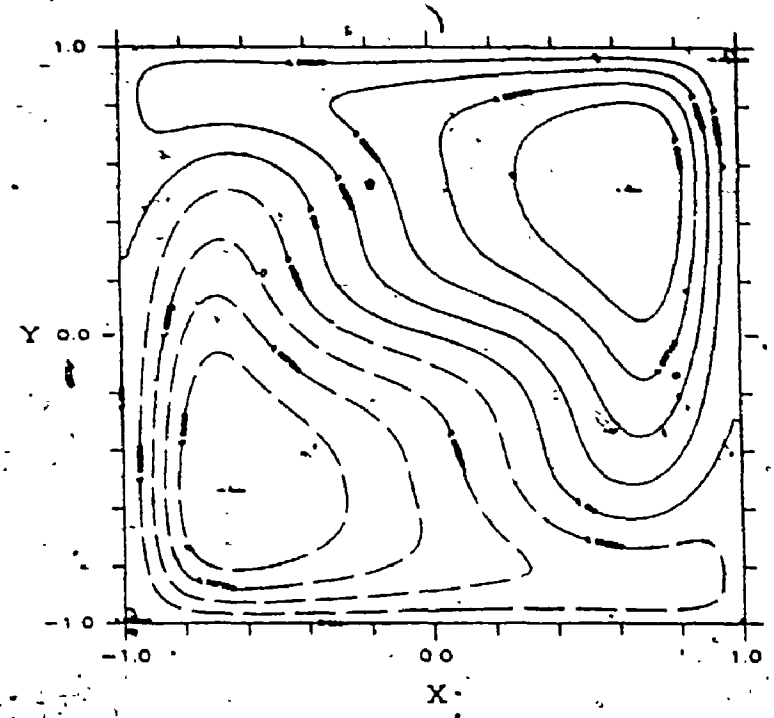

2.9e) $\zeta=0$, $Ra_{cr}=10^5$.

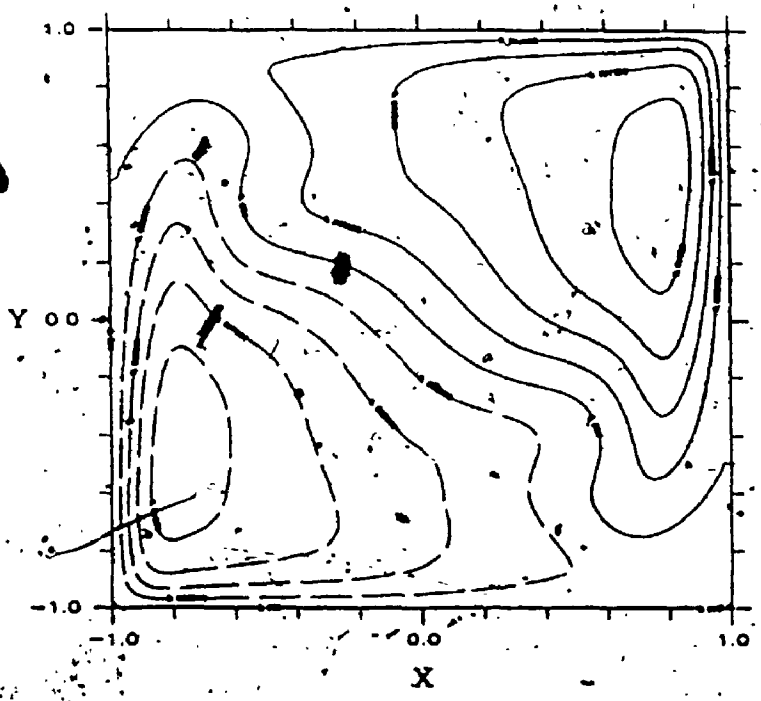

2.9f) $\zeta=0$; $Ra_{cr}=10^6$

fluid motion is in the positive Z direction for the left half of the duct next to the heated surface at X=-1, and in the negative Z direction on the right half of the duct near the cooled surface. For Ra_{cr} greater than 10^2, the axial velocity field is significantly influenced by the duct inclination. Since the fully developed temperature field is strongly distorted by the cross-plane fluid motion, and the axial velocity motion is driven by the buoyancy force in the axial direction, the axial velocity field is affected by the cross-plane circulation.

The maximum axial velocities are 0.0293, 0.0294, 0.0308, 0.0167, 0.0133 and 0.011 for $Ra_{cr}=0, 10^2, 10^3, 10^4, 10^5$ and 10^6. The maximum amplitude is reduced for larger Rayleigh numbers since larger shear stresses exist because of the stronger cross-plane motion. The accuracy of these values decreases with increasing Ra_{cr}. The maximum axial velocities on the next coarser grid are 0.01, 0.03, -0.4, 2, 9, and 59% higher than the values indicated here. The large difference for $Ra_{cr}=10^6$ is due to the 40x40 grid being inadequate to model the strong cross-plane motion.

It is interesting to note the shifting of the location of the maximum and minimum axial velocities as the cross-plane Rayleigh number is increased. For Ra_{cr} up to 10^2, the maximum and minimum velocities are located half way up the heated and cooled duct side surfaces, near Y=0.0. For $Ra_{cr}=10^3$ the maximum velocity location has moved to the top portion of the heated side, and the minimum velocity location has moved to the lower portion of the cooled side. For higher cross-plane Rayleigh numbers, these locations are shifted

along the adiabatic surfaces until they are positioned near the opposite side surface.

The axial velocity field W is shown in figures 2.10a-f for a differentially heated duct with temperature ratio ζ=0.5 . For this case, the left duct side surface is heated above the ambient temperature, while the right side surface is maintained at the ambient temperature. The fluid temperature is everywhere greater than the ambient, and as a result, the axial fluid motion is in the positive Z direction.

The axial velocity field W is shown in figures 2.11a-f for a differentially heated duct with temperature ratio ζ=1.5 . Both the left and right duct side surfaces are heated above the ambient temperature.

Results for the maximum and average axial velocities, as well as the net heat transfer to the fluid H have been tabulated in table 2.4a for temperature ratios 0.5 and 1.5 . The average axial velocity for the two ratios are essentially identical, however the maximum axial velocities for ζ=0.5 are from 6% to 2% higher than for the temperature ratio ζ=1.5, with this difference decreasing with Ra_{cr}. The net heat transfer to the fluid H for ζ=0.5 are from 10% to 4% higher than those values for ζ=1.5 .

In order to evaluate the accuracy of these solutions, the maximum and average velocities, and the net heat transfer H are shown in table 2.4b for the next coarsest grid. The coarse grid solutionsare from 1% lower for low Ra_{cr}, to 4% lower for $Ra_{cr}=10^5$, to 25% lower for $Ra_{cr}=10^6$. The accuracy of the resulting solution

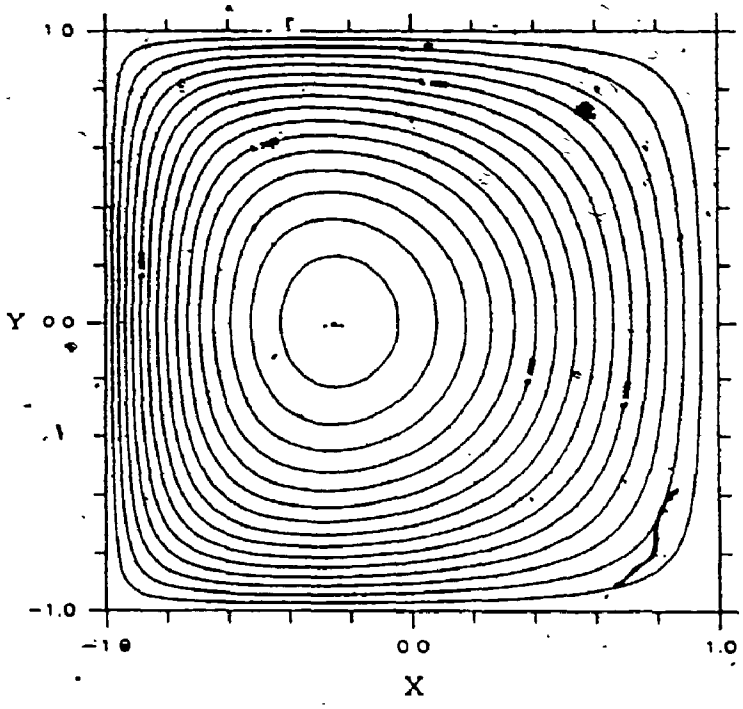

2.10a) ζ=0.5, Ra_{cr}=0

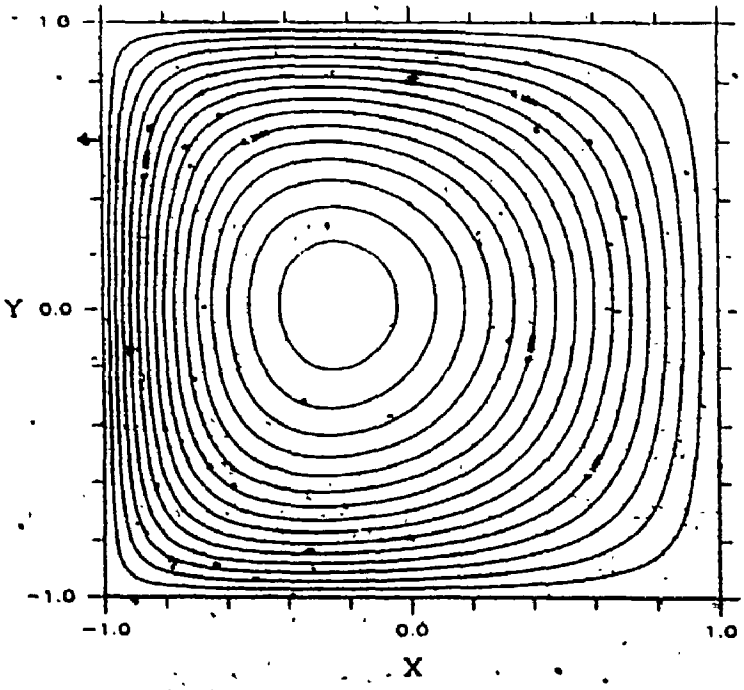

2.10b) ζ=0.5, $Ra_{cr}=10^2$

Figure 2.10 · Fully Developed Axial Velocity Field W for Temperature Ratio ζ=0.5 . (ΔW=0.02)

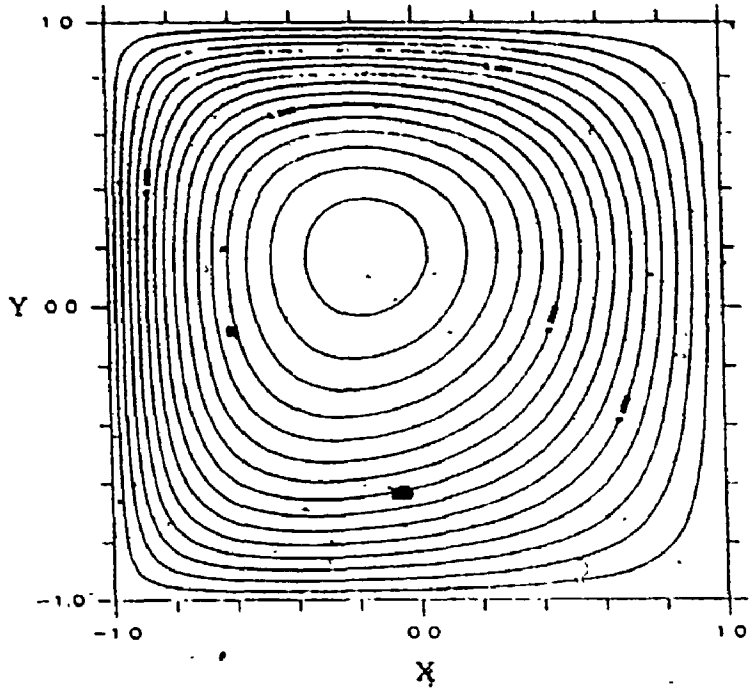

2.10c) $\zeta=0.5$, $Ra_{cr}=10^3$

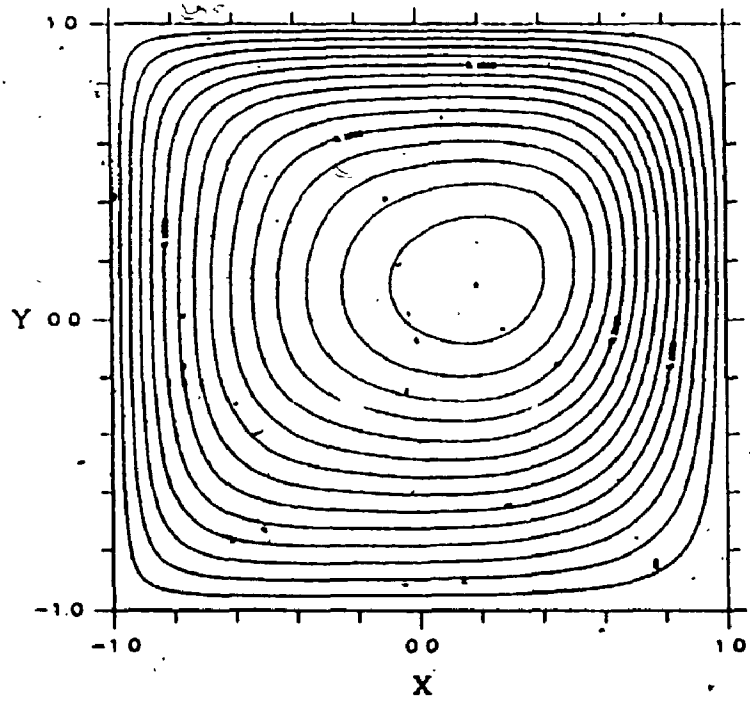

2.10d) $\zeta=0.5$, $Ra_{cr}=10^4$

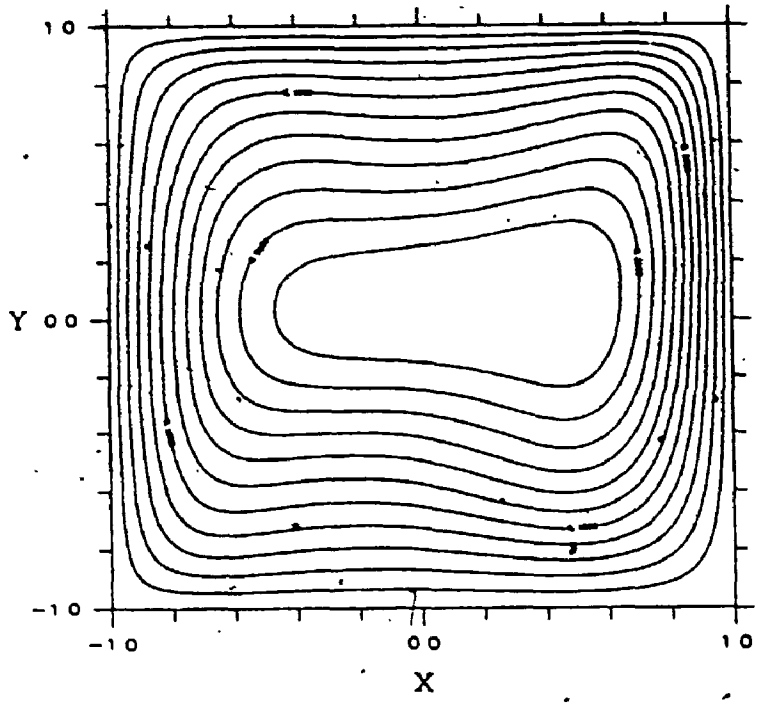

2.10e) ζ=0.5, $Ra_{cr}=10^5$

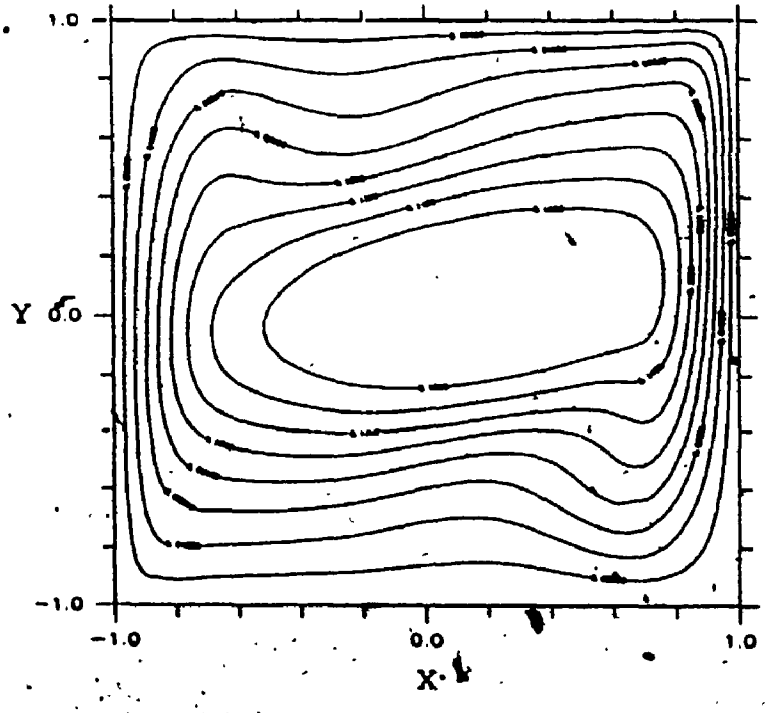

2.10f) ζ=0.5, $Ra_{cr}=10^6$

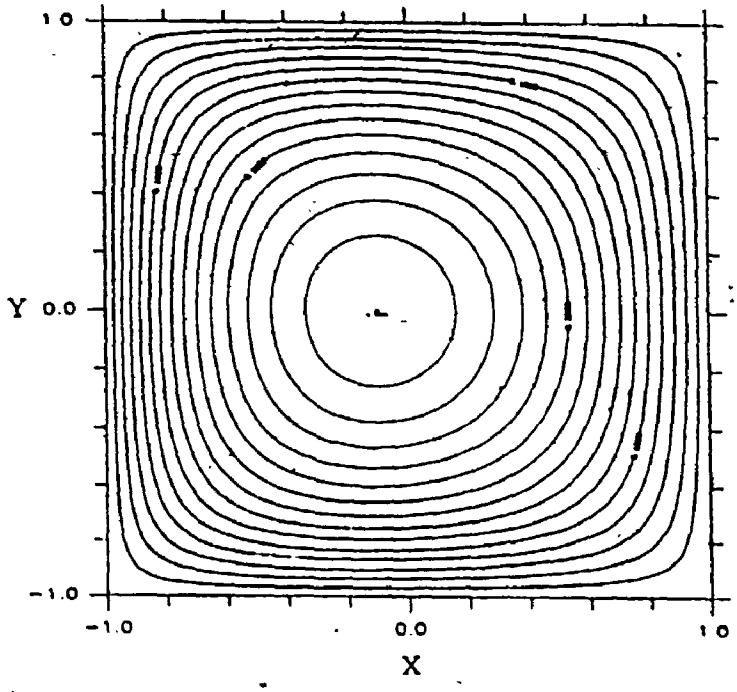

2.11a) ζ=1.5, Ra_{cr}=0

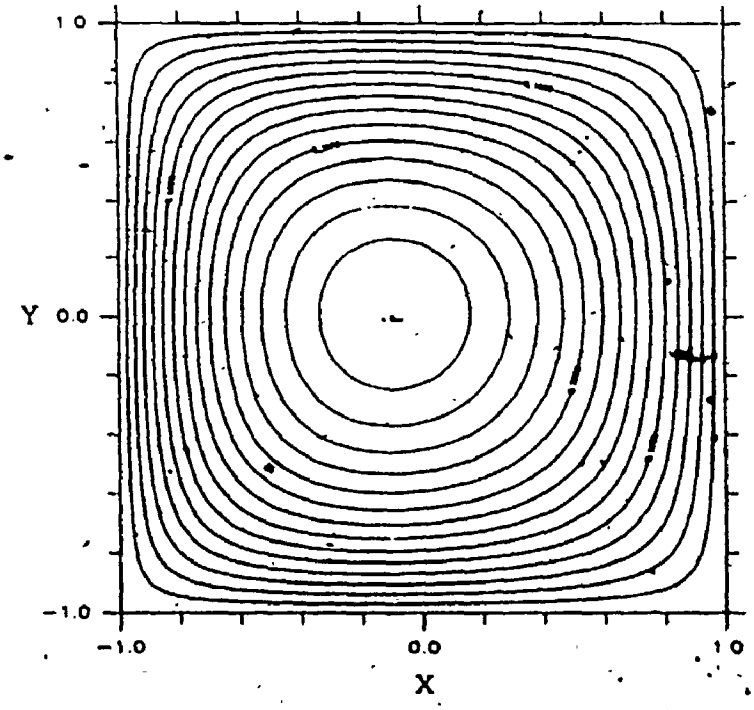

2.11b) ζ=1.5, Ra_{cr}=10^2

Figure 2.11 Fully Developed Axial Velocity Field W for Temperature Ratio ζ=1.5 , (ΔW=0.02)

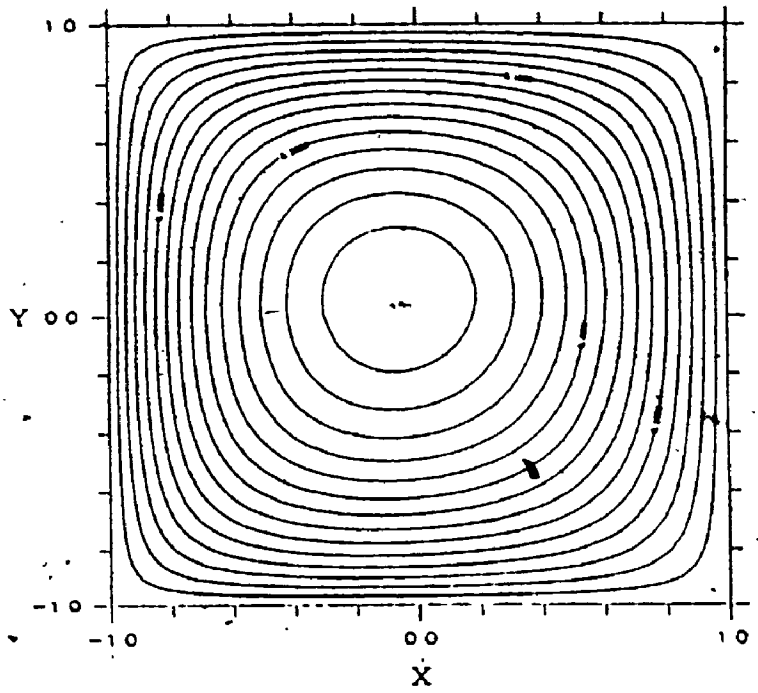

2.11c) $\zeta=1.5$, $Ra_{cr}=10^3$

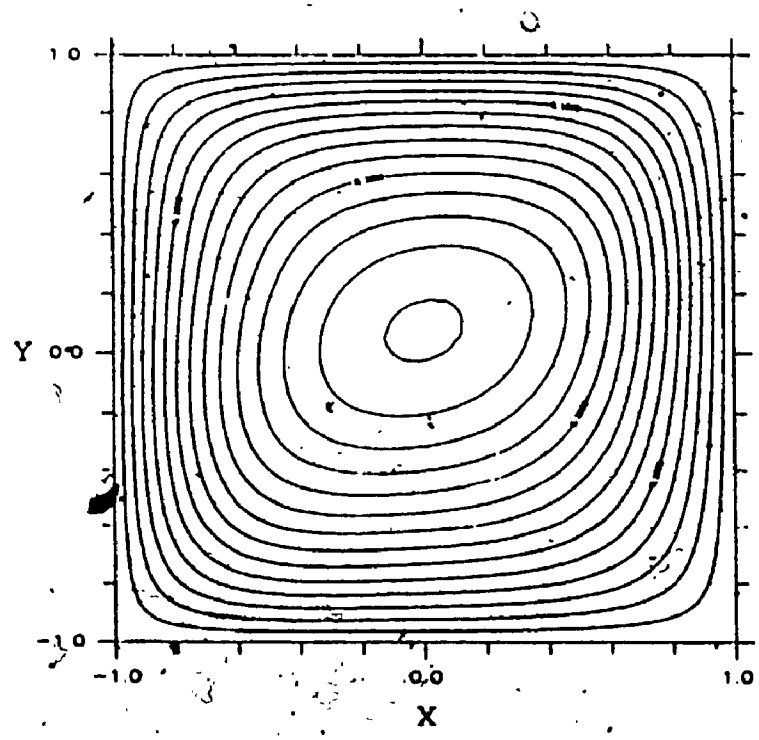

2.11d) $\zeta=1.5$, $Ra_{cr}=10^4$

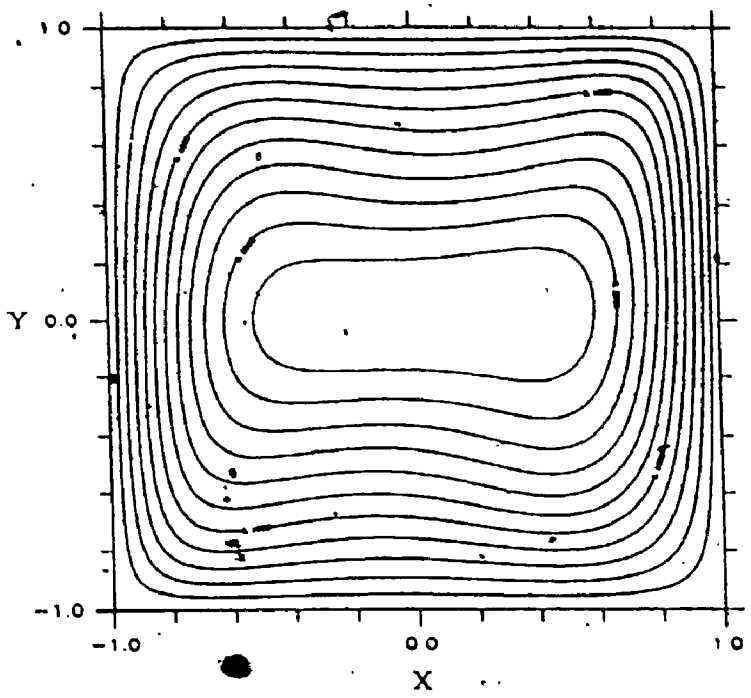

2.11e) ζ=1.5, Racr=10^5

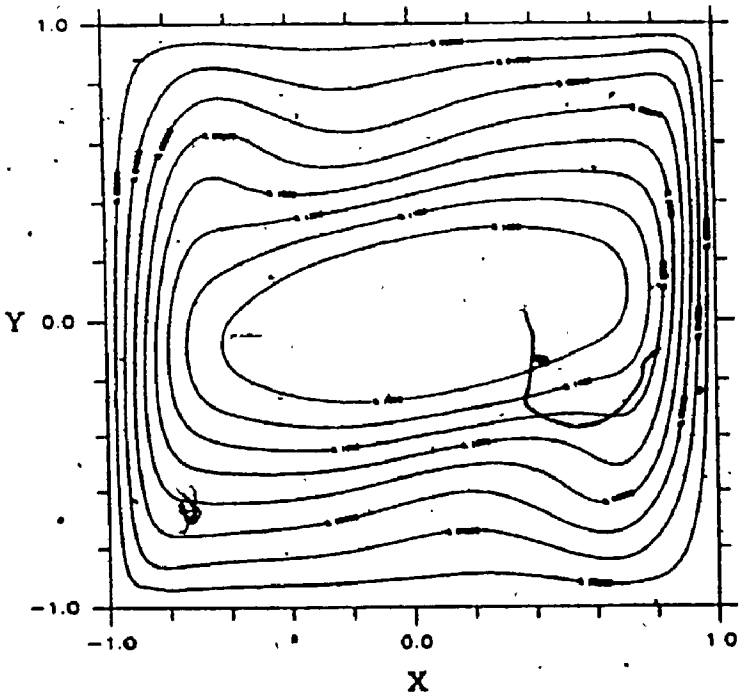

2.11f) ζ=1.5, Racr=10^6

Table 2.4a Summary of Axial Flow Results -Fine Grid

		ζ=0.0	ζ=0.5			ζ=1.5		
Ra_{cr}	grid	W_{max}	W_{max}	W_{ave}	H	W_{max}	W_{ave}	H
0	40x40	0.0293	0.314	0.140	0.622	0.297	0.140	0.568
10^2	40x40	0.0294	0.314	0.140	0.622	0.297	0.140	0.568
10^3	40x40	0.0308	0.312	0.140	0.618	0.296	0.140	0.568
10^4	80x80	0.0167	0.295	0.136	0.571	0.283	0.136	0.549
10^5	80x80	0.0133	0.246	0.123	0.506	0.240	0.123	0.494
10^6	80x80	0.0112	0.194	0.088	0.368	0.191	0.088	0.355

Table 2.4b Summary of Axial Flow Results -Coarse Grid

		ζ=0.0	ζ=0.5			ζ=1.5		
Ra_{cr}	grid	W_{max}	W_{max}	W_{ave}	H	W_{max}	W_{ave}	H
0	20x20	0.0294	0.313	0.139	0.619	0.297	0.139	0.564
10^2	20x20	0.0294	0.313	0.139	0.618	0.297	0.139	0.564
10^3	20x20	0.0307	0.311	0.139	0.613	0.296	0.139	0.564
10^4	40x40	0.0170	0.296	0.139	0.579	0.290	0.139	0.558
10^5	40x40	0.0145	0.240	0.118	0.487	0.233	0.118	0.474
10^6	40x40	0.0179	0.156	0.065	0.291	0.143	0.065	0.264

on the coarse grid for $Ra_{cr}=10^6$ is limited since this grid is too coarse to accurately model the cross-plane velocity and temperature fields.

The fine grid solution for the average axial velocity has been plotted in figure 2.12 . Since the values with the temperature ratios 0.5 and 1.5 do not differ significantly, only one curve is shown. The average axial velocity is constant for Ra_{cr} up to 10^4, and decreases for larger cross-plane Rayleigh numbers.

Curves for the net heat transfer H are shown in figure 2.13 with $\zeta=0.5$ and 1.5 . This thermal energy convected out of the duct decreased for larger cross-plane Rayleigh numbers since the axial flow rate decreases. Note a curve for the temperature ratio $\zeta=0$ was not included in figure 2.12 or 2.13 since the expression for the dimensionless axial velocity W for this temperature ratio differs from that for the temperature ratios 0.5 and 1.5 .

The axial velocity W for temperature ratios 0.5 and 1.5 is not a strong function of the cross-plane fluid motion. Indeed, for the limit $\zeta\to\infty$, the axial velocity approaches that of the isothermal duct, and is independent of the cross-plane Rayleigh number. In this limit, $W_{max}=0.295$, $W_{ave}=0.1405$ and $H=0.5620$. Because of this moderate dependence, the accuracy of the solutions for the axial velocity and net heat transfer H with $\zeta=0.5$ and 1.5 is sufficient for design calculations, even for $Ra_{cr}=10^6$.

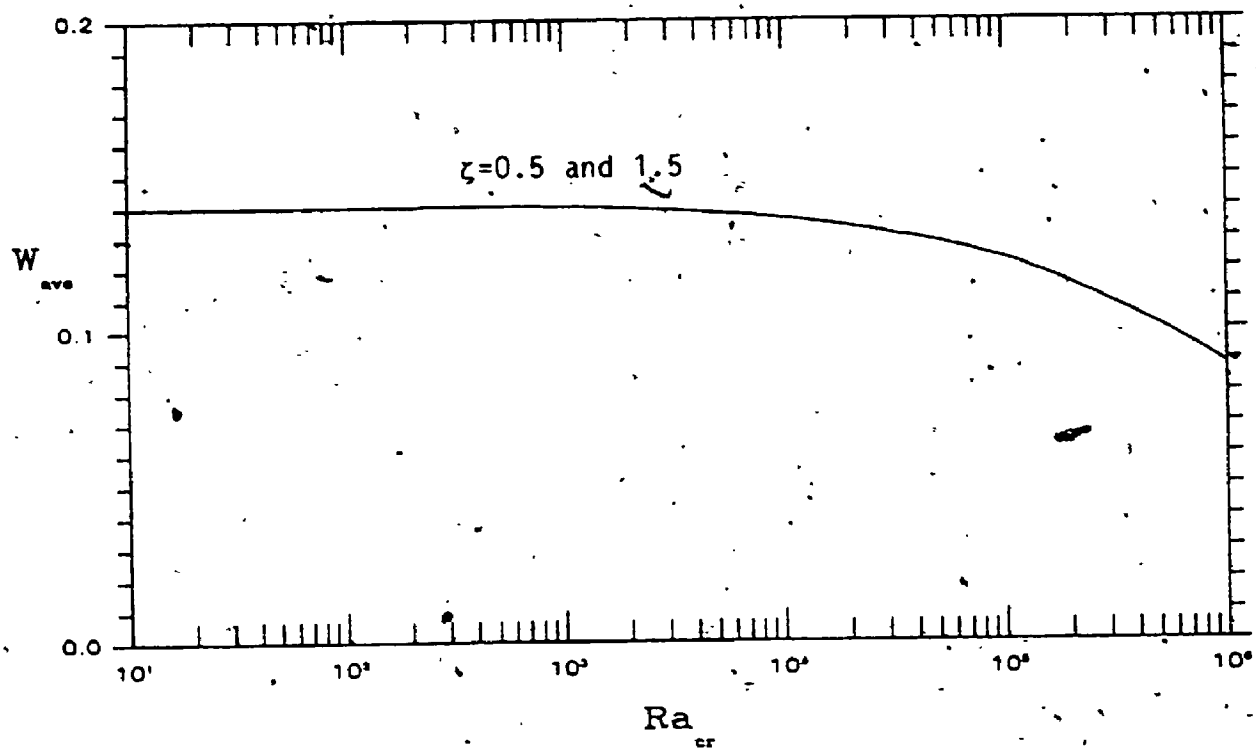

Figure 2.12 Fully Developed Average Axial Velocity

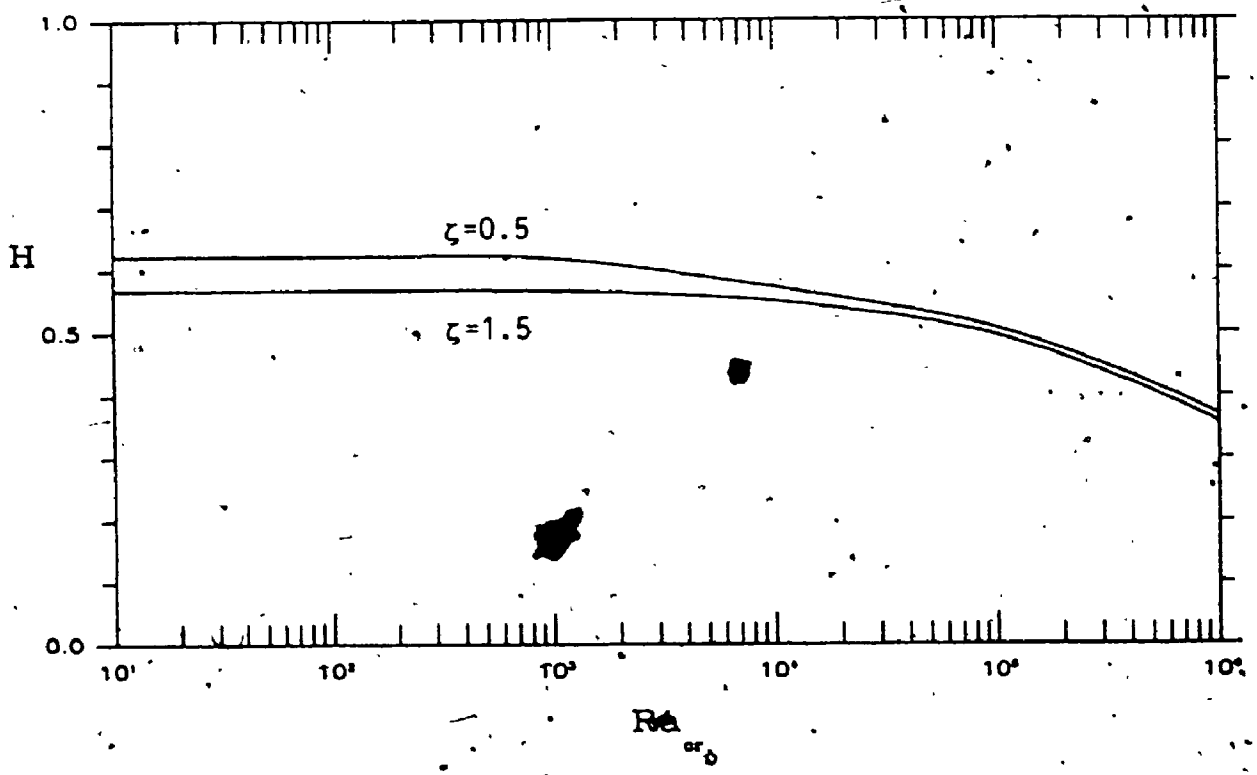

Figure 2.13 Fully Developed Net Heat Transfer

2.11 Summary

The results presented here for the isothermal and the differentially heated ducts show that solutions for fully developed natural convective duct flows can be obtained. It is the opinion of the author that solutions could also be obtained, at a reasonable cost, using existing computing facilities, for developing flow in isothermal ducts and differentially heated square ducts with small cross-plane Rayleigh numbers (up to 10^4). At these Rayleigh numbers, a 20x20 or 40x40 grid would suffice in the cross-plane.

CHAPTER 3

FRINGE ANALYSIS TECHNIQUE

3.1 Introduction

One objective in this thesis was to develop an interferometric technique for obtaining heat transfer rates for flows with three-dimensional temperature fields. This method is discussed in this chapter, together with a listing of possible applications. Chapter 4 contains a description of how this method was employed in the study of developing natural convective flow in inclined ducts.

The method described here is mathematically exact in that no approximations were made in deriving the relevant equations, other than the approximations normally made in the study of two-dimensional flows. The surface of the model is parallel to the interferometer test beam, and the temperature of this surface is constant in the direction of the test beam. The refractive index gradients normal to this surface were taken to be small so curvature of the test beam path was neglected. It was also assumed that any refractive index (or density) variations were due to temperature variations, rather than pressure variations. The fluid was taken to be an ideal gas in this thesis, although the method is valid for any fluid.

3.2 Refractive Index Variation with Temperature

The measure of the speed of light in a fluid field is given by the fluid refractive index, which is defined as the velocity of

light in free space divided by the velocity of light in the fluid. The term 'refraction' is a misnomer for interferometry. It is assumed the refraction of light is negligible. We are interested in how the light velocity is reduced in regions of high refractive index. Due to interaction with fluid (gas) molecules, light travels slower in regions of high fluid density. In the neighbourhood of a heated object, the fluid is heated and its density is low. Light travelling through this region travels slightly faster than light through the cool, surrounding fluid or alternatively, in a given time light will travel slightly farther in the warm fluid.

The interferometer integrates the 3-D refractive index field to obtain a 2-D fringe shift field or interferogram. This fringe shift field is a measure of the average refractive index along the test beam.

For many fluids it may be necessary to actually measure the index of refraction and develop an empirical relationship for the refractive index as a function of density or temperature. For an ideal gas such as air near atmospheric temperature and pressure, a solution has been derived theoretically [31]. For an ideal gas at a constant pressure, the relationship between density and refractive index is given by:

$$\frac{n^2-1}{\rho(n^2+2)} = K_{gd} \qquad (3.1)$$

where K_{gd} is the Gladstone-Dale constant for the ideal gas in question. For dry air, the Gladstone-Dale constant equals 1.504×10^{-4} m^3/Kg for light of wavelength $\lambda=6.328\times10^{-7}$m. By taking a Taylor's series of the left side for n~1,

$$\frac{n^2-1}{n^2+2} \sim \frac{2}{3}(n-1)$$

This gives:

$$\frac{n-1}{\rho} = 1.5\ K_{gd} \qquad (3.2)$$

This relationship is sufficiently accurate for the purpose of interferometry. From the ideal gas law, $\rho = \frac{P}{RT}$, and

$$(n-1) = \frac{1.5\ P\ K_{gd}}{R}\ \frac{1}{T} \qquad (3.3)$$

We now have an equation relating the refractive index n to the absolute temperature T.

3.3 Analysis of Two-Dimensional Refractive Index Fields

For a Mach-Zehnder interferometer, the fringe shift with respect to the model surface ε is related to the refractive index by the following equation.

$$\varepsilon = \frac{1}{\lambda}\int_0^l (n-n_s)\,dz \qquad (3.4)$$

The axial coordinate is given by z and n_s is the gas refractive index evaluated at the surface temperature. Substituting (3.3) in (3.4) we obtain equation (3.5).

$$\varepsilon = \frac{1}{\lambda}\int_0^l \frac{1.5\ P\ K_{gd}}{R}\left(\frac{1}{T} - \frac{1}{T_s}\right) dz \qquad (3.5)$$

If the temperature T is taken to be constant in the z direction, (3.5) can be integrated, and the following expression for the local fluid temperature is a function of the fringe shift can be obtained.

$$\frac{1}{T} - \frac{1}{T_s} = \frac{\lambda\ R\ \varepsilon}{1.5\ l\ P\ K_{gd}}$$

$$\text{or } T = \frac{T_s}{1 + \frac{\lambda\ R\ T_s}{1.5\ l\ P\ K_{gd}}\varepsilon}$$

3.4 Analysis of Three-Dimensional Refractive Index Fields

For a 3 dimensional temperature field it is not possible to invert (3.5) to obtain any temperatures by measuring the fringe shift field. Franke [1], Yousef [2,3,4] and McKeen [5] avoided this problem by taking a Taylor's series of the integrand about a temperature T_m averaged along the light path and keeping only the lowest order term.

$$f(T) = \frac{1}{T} - \frac{1}{T_s}$$
$$= \frac{1}{T_s} - \frac{1}{T_m} - \frac{1}{T_m^2}(T - T_m) + \ldots \qquad (3.6)$$

Substitute (3.6) in (3.5) and keep the lowest order term only.

$$\varepsilon = \frac{1.5\ P\ K_{gd}}{\lambda\ R} \int_0^1 \left(\frac{1}{T_m} - \frac{1}{T_s}\right) dz \qquad (3.7)$$

The integrand is constant so the integral can be evaluated.

$$\varepsilon = \frac{1.5\ 1\ P\ K_{gd}}{\lambda\ R} \left(\frac{1}{T_m} - \frac{1}{T_s}\right) \qquad (3.8)$$

The mean temperatures T_m can now be evaluated by measuring the fringe shift field from an interferogram. The accuracy of the mean temperature field T_m is dependent on the truncation error introduced by keeping only the lowest order term of (3.6).

The approach used by the author in the present study was not to try to obtain the temperature field but rather to calculate the heat transfer from the fringe shift field directly. Differentiate (3.5) in the direction y normal to the surface.

$$\frac{\partial \varepsilon}{\partial y} = \frac{1.5\ P\ K_{gd}}{\lambda\ R} \frac{\partial}{\partial y} \int_0^1 \left(\frac{1}{T} - \frac{1}{T_s}\right) dz$$
$$= \frac{1.5\ P\ K_{gd}}{\lambda\ R} \int_0^1 \frac{\partial}{\partial y}\left(\frac{1}{T} - \frac{1}{T_s}\right) dz$$
$$= \frac{1.5\ P\ K_{gd}}{\lambda\ R} \int_0^1 -\frac{1}{T^2} \frac{\partial T}{\partial y}\, dz \qquad (3.9)$$

For an isothermal model the surface temperature T_s is constant along the test beam. Evaluate (3.9) at the model surface.

$$\left.\frac{\partial \epsilon}{\partial y}\right|_s = \frac{1.5\ P\ K_{gd}}{\lambda\ R} \int_0^1 - \frac{1}{T_s^2} \left.\frac{\partial T}{\partial y}\right|_s dz$$

$$= \frac{1.5\ P\ K_{gd}}{\lambda\ R\ T_s^2} \int_0^1 - \left.\frac{\partial T}{\partial y}\right|_s dz$$

In dimensionless form, $Y=y/a$ $Z=z/a$ $L=l/a$ $Nu = -\frac{a}{(T_s-T_\infty)} \left.\frac{\partial T}{\partial y}\right|_s$, therefore

$$\left.\frac{\partial \epsilon}{\partial Y}\right|_s = \frac{1.5\ 1\ P\ K_{gd}\ (T_s-T_\infty)}{\lambda\ R\ T_s^2} \frac{1}{L} \int_0^L Nu\ dZ$$

or
$$\frac{1}{L} \int_0^L Nu\ dZ = \frac{1}{C} \left.\frac{\partial \epsilon}{\partial Y}\right|_s \qquad (3.10)$$

where
$$C = \frac{1.5\ 1\ P\ K_{gd}\ (T_s-T_\infty)}{\lambda\ R\ T_s^2} \qquad (3.11)$$

The Nusselt number, averaged along the test beam, is directly proportional to the derivative of the fringe shift normal to the model surface, evaluated at the surface. Using (3.10), the heat transfer can be calculated without calculating any fluid temperatures.

Equation (3.10) was employed by the author to analyze interferograms for vertical and inclined isothermal tubes and square ducts. A drawing of a duct end view including symbols is given in figure 3.1 . The procedure for analysing these interferograms is as follows:

1) Select a model surface to be analyzed.
2) Beginning at scanning location 0.1 along this surface, measure and record the distance from the surface to each of the first five fringes next to the surface using a measuring microscope. The resolution and accuracy of this measuring microscope in measuring these fringe locations was 1μm.
3) Fit a best-fit straight line to the first three fringes, the first four fringes and the first five fringes to obtain three estimates for the derivative of the fringe shift normal to the

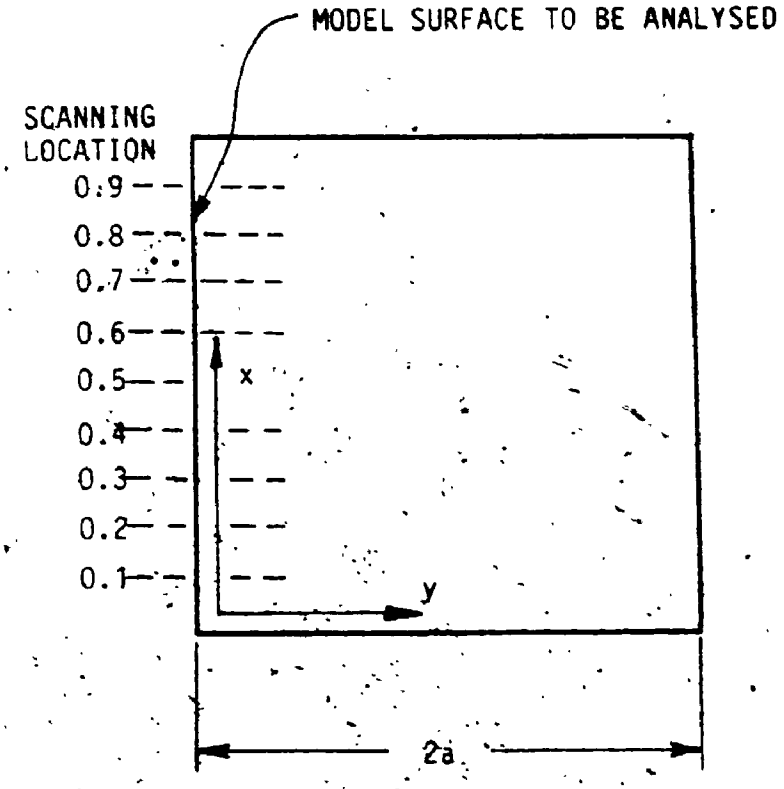

Figure 3.1 Analysis of Isothermal Square Duct Interferogram.

model surface $(\frac{\partial \varepsilon}{\partial y}|_s)$.

4) Using (3.10), calculate three estimates for the local Nusselt number, averaged along the test beam, based on these three estimates of the fringe shift derivative. These estimates differed by less than 2% for most of the scanning locations, with differences up to 19% at scanning locations 0.1 and 0.9 where only three fringes were present in a linear portion of the temperature field.

5) Repeat steps 2) through 4) for the scanning locations 0.2 to 0.9. Three estimates of the average Nusselt number were obtained by numerically integrating in the x direction the Nusselt numbers from step 4). The interferometer integrates the local Nusselt number in the z direction while the x direction integration must be done numerically. These three average Nusselt number estimates typically differed by less than 2%.

A personal computer was used for these calculations, as well as to provide plots of the fringe shift versus distance from the model surface as the fringe locations were being measured. The computer program to accomplish this task has been included in appendix C. This program was written in BASIC.

To obtain accurate heat transfer results, the experimental temperature difference T_s-T_∞ was selected so a large number of fringes, from 15 to 25, were on the interferogram. As a result, the first five fringes next to the surface were in a nearly linear portion of the fringe shift versus distance plot. A best-fit straight line through these fringes then yielded an accurate representation for the fringe shift derivative at the surface.

3.5 Application to Other Geometries

Several cases are discussed in this section where three-dimensional secondary effects are considered for nominally two-dimensional flows. The technique developed in the previous section can be used to study these flows. These cases are two-dimensional end effects, flow above horizontal heated surfaces or within horizontal and inclined rectangular cavities, and quasi-two dimensional turbulent flows.

The type of end effect considered here is that of an optical window placed at each end of a horizontal model as shown in figure 3.2. The flow within the model is two dimensional, with the exception of the ends because of the no-slip velocity boundary condition on the optical window. Since the velocity field is affected, the temperature field and the heat transfer rates near the model ends are also affected. The refractive index field and the temperature field is three-dimensional near the optical windows.

The interferometer integrates the local Nusselt numbers in the test beam direction. These test beam averaged Nusselt numbers are the correct Nusselt numbers for a particular model. The end effects are not an error in measuring the heat transfer rates for a model, but rather a discrepancy between the heat transfer rates for a model and the heat transfer rates for the idealized two dimensional case.

For flow above horizontal heated surfaces or within horizontal rectangular cavities, thermals of warm air break away from the region near the heated surface. These thermals result in temperature variations along the test beam. For horizontal heated

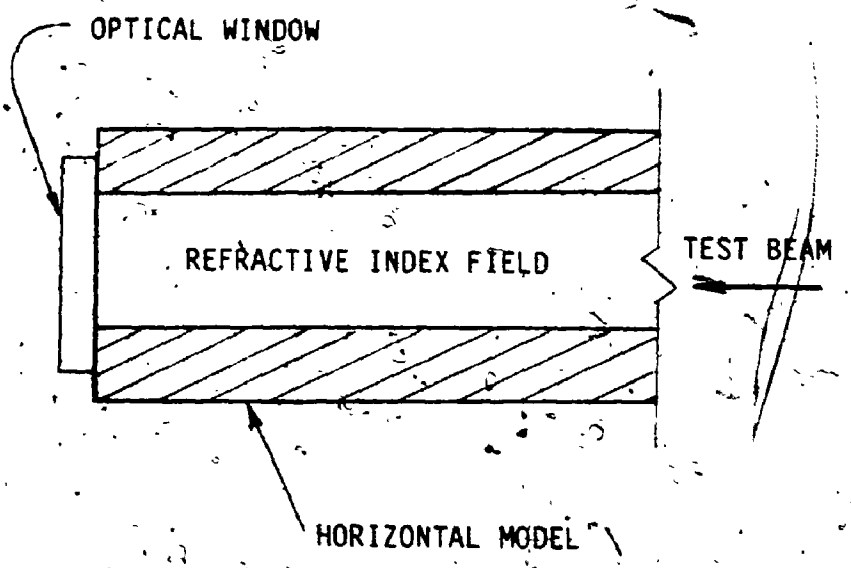

Figure 3.2 Optical Window End Effect

cavities, Benard cells may form, and end effects due to optical windows are present. In order to validate any interferometrically obtained, test beam averaged temperature profiles it would be necessary to estimate the magnitude of the truncated term in (3.6).

These same arguments apply for the study of turbulent convection in horizontal rectangular cavities using a Mach-Zehnder interferometer [32,33]. In this case the refractive index field is averaged along the test beam, as well as averaged in time. This time averaging is accomplished by using low sensitivity film and keeping the camera shutter open for about 60s. The test beam averaged Nusselt numbers can be obtained using (3.10).

For inclined rectangular cavities heated from below, for a particular Rayleigh number range, longitudinal rolls form. The interferometer arrangement described in this thesis could be used to integrate in the direction of these rolls and obtain information that has not been obtained previously.

In practice, it is not possible for a flow to be perfectly two dimensional because of end effects, or unsteadiness. A systematic error is present when two dimensional theory is employed to obtain test beam averaged temperature fields from an interferogram. These errors are greatest when large variations of the fluid temperature occur along the test beam, which is the case for three dimensional flows. Using the technique described in this chapter, it is possible to obtain accurate test beam averaged Nusselt numbers, in spite of any three dimensional variations of the refractive index field.

3.6 Summary of Fringe Analysis Technique

The technique described in this chapter for obtaining test-beam averaged heat transfer rates can be used in heat transfer studies where the flow under investigation is not two dimensional, and the fluid temperature is not constant in the direction the interferometer test beam traverses. The only restriction is the model surface temperature must be constant in the test beam direction.

The derivative of the fringe shift field normal to the model surface is proportional to the test beam averaged heat transfer rates. The accuracy of this technique is limited by the accuracy in obtaining the fringe shift derivative. Note that the accuracy in obtaining heat transfer rates for two dimensional flows is limited by the accuracy in measuring the derivative of the temperature normal to the model surface.

CHAPTER 4

EXPERIMENTAL APPARATUS

4.1 Experimental Arrangement

To measure the heat transfer from inclined geometries, a Mach-Zehnder interferometer was designed such that the optics lie in the same vertical plane, and the test beam lies in an inclined direction within this vertical plane. By shifting the optics on the lower support, δ, the angle of inclination of the test beam from the vertical can be adjusted from zero to about 48°. For the inclined ducts studied in this paper, the angle was δ=45°. Photographs of the interferometer for the vertical and inclined cases are shown in figures 4.1 and 4.2 . A schematic diagram of the vertical test-beam interferometer arangement is given in figure 4.1b .

Considerable thought was given in designing the interferometer structure or frame such that the fnterferometer would be insensitive to vibrations. The floor on which the interferometer is resting can have low frequency (less than 10 Hz) vibrations due to large vehicles passing by the building, or various activities within the building. It was also important that the structure was sufficiently rigid so the interferometer would not drift or settle from the correct alignment as the experiment was taking place.

The structure was made from 10cmx10cm, 6.4mm thick and 10cmx20cm, 6.4mm thick square stainless steel tubing (4"x4"x1/4" thick, and 4"x8"x1/4" thick). This tubing was bolted together using $\frac{1}{2}$" threaded rod. The overall length of the structure was 4.3m. Appropriate cross-bracing was used to stiffen the structure.

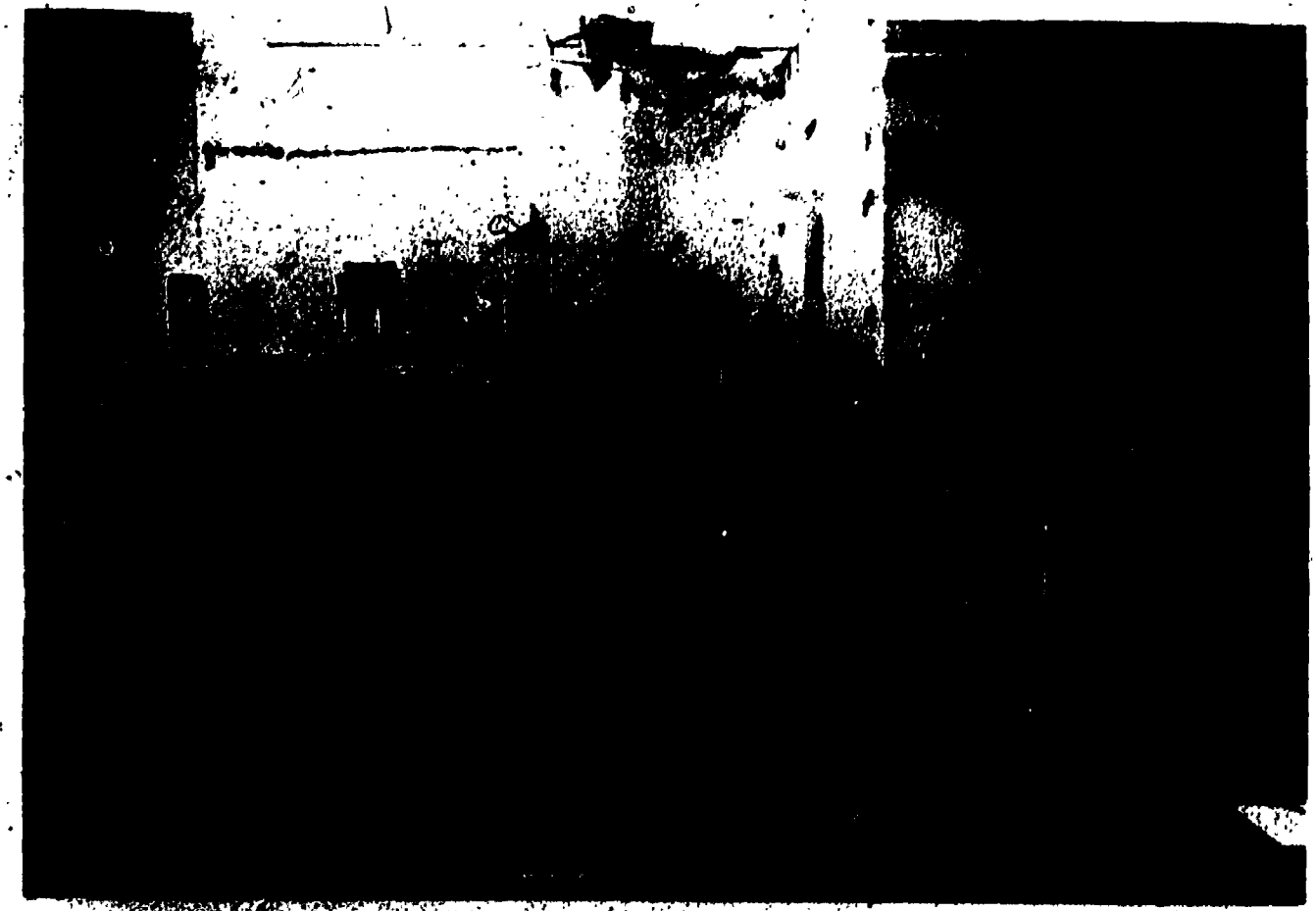

Figure 4.1 Interferometer Arrangement with Vertical Test Beam

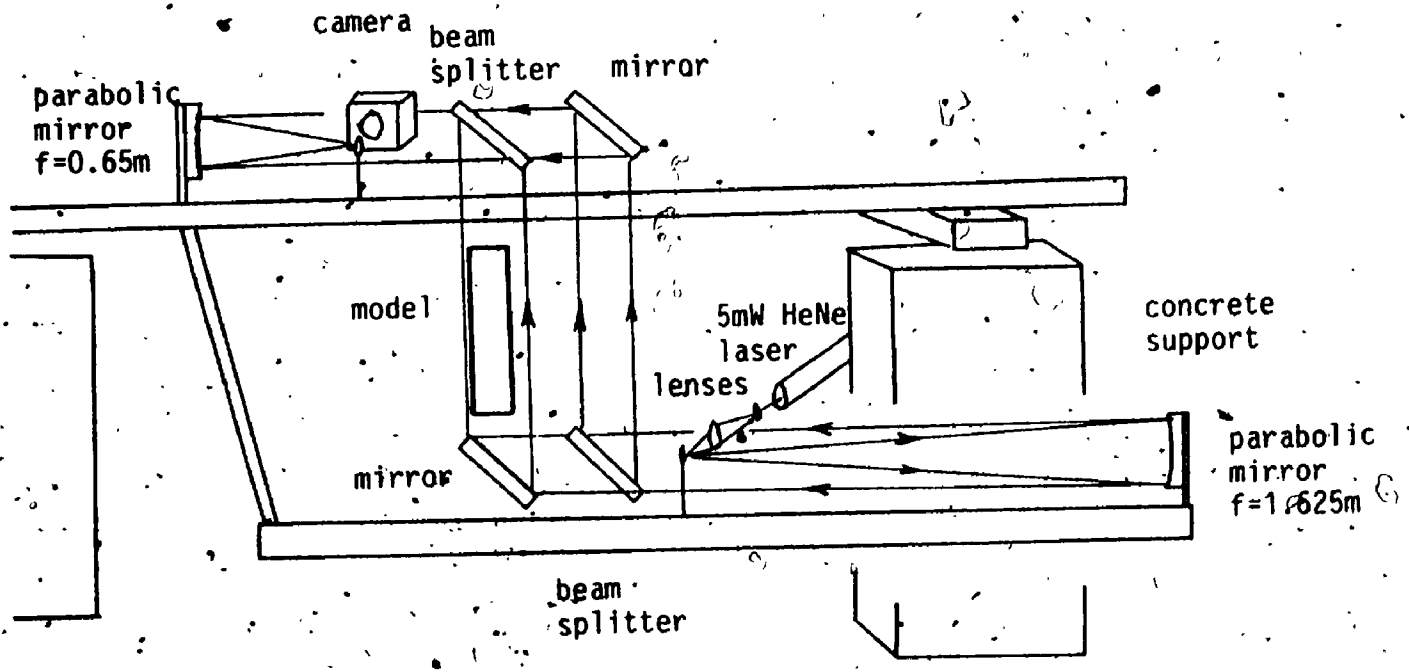

Figure 4.1b Schematic of Vertical Test Beam Interferometer

Figure 4.2 Interferometer Arrangement with Inclined Test Beam

Three concrete block columns were used to support the structure in a tripod arrangement. Air bags were used to decouple the structure from the columns. The interferometer centre of gravity was approximately the same height as the air bag supports, so no moments occur which would increase the time required for the vibrations to die out should the interferometer be bumped inadvertently.

On the lower right of the interferometer is a 5mW HeNe laser, as well as some optics for expanding the laser output to a 20cm diameter beam. In the centre is the interferometer parallelogram, where this 20cm beam is split into the test beam which passes through the model, and the reference beam which passes through the ambient air, and is finally re-combined. On the upper left is an arrangement for focusing, reducing, and photographing the interferometer output. Not shown in these photographs is a plastic sheet enclosure used to reduce velocity disturbances in the ambient air which can affect the natural convective flow at the duct entrance and exit.

A pleasant circumstance of the optics lying in a single, vertical plane is these optics are within reach of the operator. With interferometer arrangements where the optics lie in a horizontal plane, the operator must repeatedly move from one side to the opposite side to align the interferometer. The present interferometer can be aligned faster and more easily.

Polaroid land film type 55/positive-negative was used to record the interferometer output. The resulting photograph is called an interferogram. This film has a high resolution (4μm) negative, from

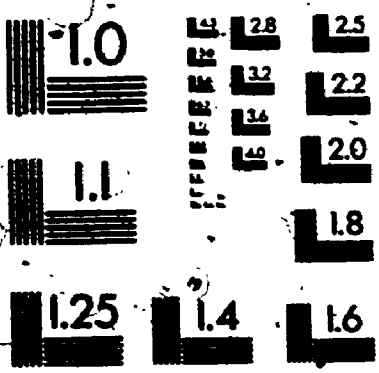

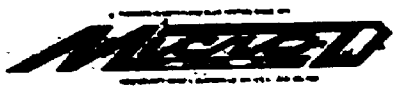

which the fringe locations were measured.

The model surface temperatures, as well as the ambient temperature, was measured and recorded by a DORIC DIGITREND 220 data logger. Twenty four gauge Copper Constantan thermocouples were employed. The resolution of the data logger was 0.1°C, and the error in measuring the temperature difference T_s-T_∞ was also 0.1°C. The absolute error in the temperature measurements was approximately 0.3°C.

4.2 Validation of Interferometric Arrangement

The interferometer arrangement was first employed to measure the number of fringes next to an inclined aluminum plate with the heated surface facing downward. The ambient fluid was air at room temperature. The plate was 60cm long and 7.5cm wide. Thermocouples were used to record the surface and ambient temperatures. The plate was inclined 45°, with the interferometer test beam traversing the plate along its length.

The interferometer was adjusted to the infinite fringe condition. Three interferograms were photographed with the plate heated 33.7, 27.8 and 21.1° above room temperature. The fringes were counted and compared with the number of fringes one should obtain theoretically. ($\epsilon_* = \frac{1.5 P}{\lambda} \frac{1}{R} K_{gd} \left(\frac{1}{T_\infty} - \frac{1}{T_s}\right)$). Agreement was excellent. The largest discrepancy was 2%.

Based on these results, the use of an interferometer for integrating refractive index fields in a direction which is not horizontal is perfectly valid. Any stratification, or variation in

the vertical direction of the ambient air temperature and pressure does not affect the interferometer operation when the test beam traverses in a non-horizontal direction. For the purpose of analysing the interferograms, a mean ambient temperature and pressure can be used.

4.3 Square Duct Model

There were several factors to consider in selecting the square duct dimensions as well as operating temperature for the experiments considered. Since only one fluid, namely air was employed in the experiments, the variation of the fluid refractive index with temperature was fixed. It was necessary to find an ideal balance between model length and temperature difference to yield 15-25 fringes for accurate fringe shift derivative measurements, while minimizing other errors such as refraction of the test beam as it passes through the model, mis-alignment of the model with the test beam, and the influence of the plume leaving the model exit on the interferogram.

In the present study a square duct model was constructed so the duct width could be varied arbitrarily from zero to 5cm. An end view of the duct is shown in figure 4.3 . A large range of Ra was thus studied by varing the duct width while keeping the temperature difference and the duct length at their optimum values for an interferometric study. The duct length was 60cm, and each surface was machined flat to ±0.1mm and polished.

The temperature difference T_s-T_∞ was maintained at 55°C for

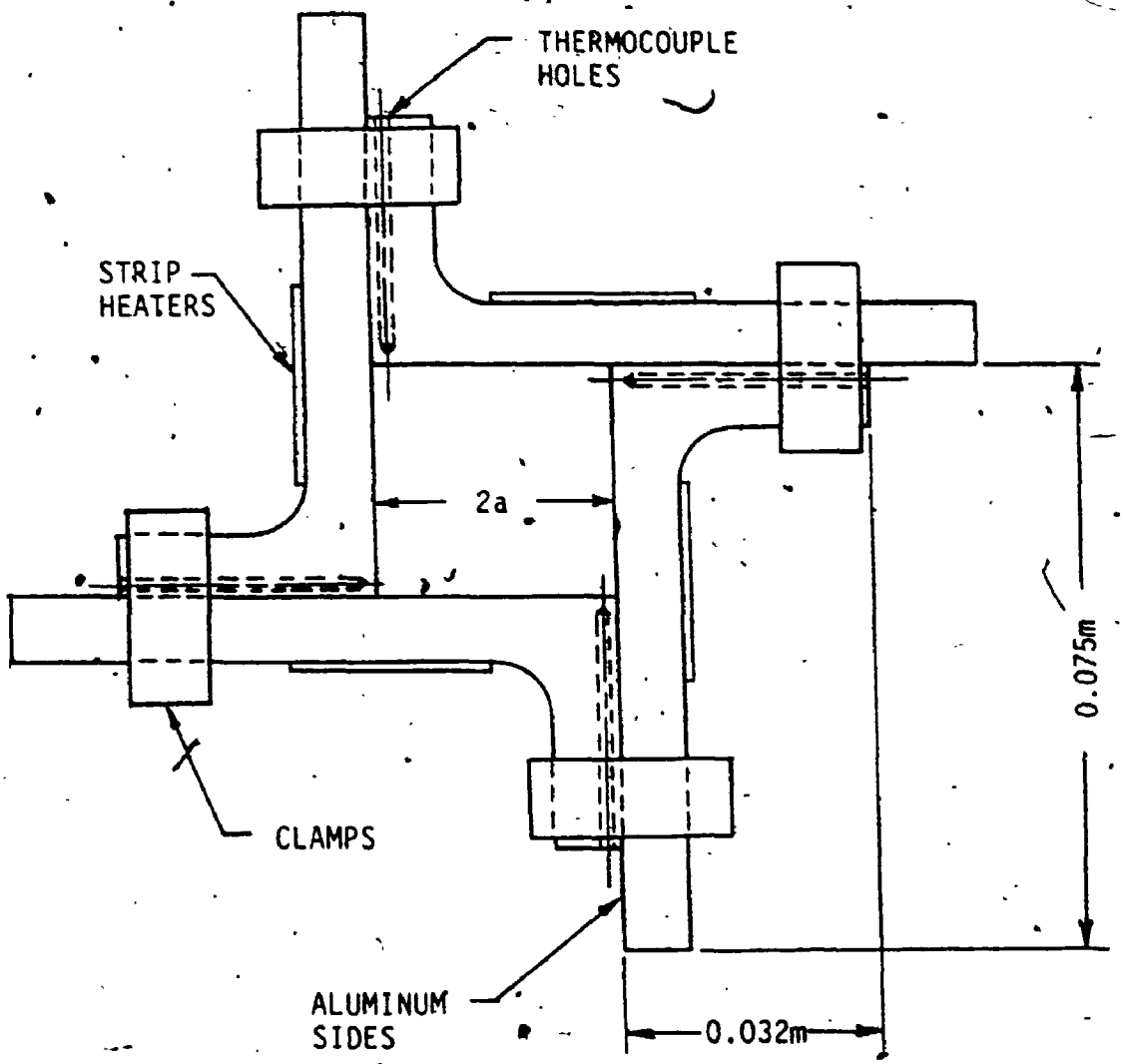

Figure 4.3 Isothermal Square Duct End View

Ra=10 and 35°C for the other values of Rayleigh number using a temperature controller connected in parallel with the strip heaters. The surface temperature was measured at five locations along the duct length, for each of the four duct surfaces. Holes were drilled in the sides to within 1mm of the duct surface. The thermocouples were then coated with a thermal conducting paste and inserted in each of these holes.

Four strip heaters were glued to the duct surfaces. These strip heaters were connected in series, and a direct current of up to four amperes was applied to heat the model. The resistance of each strip heater was 8.5Ω. The power supply was operated in a constant current mode. With this heating arrangement, the surface temperature difference was found to vary ±6% over the duct length.

A balsa wood bellmouth was placed at the duct entrance. The purpose of this was to reduce any preheating of the air before it entered the duct. The Bellmouth radius was 10mm. At the duct exit a balsa wood plate 15cmx15cmx8mm thick was installed with a square opening corresponding to the duct cross-section. The edges of this opening were rounded to act as a bellmouth, although the primary function of this plate was to deflect any warm air rising from the outside of the model, outside of the test beam.

For the vertical square duct experiments, in addition to this balsa wood plate, an optical window was mounted on an aluminum plate at a certain distance away from the duct exit. As the warm air leaves the duct exit, it forms a rising plume which strikes the optical window, then is deflected sideways by the aluminum plate

away from the interferometer test beam. Figure 4.4 contains a close-up of the duct exit, showing the optical window and its holder, as well as the aluminum plume guide. A fibreglass insulating layer was removed from the outside of the duct to make the duct outside and the strip heaters visible. The distance from the optical window to the duct exit was increased until the average heat transfer rate from the duct did not vary. This distance was found to be about 30mm. This was to ensure that the presence of the optical window did not restrict the flow through the duct.

4.4 Experimental Procedure for Square Duct Model

For the natural convective developing duct flow experiments, the interferometer was first arranged with the test beam vertical for the vertical duct experiments, or inclined 45° from the vertical for the inclined duct experiments.

The desired model width was calculated using the BASIC program included in appendix B. The problem is: given the model length l, orientation δ, and surface temperature T_s, the ambient temperature T_∞ and pressure p_∞, and the air properties, calculate the model width (2a) to obtain the desired Rayleigh number (Ra). The program RA.BAS interpolates for the air properties and then calculates the model width to use. The reference temperature at which the air properties were calculated was $T_f = \frac{1}{2}(T_s+T_\infty)$.

The next step was to adjust the square duct dimensions in the X and Y directions. This task was a matter of trial and testing. The clamps at the duct ends (see figure 4.3) were loosened and the duct

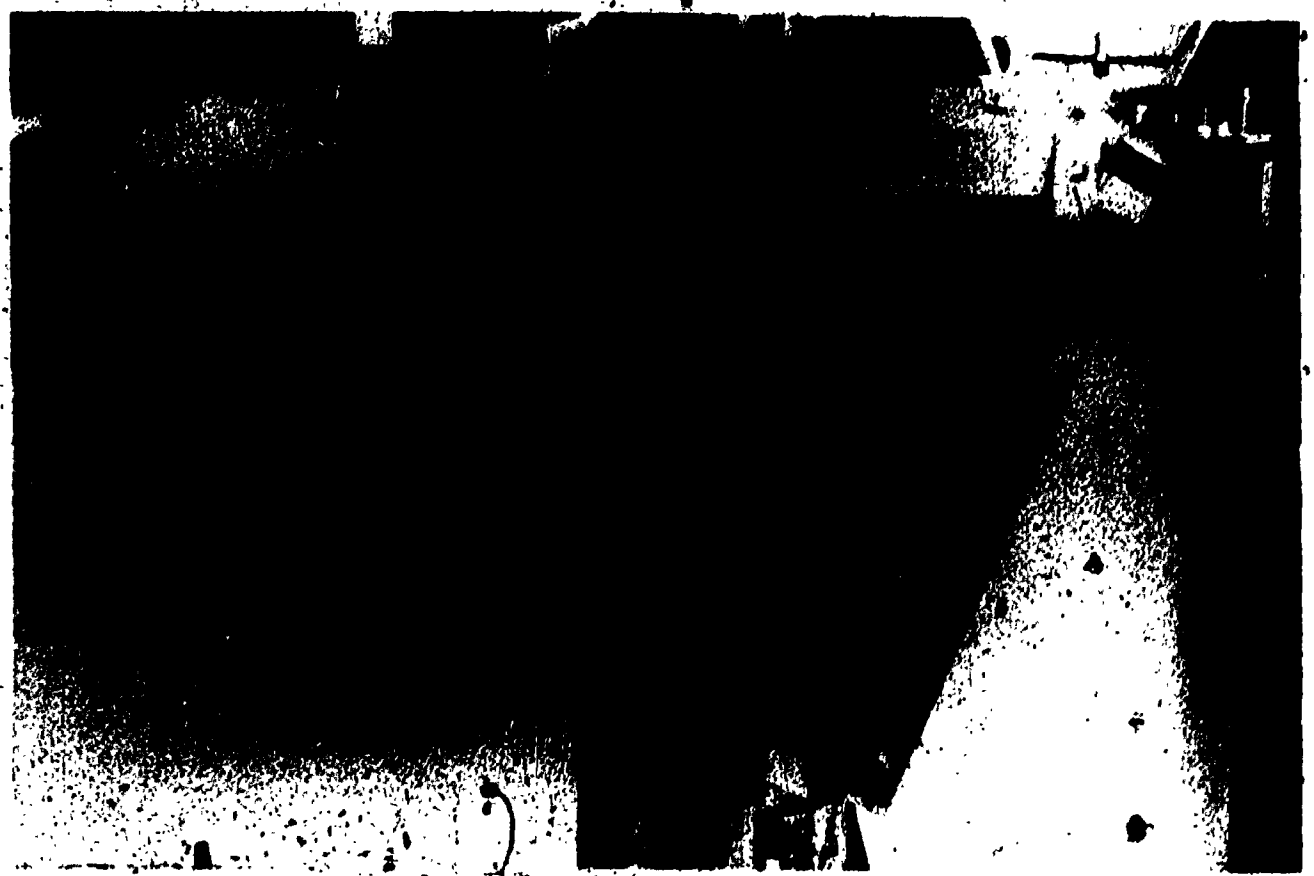

Figure 4.4 Vertical Square Duct Exit

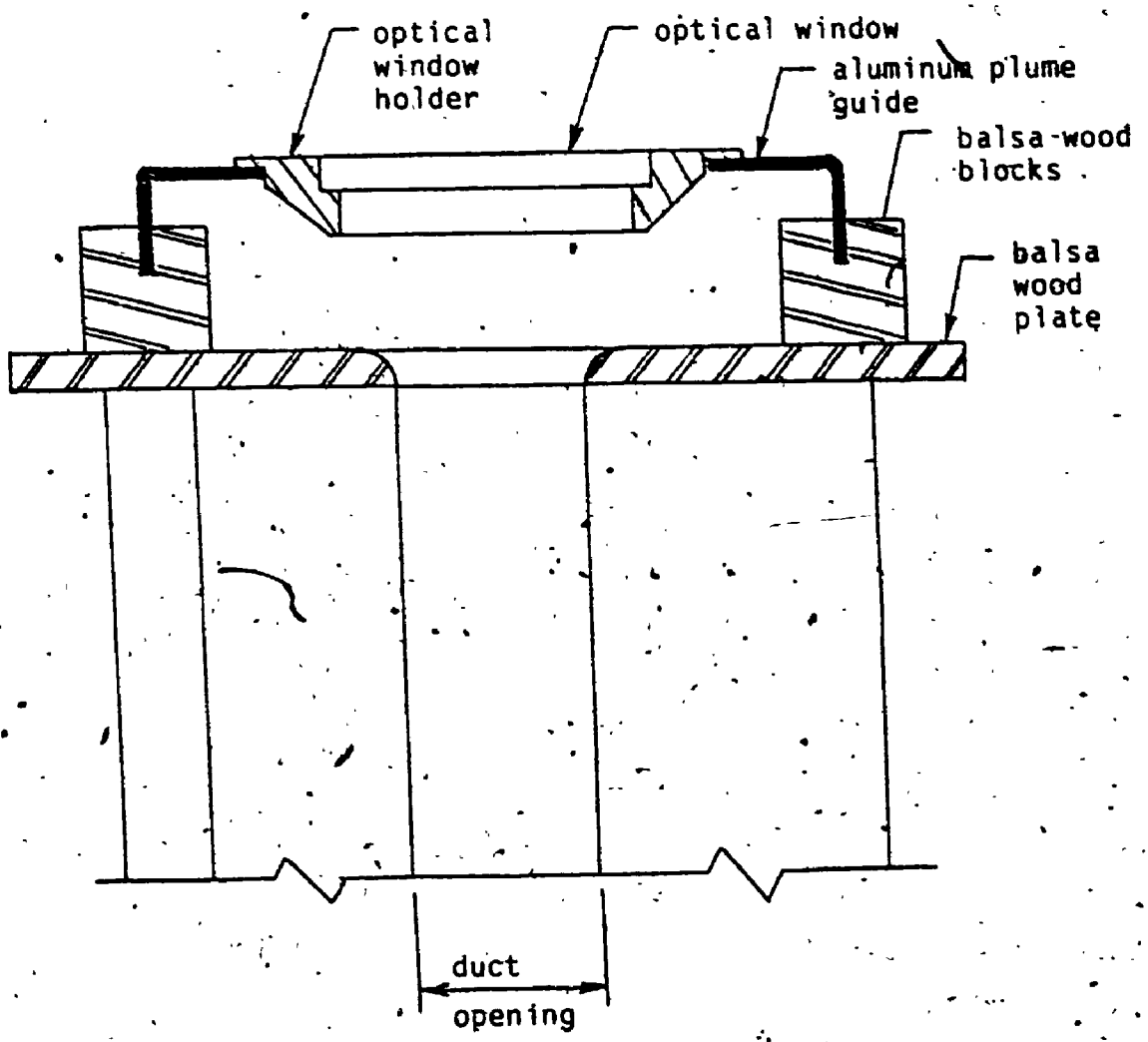

Figure 4.4b Schematic of Vertical Square Duct Exit

width was adjusted using finger pressure. The clamps were tightened and the new duct width was measured using a vernier micrometer. This process was repeated until the duct widths were the desired value. A high degree of accuracy could be achieved in this manner, the standard deviation of the duct widths about the mean value was typically 0.002mm, or 0.1%, with the mean width ranging from 13mm to 49mm. A balsa wood bellmouth was then constructed and glued to the duct entrance, and a balsa wood plate was fitted to the duct exit.

The model with the desired dimensions was then installed in the interferometer, covered with a fibreglass insulative layer, and aligned parallel with the test beam. For the vertical duct experiments, the optical window holder and aluminum plume guide were also set in place.

There were three feedback mechanisms to align the model. The unheated model was aligned to eliminate any reflections of the test beam from the duct inner surfaces. The model support provided both coarse and fine adjustments for the model orientation. A Bristol board screen was placed just after the duct exit to observe these reflections. When no reflections were present the model was parallel to the test beam. A way of checking this alignment was to observe diffraction fringes on the screen caused by the test beam passing near the duct surfaces. A third way of checking the alignment was to measure the duct widths from the interferograms and check that the two measured widths are equal.

The room ventilation was shut off and the ambient air was

dehumidified before an experiment took place. Dehumidification was more important in the summer when the absolute humidity can be high, although the air refractive index is not sensitive to water vapour content.

For interferometric studies where the temperature field, or the refractive index field is uniform along the test beam, the recommended procedure for minimizing refraction error on the interferogram is to focus the camera two thirds along the model. In the present study, where the largest refractive index gradients occur near the duct entrance, it was necessary to focus the camera closer to the entrance. This was particularly true for Ra=10 where a temperature difference of 55°C was necessary to achieve enough fringes for heat transfer measurements.

The interferometer was set to the infinite fringe condition, with no interference fringes present for the unheated model. The model was then heated by applying a DC current to the strip heaters. The temperature controller was set to the desired model temperature. This controller operates by shorting out the strip heaters when the model temperature exceeds the set point temperature. When this occurs, the current passes through the controller, rather than through the heaters.

Once the model reached the desired temperature, the interferometer output was photographed to yield an interferogram. This photograph was taken when the fringes were stationary, and were not disturbed by velocity fluctuations in the ambient air. The model and ambient temperatures were then recorded using the data

logger. The ambient pressure was read from a barometer.

The range of experimental parameters used in the present set of experiments is listed in table 4.1 .. Vertical square ducts were studied for Ra=10,31,100 and 316. Inclined square ducts were studied with δ=45° for Ra=10,31,100,316 and 1000. The corresponding cross-plane Rayleigh numbers are Ra_{cr}=872,1811,4482,10299 and 23572. Further details on each experiment is included in the next chapter with the description of the experimental results.

Table 4.1 Range of Experimental Parameters.

variable	description
duct length l	60.0 cm
inclination angle	0° and 45°±1° from vertical
duct width 2a	12.9- 48.9mm
T_s-T_∞	31.1-56.3°C
Ra	10.3-309.5 (δ=0°) 10.1-961 (δ=45°)
Ra_{cr}	0 (δ=0°) 872-23600 (δ=45°)

CHAPTER 5

EXPERIMENTAL RESULTS

5.1 Overview of Experimental Results

Four experiments for vertical square ducts and five for inclined square ducts were conducted for various Rayleigh numbers. The experimental variables for both the vertical and inclined square ducts are given in table 5.1 .

The fringe locations were measured from the resulting interferograms using a measuring microscope, as described in section 3.4 . A program for reading in the raw data, analysing this data, and displaying the final results graphically is given in appendix C. The output file for this program, for the particular experiment with Ra=10 and δ=45° is included in appendix D. This file contains both the raw data and the calculated results.

5.2 Interferograms for Vertical and Inclined Square Ducts

Interferograms for the vertical square duct experiments are shown in figures 5.1a-d. Each interferogram is qualitatively the same in that there is a centrally located core region, and the fringe shift field exhibits symmetry.

For the inclined duct interferograms, the influence of cross-plane motion on the fringes is apparent, as indicated in figures 5.2a-e. The effect of the two rolls is particularly strong for the larger Rayleigh numbers. The core region is shifted down

Table 5.1 Experimental Parameters for Vertical and Inclined Square Duct Measurements.

Ra	Ra_{cr}	δ	2a	T_s	T_∞	P_∞
10.28		0.0	0.012880	78.73	22.40	99820
32.61		0.0	0.018928	55.29	22.25	98650
101.0		0.0	0.025548	53.82	22.75	97920
309.5		0.0	0.032173	63.23	22.60	97790
10.10	872	45.0	0.013903	85.34	23.30	98800
29.49	1811	45.0	0.019538	62.07	23.25	99390
99.7	4482	45.0	0.026705	61.57	23.45	98630
319.9	10299	45.0	0.037273	50.31	21.85	100070
960.9	23572	45.0	0.048948	53.90	23.55	99340

Table 5.2 Measured Fringe Shift from Surface to Core.

Ra	Ra_{cr}	L=1/Ra	ϵ_c	ϵ_{c*}	ϵ_c/ϵ_{c*}
10.28		0.097	12.9	40.29	0.32
32.61		0.031	14.9	25.03	0.60
101.0		0.0099	19.3	23.43	0.82
309.5		0.0032	28.5	29.76	0.96
10.10	872	0.099	14.3	42.98	0.33
29.49	1811	0.034	12.9	28.81	0.45
99.7	4482	0.0100	17.7	28.10	0.63
319.9	10299	0.0031	18.0	22.15	0.81
960.9	23572	0.00104	21.8	23.05	0.95

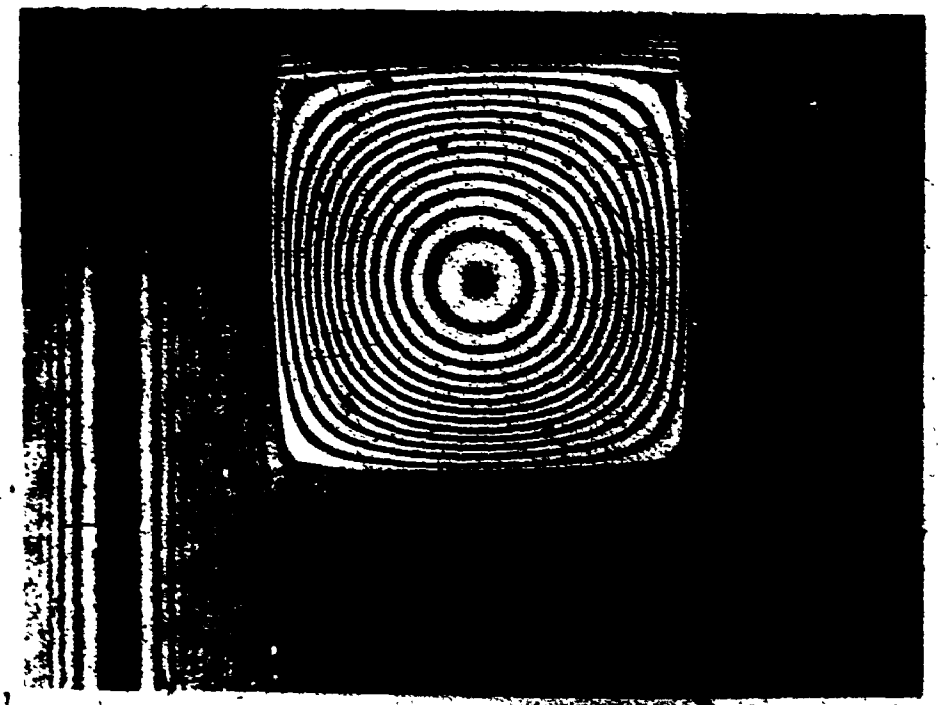

5.1a) Ra= 10.28

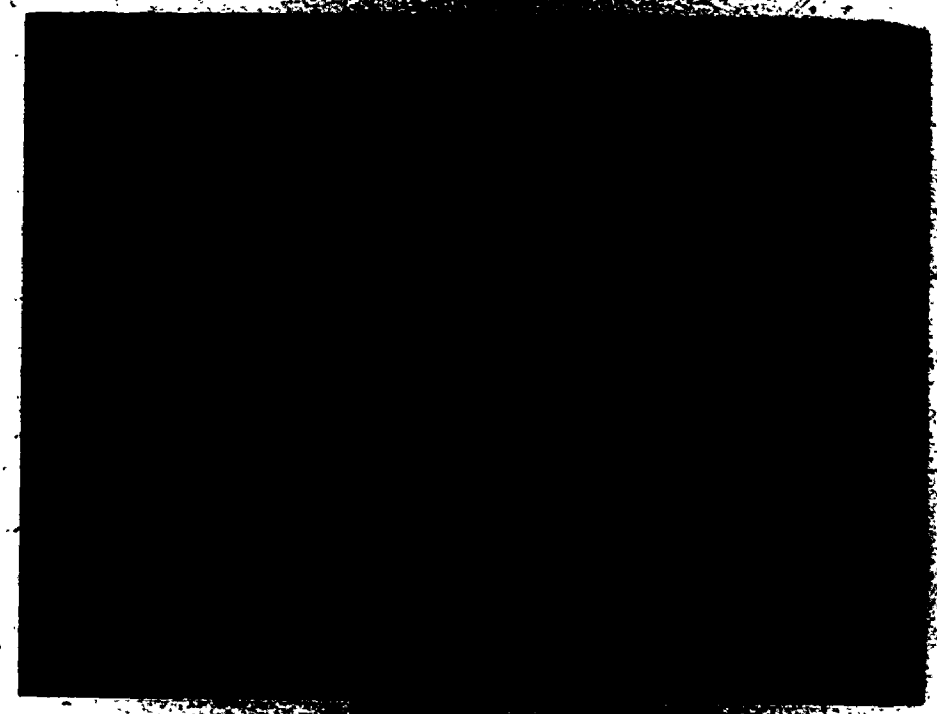

5.1b)

Figure 5.1 Interferograms of Vertical Isothermal Square Ducts.

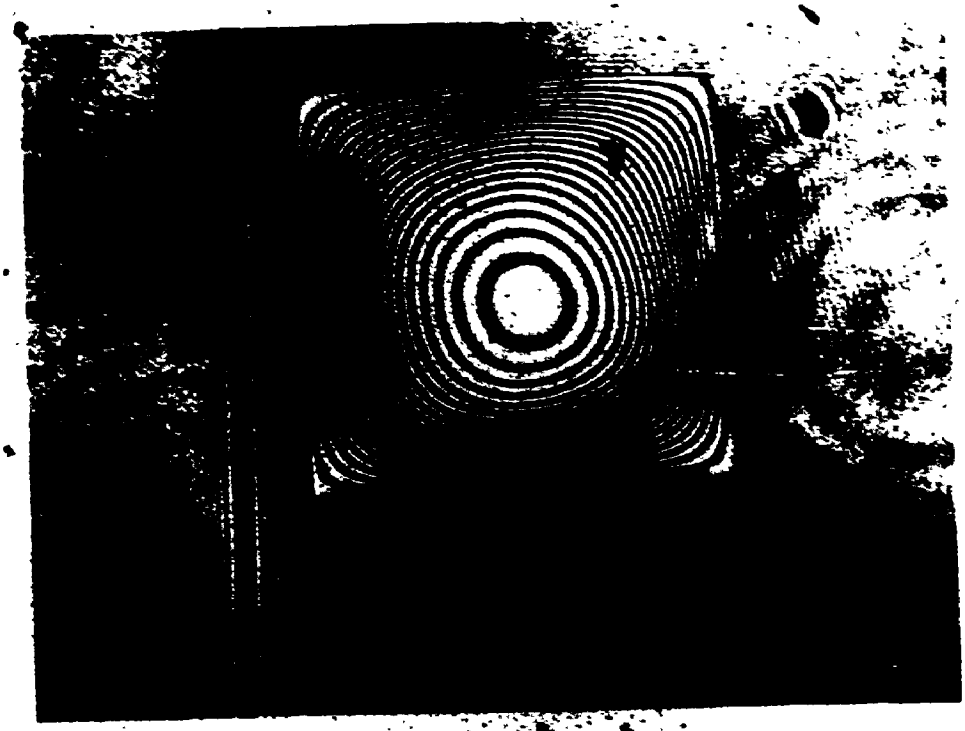

5.1c) Ra= 101.0

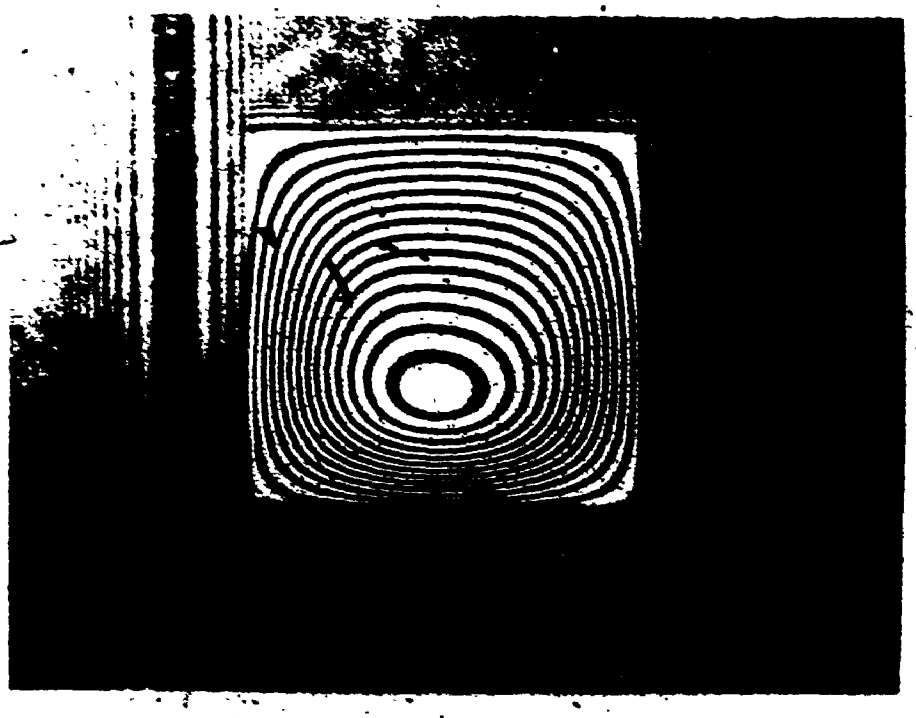

5.2a) $Ra = 10.10$ $Ra_{cr} = 872$

5.2b) [illegible]

Figure 5.2 Interferograms of Inclined Isothermal Square Ducts.

5.2c) Ra= 99.7 Racr= 4482

5.2d) Ra= 318.3 Racr= 10299

5.2e) Ra_i= 960.9 Ra_{cr}= 23572

and the fringes on the top area of the interferograms are deflected toward the lower surface as a result of this convection.

The primary difference between each of the vertical duct interferograms is that for a given temperature difference there are fewer fringes for Ra=10 than for the higher Rayleigh number interferograms. For this Rayleigh number the bulk air temperature has essentially reached that of the duct surface after the first 0.15m. Most of the refractive index and temperature variations occur in this developing region of the vertical and inclined ducts. Since the interferometer responds to refractive index variations, fewer fringes are present for lower Rayleigh numbers.

The number of fringes from the surface to the core region on each interferogram were counted, and compared with the number of fringes which would be present if the air temperature at the duct core was T_∞. The results are shown in table 5.2 . This theoretical number ε_{c*} is the maximum number that would occur, and is approached by the measured number of fringes in the limit $Ra \to \infty$. Note the ratio $\varepsilon_c/\varepsilon_{c*}$ approaches unity in this limit.

Previous investigators such as Dyer [7] studying developing natural convective flow in vertical isothermal tubes have defined a dimensionless duct length as $L=1/Ra$. The fully developed regime was specified by $L>1$ and the boundary layer regime by $L<0.0001$. The corresponding regimes for vertical square ducts as indicated by Ramakrishna [14,15] are $L>1$ for the fully developed regime and $L<0.001$ for the boundary layer regime. These regimes indicate where the average Nusselt numbers differ significantly (1%) from the

asymptotic solutions for the limits of small and large L. All the experiments of the present study fall in an intermediate regime with $0.0001<L<1$, as indicated in table 5.2 . For small L, most of the temperature variations occur near the duct walls, and the fluid near the duct centerline does not heat significantly. As a result, the ratio $\varepsilon_C/\varepsilon_{C*}$ is close to one.

5.3 Heat Transfer Rates

The test beam averaged Nusselt numbers have been plotted versus location on the duct periphery in figure 5.3 for the vertical ducts and in figure 5.4 for the inclined ducts investigated. The average heat transfer rates for each of the vertical duct surfaces are approximately the same. Any asymmetry is caused by disturbances in the ambient air entering the duct. These disturbances have a more significant effect for the larger Rayleigh numbers where the duct is wider.

The average heat transfer rates for each of the inclined duct surfaces are given in table 5.3 . The heat transfer rates for the lower surface are from 2 to 2.7 times as large as those for the upper surface.

The average Nusselt numbers for the vertical and inclined square ducts are shown in figure 5.5 . The average heat transfer rates for the inclined ducts were 5% higher than the corresponding heat transfer rates measured for vertical square ducts. This difference is within the range of uncertainty of the measurements, and could be ignored for most design calculations. The average heat transfer

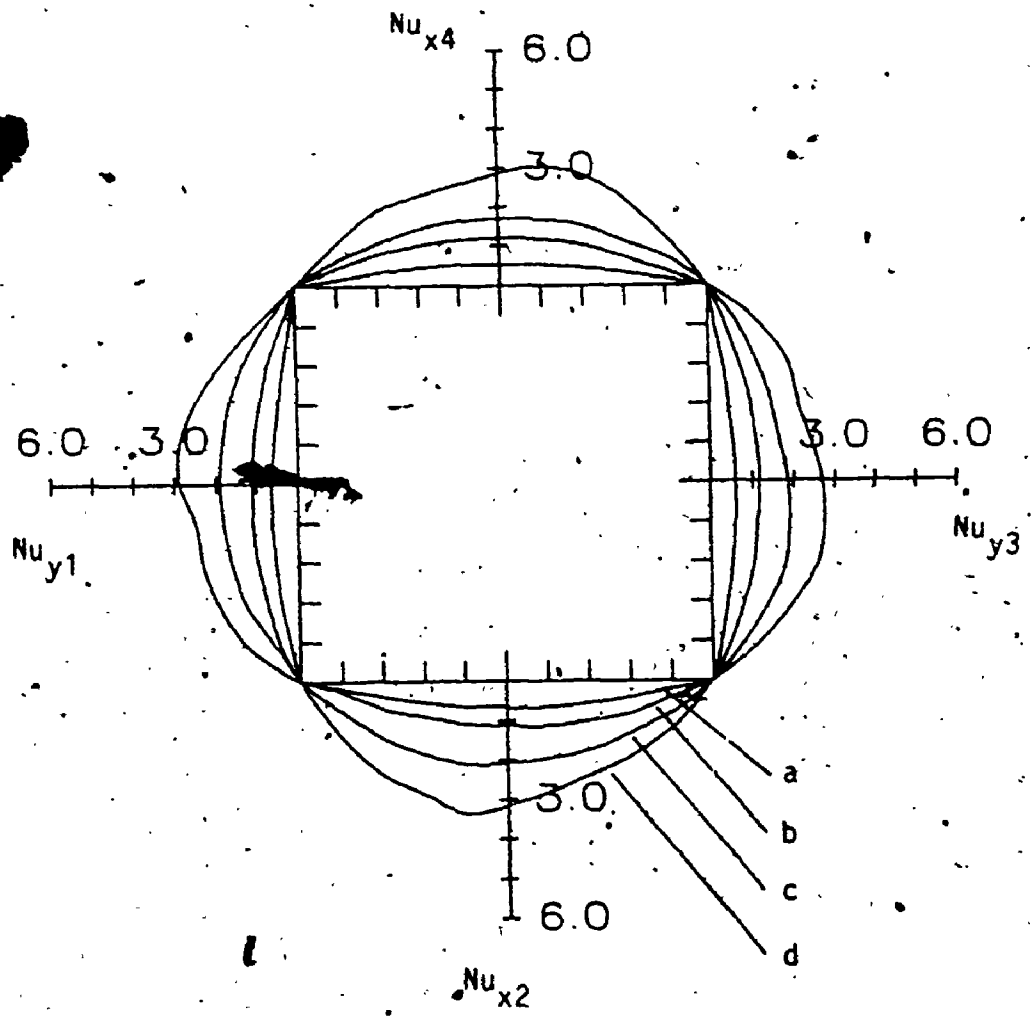

Figure 5.3 Test Beam Averaged Nusselt Numbers for Vertical Isothermal Square Ducts.
curve a: Ra=10.3 b: Ra=32.6
c: Ra=101. d: Ra=309.

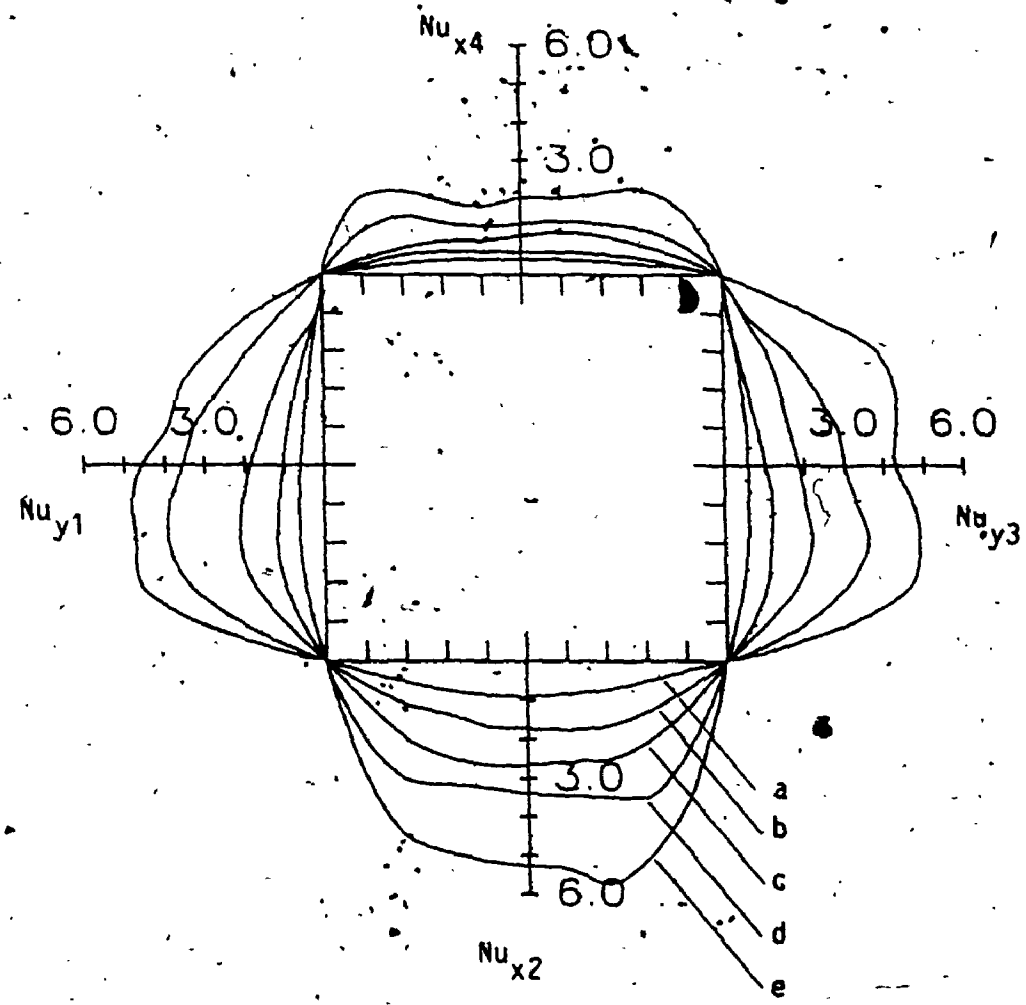

Figure 5.4 Test Beam Averaged Nusselt Numbers for Inclined Isothermal Square Ducts.
curve a: Ra=10.1 Ra_{cr}=872.
b: Ra=29.5 Ra_{cr}=1810.
c: Ra=99.7 Ra_{cr}=4480.
d: Ra=329. Ra_{cr}=10300.
e: Ra=961. Ra_{cr}=23600.

Table 5.3 Average Heat Transfer Rates for Each Inclined Square Duct Surface.

		Nu			
Ra	Ra_{cr}	upper	sides	lower	ave.
10.099	872	0.285	0.395	0.565	0.410
29.485	1811	0.444	0.715	1.195	0.767
99.733	4482	0.727	1.308	1.924	1.317
319.888	10299	1.136	2.404	2.766	2.177
960.858	23572	1.807	3.529	4.272	3.284

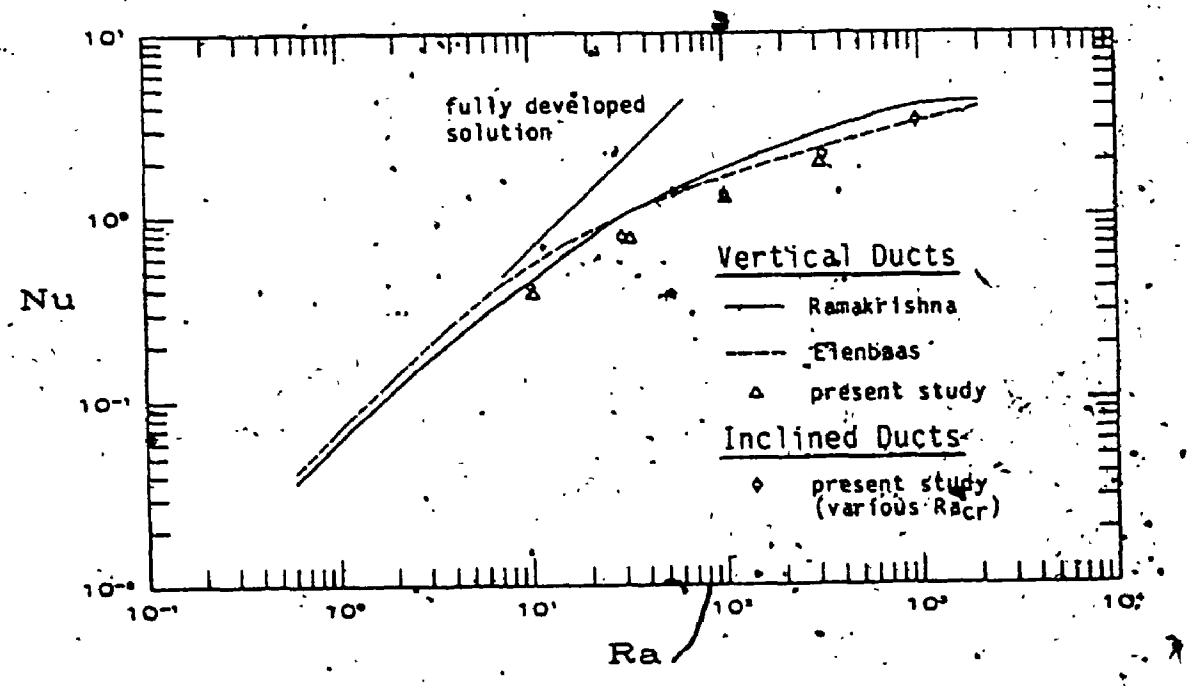

Figure 5.5 Average Nusselt Numbers for Vertical and Inclined Isothermal Square Ducts.

rates for the vertical ducts could be used for inclined ducts, for the range of Rayleigh number considered here.

Also included in figure 5.5 are numerical solution of Ramakrishna [14,15] and the combined analytical-experimental solution of Elenbass [6] for vertical square ducts. This solution is given by the following equation

$$Nu = \frac{Ra}{14.225}\left[1 - e^{-14.225\left(\frac{0.5}{Ra}\right)^{0.75}}\right] \qquad (5.1)$$

The measured average Nusselt numbers are lower (typically 8%) than these results for two possible reasons. The first reason is the air may have been preheated before entering the duct and the air refractive index variation across the duct will then be reduced. The balsa wood bellmouth at the duct entrance was heated since it was in contact with the aluminum duct sides, which would then cause the air to be preheated. Ideally, the entrance bellmouth should be maintained at the same temperature as the ambient air.

The second reason for the measured average Nusselt numbers to be lower than expected is the manner in which the heated air is treated after the duct exit. This warm air must be removed from the interferometer test beam. For the vertical ducts, the presence of the optical window may restrict the air flow through the duct. For the inclined ducts, the heated air leaves the exit, and a heated plume rises vertically. the interferometer test beam passes through part of this plume. Each of these errors are particular to interferometric studies of open-ended natural convective duct flows.

5.4 Discussion of Experimental Results

The most important point to note for these square duct flows is only two previous investigations were undertaken for vertical square ducts, and none for inclined square ducts. The results for the average heat transfer rates are not in close agreement, as indicated in figure 5.5. Ramakrishna's solution is 11% lower than that of Elenbaas in the limit of low Rayleigh number, and is higher for large Rayleigh number. Further numerical investigations are necessary to validate one or the other of these solutions. It is not obvious at present which solution is the best.

The solution of Ramakrishna for low Rayleigh number is not the same as an analytical solution in the limit of fully developed flow. For flow in vertical circular tubes, and in flow between vertical parallel plates, the corresponding analytical solutions for fully developed flow are widely accepted.

The present experimental results for average Nusselt number are about 8% lower than the results of these two investigators for vertical ducts. The results of primary importance in the present study are the variation of the test beam averaged Nusselt numbers along the duct periphery, and how these are influenced by incling the ducts.

CHAPTER 6

CONCLUSIONS

6.1 Overview

In this thesis, numerical and experimental studies were carried out on natural convection in vertical and inclined square ducts. Isothermal and differentially heated ducts were considered. The numerical and experimental studies undertaken were those considered feasible using existing computer and experimental facilities, and within time and budget requirements.

The accomplishments in this thesis in both the numerical and experimental studies are as follows:

1) The relevant parameters which specify inclined duct flows were established (Pr, Ra, Ra_{cr}, ζ).
2) The governing equations and appropriate boundary conditions for developing flow in isothermal and differentially heated open ended square ducts were derived (see sections 2.3, 2.6 and 2.7).
3) The feasibility of obtaining numerical solutions for inclined square ducts was examined. The solutions obtained in this thesis were for fully developed laminar flow in isothermal ducts, and fully developed laminar flow in differentially heated ducts. These solutions cover the entire laminar range.
4) An interferometric technique was developed for studying flow fields where the refractive index varies in the test beam direction. It was shown how the test beam averaged Nusselt numbers could be obtained with a high degree of accuracy.

The equation to calculate the heat transfer is given by;

$$\frac{1}{L}\int_0^L Nu\, dZ = \frac{1}{C}\left.\frac{\partial \varepsilon}{\partial Y}\right|_S \quad \text{where } C = \frac{1.5\ 1\ P\ Kgd\ (T_s - T_\infty)}{\lambda\ R\ \ T_s^2}$$

5) An interferometer system was constructed with the optics lying in a vertical plane, and the test beam traversing in a vertical, inclined or horizontal direction. This was believed to be the first interferometer used in heat transfer studies with the test beam traversing a heated model in a direction which was not horizontal.

6) Interferometric results were obtained for vertical and inclined, open ended square ducts. The ducts were isothermal, and heated to a temperature above that of the ambient fluid (air). This study was unique in that almost no information is available at present on natural convective flow in inclined ducts.

6.2 Summary of Numerical Study

In this section some important points concerning the numerical work in chapter 2 will be stated. These points will be related to the numerical objectives from section 6.1 .

The important parameters which specify the flow are the fluid Prandtl number Pr, the Rayleigh number Ra which indicates the flow development, and the cross-plane Rayleigh number Racr. A fourth parameter is required if axial-diffusion is significant in the flow. This effect was not considered significant for the range of experimental parameters in the present study, and was neglected in this thesis.

In deriving the governing equations for duct flows, the Rayleigh number Ra has a characteristic dimension of the duct half width 'a', while the cross-plane Rayleigh number has a characteristic dimension '2a'. This was done in this thesis for the results to be consistent with previous studies on isothermal duct flows employing the characteristic dimension 'a', and with previous studies on horizontal, differentially heated cavities which employ the characteristic dimension '2a', or the cavity width. The choice of either characteristic dimension is equally valid, and makes no difference in the final results other than to shift the value of the Rayleigh numbers or Nusselt numbers.

The applicable governing equations were discretized in such a way that they would yield an almost exact solution to the one-dimensional convection-diffusion problem. The resulting equations retain some diagonal dominance even for strong convective effects.

Solutions were obtained for fully developed flow in isothermal and differentially heated square ducts. These solutions were close agreement with existing solutions for isothermal ducts and horizontal, differentially heated cavities. In the limit of fully developed flow, the cross-plane results for inclined, differentially heated ducts are the same as the results for differentially heated horizontal cavities. There are no variations in the axial direction in either case. The new numerical results presented here are for the axial velocity for inclined, differentially heated ducts.

It is the opinion of the author that solutions could also be obtained, at a reasonable cost, using existing computing facilities,

for developing flow in isothermal ducts and differentially heated square ducts with small cross-plane Rayleigh numbers (up to 10^4).

6.3 Summary of Interferometric Study

In this section some important points concerning the experimental work in chapters 3-5 will be stated. These points will be related to the experimental objectives from section 6.1 .

It was shown in this thesis how accurate measurements of the test beam averaged Nusselt number can be made with a Mach-Zehnder interferometer, provided the model surface temperature is constant along the test beam. This study was unique in two respects; almost no information is available at present on natural convective flow in inclined ducts, and to the best of the authors' knowledge this is the first heat transfer study to employ an interferometer with the test beam traversing the heated model in a direction which was not horizontal.

The Nusselt numbers, averaged along the test beam, were shown to be directly proportional to the derivative of the fringe shift normal to the model surface. The heat transfer rates for three dimensional flows can be obtained, using the method outlined here, with the same accuracy as the heat transfer rates for two dimensional flows. This method is valid for any transparent fluid, liquid or gas, although the fluid was taken to be an ideal gas in this paper. The accuracy of the method is limited by the accuracy in calculating the derivative of the fringe shift normal to the model surface.

Results are presented for vertical and inclined square ducts. For inclined square ducts, for a given Prandtl number there are two dependent variables which specify the flow, Ra and Ra_{cr}. In the present study it was not feasible to study all possible combinations of these two variables, so only selected experimental measurements were obtained.

The average heat transfer rates for the inclined ducts were 5% higher than the corresponding heat transfer rates measured for vertical square ducts. This difference could be ignored for most design calculations.

The most significant effects of inclining the ducts are to cause two rolls to form in the developing length of the duct, and to reduce the heat transfer rates on the upper and increase those on the lower surface.

Natural convective developing flow in two other duct types were also looked at briefly, inclined isothermal circular tubes, and inclined differentially heated square ducts. For the circular tube geometry, a wide range of Rayleigh number could not be covered since it was not possible to vary the tube radius without constructing a number of models. This was not economically feasible. The results that were obtained are similar to the results for isothermal square ducts in that the average heat transfer results for the inclined tubes are close to those for the vertical tubes, and for inclined tubes, the heat transfer rates on the lower region of the tube surface are higher than those on the upper region.

Preliminary experiments on differentially heated horizontal cavities were unsuccessful because the upper and lower surfaces were not adiabatic. Balsa wood was used on these surfaces, and the resulting thermal boundary condition was a combination of a constant heat flux and a linear temperature variation. The interferograms were clearly different from what would expect from the idealized, adiabatic boundary condition.

Some of the material in this thesis has been presented at two conferences by the author. An abstract of the numerical work was presented at the CANCAM conference on July 1-4, 1987 in Edmonton, Alberta. A full paper of the experimental work was presented at the AIAA Thermophysics conference on July 8-10, 1987 in Oahu, Hawaii. The co-authors of each of these publications were M.L.C. Papple and J.D. Tarasuk.

APPENDIX A

FULLY DEVELOPED DIFFERENTIALLY HEATED DUCT

The following program, TS8, was used to solve the governing equations for fully developed flow in differentially heated, inclined square ducts. This program was written in FORTRAN 77. The finite difference grid used in the cross-plane was 80x80. The discretization method used in this program was that of a Taylor's series expansion of the numerator and denominator of the discretization factor. This program was typical of the programs used by the author to obtain the numerical solutions described in chapter 2 of this thesis.

```
      PROGRAM TS8(INPUT,OUTPUT,TAPE1=INPUT,TAPE2=OUTPUT)
C
C         FULLY DEVELOPED FLOW IN DIFFERENTIALLY HEATED
C         INCLINED SQUARE DUCTS.
C
C         Characteristic dimension - duct width.
C
C         GOVERNING EQUATIONS (steady, laminar)
C                 vorticity transport  (Z)
C                 Poisson              (S)
C                 velocity definition  (U,V)
C                 energy               (T)
C
C                 axial momentum       (W)
C
C         Taylor's discretization method was used.
C         (num and denom)
C         Source term linearization -constant.
C
C
      DIMENSION U(0:80,0:80),V(0:80,0:80),W(0:80,0:80),WOLD(0:80,0:80)
      REAL      LNU1(0:80),LNU2(0:80),NU1,NU10,NU100,NU2,NU20,NU200,
     *         LNO,KX,KY,NMN1,NMX1,NMN2,NMX2
      COMMON /AREA01/ NI,NJ
      COMMON /AREA11/ AG(79,79),AL(79,79),AE(79,79),AW(79,79)
      COMMON /AREA12/ AB(79,79)
      COMMON /AREA13/ ASG,ASL,ASE,ASW
      COMMON /AREA31/ Z(0:80,0:80)
      COMMON /AREA32/ S(0:80,0:80)
      COMMON /AREA34/ T(0:80,0:80)
      COMMON /AREA41/ ADD
      COMMON /AREA42/ AP
      EQUIVALENCE (Z,W)
      EQUIVALENCE (S,WOLD)
      DATA NI,  NJ  /80,80/
      DATA Z,U,V,S  /26244*0.0/
       NI2 = NI/2
       NJ2 = NJ/2
       ISC = NI/2
       JSC = NJ/2
       ITC = NI/4
       JTC = NJ*3/4
       IWMX= NI/4
       JWMX= NJ/2
      OPEN(UNIT=6,FILE='TS80',     STATUS='UNKNOWN')
      OPEN(UNIT=7,FILE='TS87',     STATUS='UNKNOWN')
C
C         parameters in SI units.
      PR  = 0.7
      T1  = 1.0
      T2  =-1.0
      RNI= FLOAT(NI)
```

```
      DX = 2.0/RNI
      RNJ= FLOAT(NJ)
      DY = 2.0/RNJ
C
       WRITE(2,3101)
 3101  FORMAT(' ',T10,'ENTER    - RAcr')
       READ(1,*) RACR
C
      WRITE(6,3103)
 3103 FORMAT('1'///' ',T10,'DEVELOPED LAMINAR NATURAL CONVECTION IN AN '
     *,'INCLINED SQUARE DUCT'/' ',T10,'WITH ANTI-SYMMETRIC TEMPERATURES'
     *                      /' ',T10,'- from TS8 using',
     *' VORTICITY,TRANSPORT, POISSON,',
     *' ENERGY and MOMENTUM Z equations.'////)
      WRITE(6,3104) T1,T2,PR,RACR
      WRITE(7,3154)
      WRITE(7,3104) T1,T2,PR,RACR
 3104 FORMAT(' '//
     *       ' ',T38,'DIMENSIONLESS UNITS'//
     *       ' ',T30,'T1    = ',     T41,F7.4/
     *       ' ',T30,'T2    = ',     T41,F7.4/
     *       ' ',T30,'Pr    = ',     T41,F7.4/
     *       ' ',T30,'RAcr  = ',     T41,E11.4)
C
C++++++++ STEP 1    set BC's and guess T.                          +++++++
C++++++++ .          (the others were initialized as 0.0)          +++++++
 4001  WRITE(2,3109)
 3109  FORMAT('    read ZUVST from TS8GST          -0=NO '/
     *                                    40x40    -1=YES'/
     *                                    80x80    -2=YES'/
     *                                    abort    -3=YES')
       READ(1,*,END=4001,ERR=4001) IG
      IF( IG.EQ.3 ) GO TO 4009
      IF( IG.NE.0 .AND. IG.NE.1 .AND. IG.NE.2 ) GO TO 4001
      IF( IG.EQ.0 ) THEN
       DO 3003 J=0,NJ
        T(0, J)= T1
        T(NI,J)= T2
       DO 3003 I=1,NI-1
 3003   T(I, J) = T1 +(T2-T1)*FLOAT(I)/RNI
      END IF
C
      LNU1(0)= T1-T2
      LNO    = T1-T2
      ELN    = 1.0
       NU1   = T1-T2
       NU10  = T1-T2
       ENU1  = 1.0
       NU2   = T1-T2
       NU20  = T1-T2
       ENU2  = 1.0
        SC   = 1.0
```

```
      SCO = 1.0
      ESC = 1.0
C
      DXT2 = DX*2.0
      DYT2 = DY*2.0
      DXPR2= DXT2*PR
      DYPR2= DYT2*PR
      RO64DX= RACR /(64.0*DX)
      DXDX = DX*DX
      DYDY = DY*DY
      ODXDX= 1.0 /DXDX
      ODYDY= 1.0 /DYDY
      ASG  = -ODYDY
      ASL  = -ODYDY
      ASE  = -ODXDX
      ASW  = -ODXDX
      APC  = ODXDX +ODYDY
      APS  = 2.0*(ODXDX +ODYDY)
C
C         restart by reading initial guess from TS8GST
C
       IF( IG.EQ.1 .OR. IG.EQ.2 ) THEN
        OPEN(UNIT=5,FILE='TS8GST', STATUS='OLD')
         READ(5,3110)
 3110    FORMAT()
        IF( IG.EQ.1 ) THEN
         READ(5,3112) ( (Z(I,J),I=0,NI,2 ),J=NJ ,0,-2)
         READ(5,3112) ( (U(I,J),I=0,NI,2 ),J=NJ ,0,-2)
         READ(5,3112) ( (V(I,J),I=0,NI,2 ),J=NJ ,0,-2)
         READ(5,3112) ( (S(I,J),I=0,NI,2 ),J=NJ ,0,-2)
         READ(5,3113) ( (T(I,J),I=0,NI,2 ),J=NJ ,0,-2)
 3112    FORMAT( T4,10E10.3/T4,10E10.3/T4,10E10,3/T4,11E10.3 )
 3113    FORMAT( T4,10F10.6/T4,10F10.6/T4,10F10.6/T4,11F10.6 )
         DO 3006 I=1,NI-1,2
         DO 3006 J=0,NJ,  2
          Z(I,J) = 0.5*( Z(I-1,J) + Z(I+1,J) )
          U(I,J) = 0.5*( U(I-1,J) + U(I+1,J) )
          V(I,J) = 0.5*( V(I-1,J) + V(I+1,J) )
          S(I,J) = 0.5*( S(I-1,J) + S(I+1,J) )
 3006     T(I,J) = 0.5*( T(I-1,J) + T(I+1,J) )
         DO 3007 I=0,NI
         DO 3007 J=1,NJ-1,2
          Z(I,J) = 0.5*( Z(I,J-1) + Z(I,J+1) )
          U(I,J) = 0.5*( U(I,J-1) + U(I,J+1) )
          V(I,J) = 0.5*( V(I,J-1) + V(I,J+1) )
          S(I,J) = 0.5*( S(I,J-1) + S(I,J+1) )
 3007     T(I,J) = 0.5*( T(I,J-1) + T(I,J+1) )
        ELSE
         READ(5,3115) ( (Z(I,J),I=0,NI ),J=NJ ,0,-1)
         READ(5,3115) ( (U(I,J),I=0,NI ),J=NJ ,0,-1)
         READ(5,3115) ( (V(I,J),I=0,NI ),J=NJ ,0,-1)
         READ(5,3115) ( (S(I,J),I=0,NI ),J=NJ ,0,-1)
```

```
        READ(5,3116) ( (T(I,J),I=0,NI ),J=NJ ,0,-1)
 3115    FORMAT( T4,10E10.3/T4,10E10.3/T4,10E10.3/T4,10E10.3/
     *           T4,10E10.3/T4,10E10.3/T4,10E10.3/T4,11E10.3 )
 3116   FORMAT( T4,10F10.6/T4,10F10.6/T4,10F10.6/T4,10F10.6/
     *           T4,10F10.6/T4,10F10.6/T4,10F10.6/T4,11F10.6 )
        END IF
        CLOSE(UNIT=5)
       END IF
C
 4002  WRITE(2,3114)
 3114  FORMAT(' calculate ZUVST  -0=NO '/
     *        '                    -1=YES'/
     *        ' and dump values  -2=YES')
       READ(1,*,END=4002,ERR=4002) IZUVST
       IF( IZUVST.EQ.0 ) GO TO 3046
       IF( IZUVST.NE.1 .AND. IZUVST.NE.2 ) GO TO 4002
C
       STL  = 1.0
       WRITE(2,3102) STL
 3102  FORMAT('    . STL =',F10.5,'    Enter STL')
       READ(1,*) STL
      WRITE(2,3103)
      WRITE(2,3104) T1,T2,PR,RACR
C
       WRITE(6,3107) ISC,JSC
       WRITE(7,3107) ISC,JSC
 3107  FORMAT('1'////' ','ITERATION CHECK USING NUSSELT NUMBERS'///
     *    ' ',T3,'ITERATION',T18,'NU1',T29,'ENU1',T37,'NU2',T48,'ENU2',
     *     T56,'S(',I3,',',I3,')',T67,'ES'/)
       WRITE(2,3108) ISC,JSC
 3108  FORMAT(' '//' ','ITERATION CHECK USING NUSSELT NUMBERS'///
     *    ' ',T3,'ITERATION',T18,'NU1',T29,'ENU1',T37,'NU2',T48,'ENU2',
     *     T56,'S(',I3,',',I3,')',T67,'ES'/)
      WRITE(2,3106)
 3106 FORMAT(T7,
     * 'Enter starting iteration no.')
      READ(1,*) NO
 3010 WRITE(2,3105)
 3105 FORMAT('      Enter pause interval')
      READ(1,*,END=3010,ERR=3010) INCR
      DO 3041 L=NO+1,NO+INCR
C+++++++++++++++++++++++++++++++++++++++++++++++++++++++++++++++++++++++++++++
C
C++++++++ STEP 2     calculate Z (cross-plane vorticity)          +++++++
C
C         update Z on boundaries.
      DO 3012 I=1,NI-1
       Z(I,0) = (8.0*S(I,   1) -S(I,   2)) /(2.0*DYDY)
 3012  Z(I,NJ)= (8.0*S(I,NJ-1) -S(I,NJ-2)) /(2.0*DYDY)
      DO 3013 J=1,NJ-1
       Z(0,J) = (8.0*S(   1,J) -S(   2,J)) /(2.0*DXDX)
 3013  Z(NI,J)= (8.0*S(NI-1,J) -S(NI-2,J)) /(2.0*DXDX)
```

```
C
C         update Z.
C
      DO 3014 I=1,NI-1
      DO 3014 J=1,NJ-1
       PY = V(I,J)*DYT2/PR
       IF( PY.LT. 0.0 ) THEN
        KY = 1.0 -
     *       0.5*(1.0 +PY*(-0.25+PY*(1./24.0+PY*(-1./192.0+PY/1920.0))))
     *          /(1.0 +PY*(-0.5 +PY*(1./6.0 +PY*(-1./24.0 +PY/120.0 ))))
       ELSE
        KY = 0.5*(1.0 +PY*( 0.25+PY*(1./24.0+PY*( 1./192.0+PY/1920.0))))
     *          /(1.0 +PY*( 0.5 +PY*(1./6.0 +PY*( 1./24.0 +PY/120.0 ))))
       END IF
        AG(I,J) = -KY        *ODYDY
        AL(I,J) = (KY -1.0) *ODYDY
       PX = U(I,J)*DXT2/PR
       IF( PX.LT. 0.0 ) THEN
        KX = 1.0 -
     *       0.5*(1.0 +PX*(-0.25+PX*(1./24.0+PX*(-1./192.0+PX/1920.0))))
     *          /(1.0 +PX*(-0.5 +PX*(1./6.0 +PX*(-1./24.0 +PX/120.0 ))))
       ELSE
        KX = 0.5*(1.0 +PX*( 0.25+PX*(1./24.0+PX*( 1./192.0+PX/1920.0))))
     *          /(1.0 +PX*( 0.5 +PX*(1./6.0 +PX*( 1./24.0 +PX/120.0 ))))
       END IF
        AE(I,J) = -KX        *ODXDX
        AW(I,J) = (KX -1.0) *ODXDX
 3014   AB(I,J) = -(T(I+1,J) -T(I-1,J)) *RO64DX
        FPX      = STL/(2.0*PR)
        FPY      = STL/(2.0*PR)
        ADD      = FPX/DXDX +FPY/DYDY
        AP = APC
C
      DO 3017 J=1,NJ2-1
       CALL THMZX(J)
 3017  CONTINUE
      DO 3018 J=NJ-1,NJ2,-1
       CALL THMZX(J)
 3018  CONTINUE
C
      DO 3015 I=1,NI2-1
       CALL THMZY(I)
 3015  CONTINUE
      DO 3016 I=NI-1,NI2,-1
       CALL THMZY(I)
 3016  CONTINUE
C
C++++++++ STEP 3    calculate S.                                    +++++++
C
C         COEFFICIENTS OF POISSON. (for S)
       AP  =  APS
      DO 3022 I=1,NI-1
```

```
      DO 3022 J=1,NJ-1
 3022   AB(I,J) = -Z(I,J)
C
C          S.
C
       SERR = 1.0
      DO 3032 LL=1,6
       SEO = SERR
       SO  = S(ISC,JSC)
C
      IF( (1 +2*((LL-1)/2)) .EQ. LL ) THEN
      DO 3023 I=1,NI2-1
       CALL THMSY(I)
 3023  CONTINUE
      DO 3024 I=NI-1,NI2,-1
       CALL THMSY(I)
 3024  CONTINUE
      ELSE IF( (2 +2*((LL-2)/2)) .EQ. LL ) THEN
      DO 3025 J=1,NJ2-1
       CALL THMSX(J)
 3025  CONTINUE
      DO 3026 J=NJ-1,NJ2,-1
       CALL THMSX(J)
 3026  CONTINUE
      END IF
C
 3032 SERR = ABS( (S(ISC,JSC) -SO)/SO )
C
C++++++++ STEP 4     calculate U and V.                              +++++++
C
      DO 3029 I=1,NI-1
      DO 3029 J=1,NJ-1
       U(I,J) =  (S(I,J+1) -S(I,J-1)) /DYT2
 3029  V(I,J) = -(S(I+1,J) -S(I-1,J)) /DXT2
C
C++++++++ STEP 5     calculate T.                                    +++++++
C
C          COEFFICIENTS OF ENERGY EQUATION.
C
      DO 3036 I=1,NI-1
      DO 3036 J=1,NJ-1
       PY = V(I,J)*DYT2
       IF( PY.LT. 0.0 ) THEN
        KY = 1.0 -
     *       0.5*(1.0 +PY*(-0.25+PY*(1./24.0+PY*(-1./192.0+PY/1920.0))))
     *          /(1.0 +PY*(-0.5 +PY*(1./6.0 +PY*(-1./24.0 +PY/120.0 ))))
       ELSE
        KY = 0.5*(1.0 +PY*( 0.25+PY*(1./24.0+PY*( 1./192.0+PY/1920.0))))
     *          /(1.0 +PY*( 0.5 +PY*(1./6.0 +PY*( 1./24.0 +PY/120.0 ))))
       END IF
        AG(I,J) = -KY       *ODYDY
        AL(I,J) = (KY -1.0) *ODYDY
```

```
        PX = U(I,J)*DXT2
        IF( PX.LT. 0.0 ) THEN
         KX = 1.0 -
     *       0.5*(1.0 +PX*(-0.25+PX*(1./24.0+PX*(-1./192.0+PX/1920.0))))
     *          /(1.0 +PX*(-0.5 +PX*(1./6.0 +PX*(-1./24.0 +PX/120.0 ))))
        ELSE
         KX = 0.5*(1.0 +PX*( 0.25+PX*(1./24.0+PX*( 1./192.0+PX/1920.0))))
     *          /(1.0 +PX*( 0.5 +PX*(1./6.0 +PX*( 1./24.0 +PX/120.0 ))))
        END IF
         AE(I,J) = -KX        *ODXDX
 3036    AW(I,J) = (KX -1.0) *ODXDX
         FPX      = STL/2.0
         FPY      = STL/2.0
         ADD      = FPX/DXDX +FPY/DYDY
         AP       = APC
C
       DO 3039 LT=1,2
        DO 3037 J=1,NJ2-1
         CALL THMTX(J)
 3037    CONTINUE
        DO 3038 J=NJ-1,NJ2,-1
         CALL THMTX(J)
 3038    CONTINUE
C
C          update T on Y=0,1 boundaries.
      DO 3039 I=0,NI
       T(I, 0) =  T(I,1)*4.0/3.0 -T(I,2)/3.0
 3039  T(I,NJ) = -T(I,NJ-2)/3.0  +T(I,NJ-1)*4.0/3.0
C
C++++++++++++++++++++++++++++++++++++++++++++++++++++++++++++++++++++++++++++++
C++++++++ STEP 6     CALCULATE NUSSELT NUMBERS and CHECK          +++++++
C++++++++             FOR CONVERGENCE.                            +++++++
       LNOO = LNO
       LNO  = LNU1(0)
       ELNO = ELN
       NU10O= NU10
       NU10 = NU1
       ENU10= ENU1
       NU20O= NU20
       NU20 = NU2
       ENU20= ENU2
       SUM1 = 0.0
       SUM2 = 0.0
      DO 3042 J=0,NJ
       LNU1(J) =-(-1.5 *T(0,J)    +2.0 *T(1,J)    -0.5*T(2,J)  ) /DX
       LNU2(J) =-( 0.5*T(NI-2,J)  -2.0*T(NI-1,J)  +1.5*T(NI,J) ) /DX
       IF(J.EQ.0 .OR. J.EQ.NJ) THEN
        SUM1= SUM1 +LNU1(J)*0.5
        SUM2= SUM2 +LNU2(J)*0.5
       ELSE
        SUM1= SUM1 +LNU1(J)
        SUM2= SUM2 +LNU2(J)
```

```
      END IF
3042  CONTINUE
      NU1 = SUM1 /RNJ
      NU2 = SUM2 /RNJ
      ELN  = ABS( (LNU1(0) -LNO )/LNO )
      ENU1 = ABS( (NU1 -NU10 )/NU1 )
      ENU2 = ABS( (NU2 -NU20 )/NU2 )
      SC0 = SC
      SC  = S(ISC,JSC)
      ESC0= ESC
      IF( ABS(RACR) .LE. 0.001 ) THEN
       ESC = ABS( SC -SC0 )
      ELSE
       ESC = ABS( ( SC -SC0 )/SC )
      END IF
       IF( L/10*10 .EQ. L ) THEN
        WRITE(2,3128) L,NU1,ENU1,NU2,ENU2,SC,ESC
        WRITE(6,3128) L,NU1,ENU1,NU2,ENU2,SC,ESC
       END IF
3041  WRITE(7,3128)  L,NU1,ENU1,NU2,ENU2,SC,ESC
3128  FORMAT(' ',T5,I4,T13,F11.4,F8.4,F11.4,F8.4,T51,F11.4,F8.4)
      L = L -1
      NO = NO +INCR
      IF( MAX(ENU1,ENU10,ENU2,ENU20,ESC,ESC0,ELN,ELN0)
     *                                .LT. 0.004 ) THEN
4003  WRITE(2,3131)
3131  FORMAT(' CONVERGED  :terminate          -0=YES'/
     *       '            :more iterations    -1=YES'/
     *       '            :new STL            -2=YES',
     *       '  /enter STL')
       IF( IZUVST.NE.2 ) THEN
        READ(1,*,END=4003,ERR=4003) MI
        IF( MI.EQ.2 ) READ(1,*) STL
        IF( MI.EQ.1 .OR. MI.EQ.2 ) GO TO 3010
        IF( MI.NE.0 ) GO TO 4003
       END IF
       WRITE(6,3129) (J,LNU1(J),LNU2(J),J=NJ,0,-1)
3129  FORMAT(' ',T30,'CONVERGED'////
     *       ' ',T20,'LOCAL NUSSELT NUMBERS'//
     *       ' ',T20,'    HOT      COLD    '//' ',
     *      (' ',T14,I3,T20,F8.4,T30,F8.4) )
       WRITE(6,3127) NU1,NU2,L
3127  FORMAT(' ',T15,'NU1=',F8.4,'  NU2=',F8.4,'  ITER=',I5)
      ELSE
4004  WRITE(2,3130)
3130  FORMAT('            :terminate          -0=YES'/
     *       '            :more iterations    -1=YES'/
     *       '            :new STL            -2=YES',
     *       '  /enter STL')
       IF( IZUVST.NE.2 ) THEN
        READ(1,*,END=4004,ERR=4004) MI
        IF( MI.EQ.2 ) READ(1,*) STL
```

```
          IF( MI.EQ.1 .OR. MI.EQ.2 ) GO TO 3010
          IF( MI.NE.0 ) GO TO 4004
         END IF
         WRITE(6,3132) L
 3132  FORMAT(' '//' ',T30,'ITERATIONS TERMINATED AFTER',I4//)
       END IF
C
C
C+++++++++ Write out info for contouring and plotting ++++++++++++++++
       OPEN(UNIT=8,FILE='TS8G',      STATUS='UNKNOWN')
         IF( RACR.LT. 0.0001 ) THEN
          RALOG = -.9
         ELSE
          RALOG = LOG10(RACR*1.00001)
         END IF
         WRITE(8,3133) RALOG,RACR,PR,NI,NJ
 3133  FORMAT('1 T',F3.1,T15,E10.3,T30,F8.4,T42,2I4,
     *          '     RAcr,Pr,NI,NJ' )
         WRITE(8,3136) (J,(Z(I,J),I=0,NI),J=NJ,0,-1)
         WRITE(8,3137) (J,(U(I,J),I=0,NI),J=NJ,0,-1)
         WRITE(8,3138) (J,(V(I,J),I=0,NI),J=NJ,0,-1)
         WRITE(8,3139) (J,(S(I,J),I=0,NI),J=NJ,0,-1)
         WRITE(8,3140) (J,(T(I,J),I=0,NI),J=NJ,0,-1)
 3136 FORMAT(' ',T118,'VORTICITY Z  ',
     *      (' ',T113,I3,T1,'0',T4,10E10.3/' ',T4,10E10.3/
     *       ' ',T4,10E10.3/' ',T4,10E10.3/' ',T4,10E10.3/
     *       ' ',T4,10E10.3/' ',T4,10E10.3/' ',T4,11E10.3) )
 3137 FORMAT(' ',T118,'VELOCITY U  ',
     *      (' ',T113,I3,T1,'0',T4,10E10.3/' ',T4,10E10.3/
     *       ' ',T4,10E10.3/' ',T4,10E10.3/' ',T4,10E10.3/
     *       ' ',T4,10E10.3/' ',T4,10E10.3/' ',T4,11E10.3) )
 3138 FORMAT(' ',T118,'VELOCITY V  ',
     *      (' ',T113,I3,T1,'0',T4,10E10.3/' ',T4,10E10.3/
     *       ' ',T4,10E10.3/' ',T4,10E10.3/' ',T4,10E10.3/
     *       ' ',T4,10E10.3/' ',T4,10E10.3/' ',T4,11E10.3) )
 3139 FORMAT(' ',T118,'STR. FUNCT. S',
     *      (' ',T113,I3,T1,'0',T4,10E10.3/' ',T4,10E10.3/
     *       ' ',T4,10E10.3/' ',T4,10E10.3/' ',T4,10E10.3/
     *       ' ',T4,10E10.3/' ',T4,10E10.3/' ',T4,11E10.3) )
 3140 FORMAT(' ',T118,'TEMPERATURE T',
     *      (' ',T113,I3,T1,'0',T4,10F10.6/' ',T4,10F10.6/
     *       ' ',T4,10F10.6/' ',T4,10F10.6/' ',T4,10F10.6/
     *       ' ',T4,10F10.6/' ',T4,10F10.6/' ',T4,11F10.6) )
       WRITE(8,3141)  (LNU1(J),LNU2(J),J,J=NJ,0,-1)
 3141 FORMAT('0',T50,'NU  :HOT 1  COLD 2',
     *      (' ',T15,F8.4,T25,F8.4,T5,I3))
       WRITE(8,3142) NU1,NU2
 3142 FORMAT(' ',T15,F8.4,T25,F8.4,' ',T50,'ave')
       WRITE(8,3154)
       CLOSE(UNIT=8)
C
        ZMN    = .1000000.0
```

```
      ZMX    = -1000000.0
      UMN    =  1000000.0
      UMX    = -1000000.0
      VMN    =  1000000.0
      VMX    = -1000000.0
      SMN    =  1000000.0
      NMN1   =  1000000.0
      NMX1   = -1000000.0
      NMN2   =  1000000.0
      NMX2   = -1000000.0
     DO 3047 J=0,NJ
      IF( LNU1(J) .GT. NMX1 ) NMX1=LNU1(J)
      IF( LNU1(J) .LT. NMN1 ) NMN1=LNU1(J)
      IF( LNU2(J) .GT. NMX2 ) NMX2=LNU2(J)
      IF( LNU2(J) .LT. NMN2 ) NMN2=LNU2(J)
     DO 3047 I=0,NI
      IF( Z(I,J) .GT. ZMX ) THEN
       ZMX  = Z(I,J)
       IZMX = I
       JZMX = J
      ELSE IF( Z(I,J) .LT. ZMN ) THEN
       ZMN  = Z(I,J)
       IZMN = I
       JZMN = J
      END IF
      IF( U(I,J) .GT. UMX ) THEN
       UMX  = U(I,J)
       IUMX = I
       JUMX = J
      ELSE IF( U(I,J) .LT. UMN ) THEN
       UMN  = U(I,J)
       IUMN = I
       JUMN = J
      END IF
      IF( V(I,J) .GT. VMX ) THEN
       VMX  = V(I,J)
       IVMX = I
       JVMX = J
      ELSE IF( V(I,J) .LT. VMN ) THEN
       VMN  = V(I,J)
       IVMN = I
       JVMN = J
      END IF
      IF( S(I,J) .LT. SMN ) THEN
       SMN  = S(I,J)
       ISMN = I
       JSMN = J
      END IF
 3047 CONTINUE
C
     PMAX = MAX( UMX*DXT2, VMX*DYT2 ) /PR
     PMIN = MIN( UMN*DXT2, VMN*DYT2 ) /PR
```

```
      WRITE(6,3143) PR,NI,STL,RACR,NJ,
     *     NMN1,NMN2,NMX1,NMX2,NU1,NU2
 3143 FORMAT('1///
     *       ' ,T20,'Pr    =',F7.4,,T50,'NI =',I3,T65,'STL=',F10.5/
     *       ' ,T20,'RAcr  =',E10.3,T51,'NJ =',I3//
     *       ' ,T20,'NUmin =',F7.4,F11.4/
     *       ' ,T20,'NUmax =',F7.4,F11.4/
     *       ' ,T20,'NU    =',F7.4,F11.4)
      IF( RACR .GT. 0.001 ) THEN
       WRITE(6,3144) IZMX,JZMX,ZMX,     L,IZMN,JZMN,ZMN,
     *                                    ISMN,JSMN,SMN,
     *               IUMX,JUMX,UMX,     IUMN,JUMN,UMN,
     *               IVMX,JVMX,VMX,     IVMN,JVMN,VMN,
     *               PMAX,PMIN
 3144  FORMAT(     ' ',T20,'ZMAX(',I3,',',I3,') =',E10.3,
     *                        T65,'ITER=',I4/
     *          ' ',T20,'Zmin(',I3,',',I3,') =',E10.3/
     *          ' ',T20,'Smin(',I3,',',I3,') =',E10.3//
     *          ' ',T20,'Umax(',I3,',',I3,') =',E10.3/
     *          ' ',T20,'Umin(',I3,',',I3,') =',E10.3/
     *          ' ',T20,'Vmax(',I3,',',I3,') =',E10.3/
     *          ' ',T20,'Vmin(',I3,',',I3,') =',E10.3/
     *          ' ',T20,'Pmax =',E10.3/
     *          ' ',T20,'Pmin =',E10.3)
      END IF
      IF( IZUVST.EQ.2 ) GO TO 3075
C
C++++++++ STEP 7     update W.                                    +++++++
C
 3046 WRITE(2,3172)
 3172 FORMAT('    calculate W   0=NO '/
     *                          1=YES')
      READ(1,*,END=3046,ERR=3046) IW
      IF( IW.EQ.0 ) GO TO 3075
      IF( IW.NE.1 ) GO TO 3046
C
C         UNIVERSAL W PROFILES
C           FOR Pr, ZETA=TB-TI/T1-T2, and RAcr specified.
C
C      coefficients of MOMENTUM Z Navier-Stokes equation.
C
      DO 3048 I=1,NI-1
      DO 3048 J=1,NJ-1
       PY = V(I,J)*DYT2/PR
       IF( PY.LT. 0.0 ) THEN
        KY = 1.0 -
     *       0.5*(1.0 +PY*(-0.25+PY*(1./24.0+PY*(-1./192.0+PY/1920.0))))
     *         /(1.0 +PY*(-0.5 +PY*(1./6.0 +PY*(-1./24.0 +PY/120.0 ))))
       ELSE
        KY = 0.5*(1.0 +PY*( 0.25+PY*(1./24.0+PY*( 1./192.0+PY/1920.0))))
     *         /(1.0 +PY*( 0.5 +PY*(1./6.0 +PY*( 1./24.0 +PY/120.0 ))))
       END IF
```

```
      AG(I,J) = -KY          *ODYDY
      AL(I,J) = (KY -1.0) *ODYDY
     PX = U(I,J)*DXT2/PR
     IF( PX.LT. 0.0 ) THEN
      KX = 1.0 -
     *      0.5*(1.0 +PX*(-0.25+PX*(1./24.0+PX*(-1./192.0+PX/1920.0))))
     *         /(1.0 +PX*(-0.5 +PX*(1./6.0 +PX*(-1./24.0 +PX/120.0 ))))
     ELSE
      KX = 0.5*(1.0 +PX*( 0.25+PX*(1./24.0+PX*( 1./192.0+PX/1920.0))))
     *         /(1.0 +PX*( 0.5 +PX*(1./6.0 +PX*( 1./24.0 +PX/120.0 ))))
     END IF
      AE(I,J) = -KX          *ODXDX
3048  AW(I,J) = (KX -1.0) *ODXDX
      AP      = APC
C
     OPEN(UNIT=8,FILE='TS8W',      STATUS='UNKNOWN')
     DO 3062 IZ=1,3
      IF( IZ .EQ. 1 ) THEN
       ZETA = 0.0
      ELSE IF( IZ .EQ. 2 ) THEN
       ZETA = 0.5
      ELSE IF( IZ .EQ. 3 ) THEN
       ZETA = 1.5
      END IF
C
     IF( IZ .EQ. 1 ) THEN
      DO 3049 I=1,NI-1
      DO 3049 J=1,NJ-1
3049   AB(I,J) =  T(I,J) /4.0
     ELSE
      DO 3050 I=1,NI-1
      DO 3050 J=1,NJ-1
3050   AB(I,J) = (T(I,J)/(2.0*ZETA) +1.0)/2.0
     END IF
C
C          restart for W from TS8WST
4005  WRITE(2,3155)
3155  FORMAT('     read W from TS8WST              -0=NO '/
     *                                  40x40     -1=YES'/
     *                                  80x80     -2=YES'/
     *                                  abort     -3=YES')
      READ(1,*,END=4005,ERR=4005) IG
     IF( IG.EQ.3 ) GO TO 4009
     IF( IG.NE.0 .AND. IG.NE.1 .AND. IG.NE.2 ) GO TO 4005
     IF( IG.EQ.1 .OR. IG.EQ.2 ) THEN
      OPEN(UNIT=5,FILE='TS8WST',  STATUS='OLD')
       READ(5,3110)
      IF( IG.EQ.1 ) THEN
       READ(5,3112) ( (W(I,J),I=0,NI,2),J=NJ ,0,-2)
       DO 3071 I=1,NI-1,2
       DO 3071 J=0,NJ,  2
3071    W(I,J) = 0.5*( W(I-1,J) + W(I+1,J) )
```

```
        DO 3072 I=0,NI
        DO 3072 J=1,NJ-1,2
3072     W(I,J) = 0.5*( W(I,J-1) + W(I,J+1) )
       ELSE
        READ(5,3115) ( (W(I,J),I=0,NI ),J=NJ ,0,-1)
       END IF
      ELSE
       DO 3051 I=0,NI
       DO 3051 J=0,NJ
3051    W(I,J) = 0.0
      END IF
C
      WRITE(2,3145) IWMX,JWMX
3145 FORMAT(' '//' ',T10,'ITERATION FOR W, W(',I3,',',I3,')'//
     *  ' ',T12,'iteration    W       ',
     *                    Werr          Wres')
      WRITE(7,3146) IWMX,JWMX
3146 FORMAT('1'/' ',T10,'ITERATION FOR W, W(',I3,',',I3,')'//
     *  ' ',T12,'iteration    W       ',
     *                    Werr          Wres')
      WEQ  = 1.0
      WERR = 1.0
      W(IWMX,JWMX) = 0.01
      MI = 0
      NO = -50
3052  NO = NO +50
      DO 3059 LLW=NO+1,NO+50
       IF( MI.EQ.0 ) WREL = 1.25
        WO  = W(IWMX,JWMX)
       DO 3053 I=1,NI-1
       DO 3053 J=1,NJ-1
3053    WOLD(I,J) = W(I,J)
C
      IF( (1 +2*((LLW-1)/2)) .EQ. LLW ) THEN
      DO 3054 I=1,NI2-1
       CALL THMWY(I)
3054   CONTINUE
      DO 3055 I=NI-1,NI2,-1
       CALL THMWY(I)
3055   CONTINUE
      ELSE IF( (2 +2*((LLW-2)/2)) .EQ. LLW ) THEN
      DO 3056 J=1,NJ2-1
       CALL THMWX(J)
3056   CONTINUE
      DO 3057 J=NJ-1,NJ2,-1
       CALL THMWX(J)
3057   CONTINUE
      END IF
C
      DO 3058 I=1,NI-1
      DO 3058 J=1,NJ-1
3058   W(I,J) = WOLD(I,J) +WREL*( W(I,J) -WOLD(I,J) )
```

```
C
C         calculate W residuals.
      WRES = 0.0
      DO 3066 K=1,NI-1
3066  WRES = WRES +ABS( AG(K,K)*W(K,K+1) +AL(K,K)*W(K,K-1)
     *                 +AE(K,K)*W(K+1,K) +AW(K,K)*W(K-1,K)
     *                 +AP*W(K,K) -AB(K,K) )
      WEOO = WEO
      WEO  = WERR
      WERR = ABS( (W(IWMX,JWMX)-WO)/WO )
      IF( WERR.GT.0.0005 .OR. WEO.GT.0.0005 .OR. WEOO.GT.0.0005 ) THEN
       IF( LLW/10*10 .EQ. LLW ) THEN
        WRITE(2,3147) LLW,W( IWMX, JWMX ),WERR,WRES
       END IF
       WRITE(7,3147)  LLW,W( IWMX, JWMX ),WERR,WRES
3147   FORMAT(' ',T15,I4,T22,F9.6,T39,F8.4,T52,F8.4)
      ELSE
       IF( LLW/10*10 .EQ. LLW ) THEN
        WRITE(2,3148) LLW,W( IWMX, JWMX ),WERR,WRES
       END IF
       WRITE(7,3148)  LLW,W( IWMX, JWMX ),WERR,WRES
3148   FORMAT(' ',T15,I4,T22,F9.6,T39,F8.4,T52,F8.4,'   CONVERGED')
      END IF
3059  CONTINUE
      WMN = 1000000.0
      WMX =-1000000.0
      DO 3068 I=0,NI
      DO 3068 J=0,NJ
       IF( W(I,J).GT.WMX ) THEN
        WMX = W(I,J)
        IWMX = I
        JWMX = J
       ELSE IF( W(I,J).LT.WMN ) THEN
        WMN = W(I,J)
        IWMN = I
        JWMN = J
       END IF
3068  CONTINUE
4006  WRITE(2,3149) IWMX,JWMX,WMX
3149  FORMAT('    WMX(',I3,',',I3,') =',F9.6/
     *       ' terminate        -0=YES'/
     *       ' more iterations  -1=YES'/
     *       ' new WREL         -2=YES')
      READ(1,*,END=4006,ERR=4006) MI
      IF( MI.EQ.2 ) THEN
       WRITE(2,3150) WREL
3150   FORMAT(' '/' ',T5,'WREL =',F4.2,'   enter WREL')
       READ(1,*) WREL
      END IF
      IF( MI.EQ.1 .OR. MI.EQ.2 ) THEN
       WRITE(2,3145) IWMX,JWMX
       WRITE(7,3145) IWMX,JWMX
```

```
        GO TO 3052
       END IF
       IF( MI.NE.0 ) GO TO 4006
C
        WAVE = 0.0
        Q    = 0.0
       DO 3061 I=1,NI
       DO 3061 J=1,NJ
        WAVE = WAVE  +0.25 *( W(I-1,J-1) +W(I-1,J) )
      *              +0.25 *( W(I,  J-1) +W(I,  J) )
       IF( IZ.EQ.1 ) THEN
        THMM = T(I-1,J-1)
        THMO = T(I-1,J)
        THOM = T(I,J-1)
        THOO = T(I,J)
       ELSE
        THMM = T(I-1,J-1)/ZETA +1.0
        THMO = T(I-1,J)  /ZETA +1.0
        THOM = T(I,J-1)  /ZETA +1.0
        THOO = T(I,J)    /ZETA +1.0
       END IF
 3061  Q    = Q     +0.25 *( THMM*ABS(W(I-1,J-1)) +THMO*ABS(W(I-1,J)) )
      *              +0.25 *( THOM*ABS(W(I,  J-1)) +THOO*ABS(W(I,  J)) )
       WAVE = WAVE *DX *DY /4.0
       Q    = Q    *DX *DY
       WRITE(6,3151) ZETA,IWMX,JWMX,WMX,IWMN,JWMN,WMN,WAVE,WREL,LLW-1,Q
 3151 FORMAT('0',T20,'ZETA  =',F6.3/
      *       ' ',T20,'Wmax(',I3,',',I3,') =',E10.3/
      *       ' ',T20,'Wmin(',I3,',',I3,') =',E10.3/
      *       ' ',T20,'Wave  =',E10.3,
      *               T50,'WREL=',F4.2,T65,'iter=',I5/
      *       ' ',T20,'Q     =',E10.3/)
C
        WRITE(8,3152) ZETA,NI,NJ,RACR,PR,ZETA,WAVE,Q
 3152   FORMAT('1 W',F4.1,T15,2I3,E11.4,2F8.4,2E10.3,
      *       '  NI,NJ,RAcr,Pr,ZETA,Wave,Q')
       WRITE(8,3153) (J,(W(I,J),I=0,NI),J=NJ,0,-1)
 3153 FORMAT(' ',T118,'VELOCITY W   ',
      *     (' ',T113,I3,T1,'0',T4,10E10.3/' ',T4,10E10.3/
      *      ' ',T4,10E10.3/' ',T4,10E10.3/' ',T4,10E10.3/
      *      ' ',T4,10E10.3/' ',T4,10E10.3/' ',T4,11E10.3) )
 3062 CONTINUE
C
      WRITE(8,3154)
 3075 WRITE(6,3154)
      WRITE(7,3154)
 3154 FORMAT('1')
 4009 CONTINUE
C
      STOP
      END
C
```

```
      SUBROUTINE THMZX(J)
      COMMON /AREA01/ NI,NJ
      COMMON /AREA11/ AG(79,79),AL(79,79),AE(79,79),AW(79,79)
      COMMON /AREA12/ AB(79,79)
      COMMON /AREA21/ G(0:79),H(0:79)
      COMMON /AREA31/ Z(0:80,0:80)
      COMMON /AREA41/ ADD
      COMMON /AREA42/ AP
C
C         THOMAS ALGORITHM TO SOLVE FOR Z.
C
       H(0) = 0.0
       G(0) = Z(0,J)
       DO 1002 I=1,NI-1
        RD=-Z(I,J+1)*AG(I,J) -Z(I,J-1)*AL(I,J) +AB(I,J) +Z(I,J)*ADD
        RA= AE(I,J)
        RB= AP +ADD
        RC= AW(I,J)
        DEL = RB +RC*H(I-1)
        G(I) = (RD -RC*G(I-1)) /DEL
 1002   H(I) = -RA /DEL
       DO 1003 I=NI-1,1,-1
 1003   Z(I,J) = G(I) +H(I)*Z(I+1,J)
      RETURN
      END
C
      SUBROUTINE THMSX(J)
      COMMON /AREA01/ NI,NJ
      COMMON /AREA12/ AB(79,79)
      COMMON /AREA13/ ASG,ASL,ASE,ASW
      COMMON /AREA21/ G(0:79),H(0:79)
      COMMON /AREA32/ S(0:80,0:80)
      COMMON /AREA42/ AP
C
C         THOMAS ALGORITHM TO SOLVE FOR S.
C
       H(0) = 0.0
       G(0) = S(0,J)
       DO 1002 I=1,NI-1
        RD =-S(I,J+1)*ASG -S(I,J-1)*ASL  +AB(I,J)
        RA = ASE
        RB = AP
        RC = ASW
        DEL = RB +RC*H(I-1)
        G(I) = (RD -RC*G(I-1)) /DEL
 1002   H(I) = -RA /DEL
       DO 1003 I=NI-1,1,-1
 1003   S(I,J) = G(I) +H(I)*S(I+1,J)
      RETURN
      END
C
      SUBROUTINE THMTX(J)
```

```
      COMMON /AREA01/ NI,NJ
      COMMON /AREA11/ AG(79,79),AL(79,79),AE(79,79),AW(79,79)
      COMMON /AREA21/ G(0:79),H(0:79)
      COMMON /AREA34/ T(0:80,0:80)
      COMMON /AREA41/ ADD
      COMMON /AREA42/ AP
C
C        THOMAS ALGORITHM TO SOLVE FOR T.
C
       H(0) = 0.0
       G(0) = T(0,J)
       DO 1002 I=1,NI-1
        RD =-T(I,J+1)*AG(I,J) -T(I,J-1)*AL(I,J)          +T(I,J)*ADD
        RA = AE(I,J)
        RB = AP +ADD
        RC = AW(I,J)
        DEL = RB +RC*H(I-1)
        G(I) = (RD -RC*G(I-1)) /DEL
 1002   H(I) = -RA /DEL
       DO 1003 I=NI-1,1,-1
 1003   T(I,J) = G(I) +H(I)*T(I+1,J)
      RETURN
      END
C
      SUBROUTINE THMZY(I)
      COMMON /AREA01/ NI,NJ
      COMMON /AREA11/ AG(79,79),AL(79,79),AE(79,79),AW(79,79)
      COMMON /AREA12/ AB(79,79)
      COMMON /AREA21/ G(0:79),H(0:79)
      COMMON /AREA31/ Z(0:80,0:80)
      COMMON /AREA41/ ADD
      COMMON /AREA42/ AP
C
C        THOMAS ALGORITHM TO SOLVE FOR Z.
C
       H(0) = 0.0
       G(0) = Z(I,0)
       DO 2002 J=1,NJ-1
        RD=-Z(I+1,J)*AE(I,J) -Z(I-1,J)*AW(I,J) +AB(I,J) +Z(I,J)*ADD
        RA= AG(I,J)
        RB= AP +ADD
        RC= AL(I,J)
        DEL = RB +RC*H(J-1)
        G(J) = (RD -RC*G(J-1)) /DEL
 2002   H(J) = -RA /DEL
       DO 2003 J=NJ-1,1,-1
 2003  Z(I,J) = G(J) +H(J)*Z(I,J+1)
      RETURN
      END
C
      SUBROUTINE THMSY(I)
      COMMON /AREA01/ NI,NJ
```

```
      COMMON /AREA12/ AB(79,79)
      COMMON /AREA13/ ASG,ASL,ASE,ASW
      COMMON /AREA21/ G(0:79),H(0:79)
      COMMON /AREA32/ S(0:80,0:80)
      COMMON /AREA42/ AP
C
C         THOMAS ALGORITHM TO SOLVE FOR S.
C
       H(0) = 0.0
       G(0) = S(I,0)
       DO 2002 J=1,NJ-1
        RD =-S(I+1,J)*ASE -S(I-1,J)*ASW  +AB(I,J)
        RA = ASG
        RB = AP
        RC = ASL
        DEL = RB +RC*H(J-1)
        G(J) = (RD -RC*G(J-1)) /DEL
 2002   H(J) = -RA /DEL
       DO 2003 J=NJ-1,1,-1
 2003   S(I,J) = G(J) +H(J)*S(I,J+1)
      RETURN
      END
C
      SUBROUTINE THMWX(J)
      COMMON /AREA01/ NI,NJ
      COMMON /AREA11/ AG(79,79),AL(79,79),AE(79,79),AW(79,79)
      COMMON /AREA12/ AB(79,79)
      COMMON /AREA21/ G(0:79),H(0:79)
      COMMON /AREA31/ W(0:80,0:80)
      COMMON /AREA42/ AP
C
C         THOMAS ALGORITHM TO SOLVE FOR W.
C
       H(0) = 0.0
       G(0) = W(0,J)
       DO 1002 I=1,NI-1
        RD =-W(I,J+1)*AG(I,J) -W(I,J-1)*AL(I,J)  +AB(I,J)
        RA = AE(I,J)
        RB = AP
        RC = AW(I,J)
        DEL = RB +RC*H(I-1)
        G(I) = (RD -RC*G(I-1)) /DEL
 1002   H(I) = -RA /DEL
       DO 1003 I=NI-1,1,-1
 1003   W(I,J) = G(I) +H(I)*W(I+1,J)
      RETURN
      END
C
      SUBROUTINE THMWY(I)
      COMMON /AREA01/ NI,NJ
      COMMON /AREA11/ AG(79,79),AL(79,79),AE(79,79),AW(79,79)
      COMMON /AREA12/ AB(79,79)
```

```
      COMMON /AREA21/ G(0:79),H(0:79)
      COMMON /AREA31/ W(0:80,0:80)
      COMMON /AREA42/ AP
C
C         THOMAS ALGORITHM TO SOLVE FOR W.
C
       H(0) = 0.0
       G(0) = W(I,0)
       DO 2002 J=1,NJ-1
        RD =-W(I+1,J)*AE(I,J) -W(I-1,J)*AW(I,J)  +AB(I,J)
        RA = AG(I,J)
        RB = AP
        RC = AL(I,J)
        DEL = RB +RC*H(J-1)
        G(J) = (RD -RC*G(J-1)) /DEL
 2002   H(J) = -RA /DEL
       DO 2003 J=NJ-1,1,-1
 2003   W(I,J) = G(J) +H(J)*W(I,J+1)
      RETURN
      END
```

APPENDIX B

CALCULATION OF EXPERIMENTAL PARAMETERS

The following program, RA.BAS, calculates the experimental parameters to determine the model dimensions before an experiment, and the desired surface temperature during an experiment. This program was written in BASIC on a Tandy 2000 personal computer. There are no graphics in this program, so it should run on any IBM compatible personal computer.

```
1010 '       "RA.BAS"
1020 '       by Michael Papple
1030 '
1040 '      This program calculates the parameters necessary
1050 '      to run an experiment with the interferometer for:
1060 '         Horizontal square cavities
1070 '         Inclined square ducts with differentially heated sides
1080 '         Inclined isothermal square ducts
1090 '         Inclined isothermal tubes
1100 '
1110 '
1120 DEFINT I,J,M,N
1130 DIM TVMU(14),TK(14),TPR(8)
1140                                    'initialize tables.
1150 READ PI :DATA 3.141592654
1160 FOR J=1 TO 14 :READ TVMU(J) :NEXT J
1170 DATA 1.707,1.757,1.805,1.853,1.900,1.946,1.992
1180 DATA 2.037,2.081,2.125,2.168,2.211,2.252,2.294
1190 '
1200 FOR J=1 TO 14 :READ TK(J) :NEXT J
1210 DATA 0.02384,0.02461,0.02538,0.02614,0.02687,0.02759,0.02830
1220 DATA 0.02900,0.02970,0.03039,0.03107,0.03173,0.03239,0.03305
1230 '
1240 FOR J=1 TO 8 :READ TPR(J) :NEXT J
1250 DATA 0.719,0.713,0.708,0.703,0.699,0.695,0.691,0.689
1260 '
1270 READ L,KGD,R,WAVE,G
1280 DATA 0.600,1.504E-04,287.0967,6.328E-07,9.806
1290 '
1300 SCREEN 0
1310 KEY OFF
1320 WIDTH 80
1330 '
1340 CLR$="                                                                "
1350 FOR I=1  TO  3 :LOCATE I,1 :PRINT CLR$;CLR$; :NEXT I
1360 LOCATE 1,1
1370 PRINT TAB(10) "RA  - Calculation of experimental parameters"
1380 PRINT TAB(10) "for heat transfer experiments                "
1390 PRINT TAB(10) "      by Michael Papple                      "
1400 DOTS$ = "........................................."
1410 PRINT DOTS$;DOTS$
1420 '
1430 FOR I=21 TO 24 :LOCATE I,1 :PRINT CLR$;CLR$; :NEXT I
1440 FOR I=5  TO 19 :LOCATE I,1 :PRINT CLR$;CLR$; :NEXT I
1450 COLOR 1,0
1460 LOCATE 7,10 :PRINT "Available Geometries"
1470 COLOR 2,0
1480 LOCATE 20,1 :PRINT DOTS$;DOTS$
1490 LOCATE 22,1 :PRINT TAB(5) "Select geometry using ";CHR$(24);
1500 PRINT CHR$(25);" and  CR  "
1510 LOCATE 23,1 :PRINT TAB(5) "To quit enter (Q/q/E/e)";
1520 '
```

```
1530 LOCATE  9,6 :PRINT "Horizontal square cavities"
1540 LOCATE 10,6 :PRINT "Inclined square ducts with differentially";
1550 PRINT " heated sides"
1560 LOCATE 11,6 :PRINT "Inclined isothermal square ducts"
1570 LOCATE 12,6 :PRINT "Inclined isothermal tubes"
1580 '
1590 ITOP=9 :IBOTT=12 :ICH=11
1600 LOCATE ICH,5,1,0,7
1610 ANS$=INKEY$ :IF ANS$="" THEN 1610
1620 IF ANS$="Q" OR ANS$="q" OR ANS$="E" OR ANS$="e" THEN 1730
1630  IF ANS$=CHR$(31) THEN IF ICH IBOTT THEN ICH=ICH+1 ELSE ICH=ITOP
1640  IF ANS$=CHR$(30) THEN IF ICH ITOP  THEN ICH=ICH-1 ELSE ICH=IBOTT
1650 LOCATE ICH,5,1,0,7 :IF ANS$  CHR$(13) THEN 1610
1660 ISEL=CSRLIN :ISEL=ISEL-ITOP+1
1670 '
1680 ON ISEL GOTO 1760,2990,5080,6570
1690 '
1700                                    'ending program.
1710 LOCATE 23,1
1720 ANS$=INKEY$ :IF ANS$  " " AND ANS$  CHR$(13) THEN 1720
1730 CLS
1740 KEY ON
1750 END
1760 '+++++++++++++++++++++++++++++++++++++++++++++++++++++++++++++++++++++++
1770 '      This subroutine examines the horizontal square cavity.
1780 '
1790 '
1800 FOR I=21 TO 24 :LOCATE I,1 :PRINT CLR$;CLR$; :NEXT I
1810 FOR I=5  TO 19 :LOCATE I,1 :PRINT CLR$;CLR$; :NEXT I
1820 FOR I=1  TO  3 :LOCATE I,1 :PRINT CLR$;CLR$; :NEXT I
1830 COLOR 1,0
1840 LOCATE 2,10 :PRINT "HORIZONTAL SQUARE CAVITY"
1850 LOCATE 7,10 :PRINT "Select option (1 or 2)"
1860 COLOR 2,0
1870 LOCATE  9,6
1880 PRINT "1) Calculate cavity width with ";CHR$(235);"T specified."
1890 LOCATE,10,6
1900 PRINT "2) Calculate ";CHR$(235);"T for a given cavity."
1910 LOCATE 22,6 :PRINT "Select geometry again :type  space bar "
1920 LOCATE 12,20
1930 AHCS$=INKEY$ :IF AHCS$="" THEN 1930
1940  IF AHCS$="1" THEN 1990
1950  IF AHCS$="2" THEN 2430
1960  IF AHCS$=" " THEN 1330
1970 IF AHCS$="Q" OR AHCS$="q" OR AHCS$="E" OR AHCS$="e" THEN 1730
1980 END
1990 '++++++++++++
2000 '          Subroutine
2010 '          Horizontal.cavity
2020 '          2A with dT specified
2030 '
2040 FOR I=21 TO 24 :LOCATE I,1 :PRINT CLR$;CLR$; :NEXT I
```

```
2050 FOR I=5  TO 19 :LOCATE I,1 :PRINT CLR$;CLR$; :NEXT I
2060 LOCATE 7,10 :PRINT "Cavity widths with ";CHR$(235);
                        "T and RAcr specified."
2070 LOCATE 10,10 :PRINT "Enter these values:"
2080 LOCATE 12,10 :PRINT "T2 ";CHR$(248);"C     ";
2090 INPUT "",T2
2100 LOCATE 13,10 :PRINT "T1 ";CHR$(248);"C     ";
2110 INPUT "",T1
2120 LOCATE 14,10 :PRINT "P (mm Hg) ";
2130 INPUT "",PO
2140 '
2150 DT=T1-T2
2160 TF=.5*(T1+T2) +273.15 :TI =T2
2170 GOSUB 7300                              'Air properties.
2180 CDF= 1.5 *L *P *KGD /(WAVE *R)
2190 DF = CDF *(1!/(T2+273.15) -1!/(T1+273.15))
2200 FOR I=10 TO 14 :LOCATE I,1 :PRINT CLR$;CLR$; :NEXT I
2210 LOCATE 10,1
2220 PRINT "     T1 = ";T1  :PRINT "     T2 = ";T2
2230 PRINT "     PO = ";PO  :PRINT "     P  = ";P
2240 PRINT "     DT = ";DT  :PRINT "     DF = ";DF
2250 PRINT
2260 LOCATE 11,25 :PRINT "  A         2A          RAcr"
2270 C  = G *DT /TF *PR /(VNU*VNU)
2280 RACR= 1000!
2290 FOR I=1 TO 5
2300  A2 = (RACR /C) (1!/3!)
2310  A  = A2 /2!
2320 LOCATE I+12,25 :PRINT USING "#.######";A
2330 LOCATE I+12,34 :PRINT USING "#.######";A2
2340 LOCATE I+12,44 :PRINT USING "######.#";RACR
2350  RACR= RACR *SQR(10!)
2360 NEXT I
2370 FOR I=21 TO 24 :LOCATE I,1 :PRINT CLR$;CLR$; :NEXT I
2380 LOCATE 22,10 :PRINT "Press  space bar  to continue";
2390 AHSC2$=INKEY$ :IF AHSC2$="" THEN 2390
2400 IF AHSC2$=" " GOTO 1760
2410 GOTO 1730
2420 END
2430 '++++++++++
2440 '          Subroutine
2450 '          Horizontal cavity
2460 '          dT with 2A and RAcr specified
2470 '
2480 FOR I=21 TO 24 :LOCATE I,1 :PRINT CLR$;CLR$; :NEXT I
2490 FOR I=5  TO 19 :LOCATE I,1 :PRINT CLR$;CLR$; :NEXT I
2500 LOCATE 7,10 :PRINT CHR$(235);"T with cavity width and RAcr specified."
2510 LOCATE 10,10 :PRINT "Enter these values:"
2520 LOCATE 12,10 :PRINT "T2 ";CHR$(248);"C     ";
2530 INPUT "",T2 :TI =T2
2540 LOCATE 13,10 :PRINT "P (mm Hg) ";
2550 INPUT "",PO
```

```
2560 LOCATE 14,10 :PRINT "2A (m)     ";
2570 INPUT "",A2
2580 LOCATE 15,10 :PRINT "RAcr       ";
2590 INPUT "",RACRS
2600 '
2610 A   = A2 /2!
2620 CDF= 1.5 *L *KGD /(WAVE *R)
2630 C   = G*A2*A2*A2
2640 RACRO= 0!
2650 T10  = T2
2660 T1   = T2 +30!
2670 RACROO= RACRO                          'start of loop
2680  T100 = T10
2690  T10  = T1
2700  TF   = .5*(T10 +T2) +273.15
2710   GOSUB 7300
2720  RACRO= C *(T10 -T2)/TF *PR /(VNU*VNU)
2730 T1    = T10 +(T100 -T10) *(RACRS -RACRO) /(RACROO -RACRO)
2740 IF ABS(T1-T10) .1 OR ABS(T1-T100) .1 THEN 2670
2750  TF    = .5*(T1 +T2) +273.15
2760  GOSUB 7300
2770 RACR    = C *(T1-T2)/TF *PR /(VNU*VNU)
2780 CDF     = CDF *P
2790 DF   = CDF *(1!/(T2+273.15) -1!/(T1+273.15))
2800 DT   = T1 -T2
2810 '
2820 FOR I=21 TO 24 :LOCATE I,1 :PRINT CLR$;CLR$; :NEXT I
2830 FOR I=10 TO 19 :LOCATE I,1 :PRINT CLR$;CLR$; :NEXT I
2840 LOCATE 10,10 :PRINT "T2  =";  :PRINT USING "###.##";T2;
2850 PRINT TAB(30);"PO =";  :PRINT USING "####.#";PO
2860 LOCATE 11,10 :PRINT "A   = ";  :PRINT USING "#.######";A;
2870 PRINT TAB(30);"2A = ";  :PRINT USING "#.######";A2
2880 PRINT TAB(10);"RAcr= ";RACR
2890 LOCATE 14,10 :PRINT "P  =";  :PRINT USING "#######.#";P
2900 PRINT TAB(10);"T1 = ";  :PRINT USING "###.##";T1
2910 PRINT TAB(10);CHR$(235);"T = ";  :PRINT USING "###.##";DT
2920 PRINT TAB(10);CHR$(235);"F = ";  :PRINT USING "###.##";DF
2930 FOR I=21 TO 24 :LOCATE I,1 :PRINT CLR$;CLR$; :NEXT I
2940 LOCATE 22,10 :PRINT "Press  space bar  to continue";
2950 AHSC2$=INKEY$ :IF AHSC2$="" THEN 2390
2960 IF AHSC2$=" " GOTO 1760
2970 GOTO 1730
2980 END
2990 '+++++++++++++++++++++++++++++++++++++++++++++++++++++++++++++++++++++++
3000 '        This subroutine examines inclined square ducts with
3010 '        differentially heated sides.
3020 '
3030 '
3040 FOR I=21 TO 24 :LOCATE I,1 :PRINT CLR$;CLR$; :NEXT I
3050 FOR I=5  TO 19 :LOCATE I,1 :PRINT CLR$;CLR$; :NEXT I
3060 FOR I=1  TO  3 :LOCATE I,1 :PRINT CLR$;CLR$; :NEXT I
3070 COLOR 1,0
```

```
3080 LOCATE 2,10 :PRINT "INCLINED DIFFERENTIALLY HEATED DUCT"
3090 LOCATE 7,10 :PRINT "Select option (1 or 2)"
3100 COLOR 2,0
3110 LOCATE  9,6
3120 PRINT "1) Calculate duct width with ";CHR$(235);"T specified."
3130 LOCATE 10,6
3140 PRINT "2) Calculate ";CHR$(235);"T for a given duct."
3150  LOCATE 22,6 :PRINT "Select geometry again: type  space bar "
3160 LOCATE 12,20
3170 ADHS$=INKEY$ :IF ADHS$="" THEN 3170
3180  IF ADHS$="1" THEN 3230
3190  IF ADHS$="2" THEN 4030
3200  IF ADHS$=" " THEN 1330
3210 GOTO 1730
3220 END
3230 '++++++++++
3240 '          Subroutine
3250 '          Inclined differentially heated duct.
3260 '          2A with dT specified
3270 '
3280 FOR I=21 TO 24 :LOCATE I,1 :PRINT CLR$;CLR$; :NEXT I
3290 FOR I=5  TO 19 :LOCATE I,1 :PRINT CLR$;CLR$; :NEXT I
3300 LOCATE 7,10 :PRINT "Duct widths with ";CHR$(235);
                        "T and RAcr specified."
3310 LOCATE 10,10 :PRINT "Enter these values:"
3320 LOCATE 12,10 :PRINT "T";CHR$(236);" ";CHR$(248);"C          ";
3330 INPUT "",TI
3340 LOCATE 13,10 :PRINT "TB ";CHR$(248);"C          ";
3350 INPUT "",TB
3360 LOCATE 14,10 :PRINT "P (mm Hg)          ";
3370 INPUT "",PO
3380 '
3390 TF=.5*(TB+TI) +273.15
3400 GOSUB 7300                          'Air properties.
3410 CDF= 1.5 *L *P *KGD /(WAVE *R)
3420 LOCATE 15,10 :PRINT CHR$(233);" (T2-TI)/(T1-TI) ";
3430 INPUT "",THETA
3440 T2 = ( (1! -THETA)*TI +2!*THETA*TB )/(1!+THETA)
3450 T1 = 2!*TB -T2
3460 DT1=T1 -TI
3470 DT2=T2 -TI
3480 DF1= CDF *(1!/(TI+273.15) -1!/(T1+273.15))
3490 DF2= CDF *(1!/(TI+273.15) -1!/(T2+273.15))
3500 FOR I=10 TO 15 :LOCATE I,1 :PRINT CLR$;CLR$; :NEXT I
3510 LOCATE 10,1
3520 PRINT "     TI = ";TI  :PRINT "     TB = ";TB
3530 PRINT "     PO = ";PO  :PRINT "     P  = ";P
3540 LOCATE 13,1 :PRINT "     ";CHR$(233);"  = ";THETA;"      "
3550 PRINT "     T1 = ";T1  :PRINT "     T2 = ";T2
3560 PRINT "     DT1= ";DT1 :PRINT "     DT2= ";DT2
3570 PRINT "     DF1= ";DF1 :PRINT "     DF2= ";DF2
3580 '
```

```
3590 CLR2$="
3600 FOR I=10 TO 17 :LOCATE I,25 :PRINT CLR2$ :NEXT I
3610 LOCATE 22,5
3620 PRINT "Enter ";CHR$(235);" -angle in inclination (degrees)";
3630 INPUT "";DLT
3640 DDLT = DLT *PI /180!
3650 LOCATE 10,35 :PRINT CHR$(235);" =";
3660 PRINT USING "###.#";DLT; :PRINT CHR$(248)
3670 IF ABS(DLT) <1! THEN 3830
3680 LOCATE 11,25 :PRINT "  A        2A        RAcr      RA      Ratio"
3690 C   = G *SIN(DDLT) *(T1 -T2) /TF *PR /(VNU*VNU)
3700 RACR= 1000!
3710 FOR I=1 TO 5
3720  A2 = (RACR /C) (1!/3!)
3730  A  = A2 /2!
3740 RATIO= TAN(DDLT) *(T1 -T2)/(TB -TI) *8!*L /A
3750 RA   = RACR /RATIO
3760 LOCATE I+12,25 :PRINT USING "#.######";A
3770 LOCATE I+12,34 :PRINT USING "#.######";A2
3780 LOCATE I+12,44 :PRINT USING "######.#";RACR
3790 LOCATE I+12,53 :PRINT USING "####.###";RA
3800 LOCATE I+12,62 :PRINT USING "#####.##";RATIO
3810 RACR = RACR *SQR(10!) :NEXT I
3820 GOTO 3950
3830 LOCATE 11,25 :PRINT "  A        2A        RAcr      RA"
3840 C   = G *COS(DDLT) *(TB -TI)/TF *PR/(VNU*VNU*L)
3850 RACR= 0!
3860 RA  = 10!
3870 FOR I=1 TO 5
3880  A  = (RA /C) .25
3890  A2 = A *2!
3900 LOCATE I+12,25 :PRINT USING "#.######";A
3910 LOCATE I+12,34 :PRINT USING "#.######";A2
3920 LOCATE I+12,44 :PRINT USING "######.#";RACR
3930 LOCATE I+12,53 :PRINT USING "####.###";RA
3940 RA  = RA *SQR(10!) :NEXT I
3950 '
3960 FOR I=21 TO 24 :LOCATE I,1 :PRINT CLR$;CLR$; :NEXT I
3970 LOCATE 22,10 :PRINT "Another angle  (y/n) ";
3980 ANG$=INKEY$ :IF ANG$="" THEN 3980
3990 IF ANG$="Y" OR ANG$="y" THEN 3580
4000 IF ANG$="Q" OR ANG$="q" OR ANG$="E" OR ANG$="e" THEN 1730
4010 GOTO 2990
4020 END
4030 '++++++++++
4040 '          Subroutine
4050 '          Inclined differentially heated duct.
4060 '          dT with 2A and RAcr specified
4070 '
4080 FOR I=21 TO 24 :LOCATE I,1 :PRINT CLR$;CLR$; :NEXT I
4090 FOR I=5 TO 19 :LOCATE I,1 :PRINT CLR$;CLR$; :NEXT I
4100 LOCATE 7,10 :PRINT CHR$(235);"T with duct width and RAcr specified."
```

```
4110 LOCATE 10,10 :PRINT "Enter these values:"
4120 LOCATE 12,10 :PRINT "T";CHR$(236);" ";CHR$(248);"C      ";
4130 INPUT "",TI
4140 LOCATE 13,10 :PRINT "P (mm Hg) ";
4150 INPUT "",PO
4160 LOCATE 14,10 :PRINT "2A (m)  ";
4170 INPUT "",A2
4180 LOCATE 15,10 :PRINT CHR$(233);"          ";
4190 INPUT "",THETA
4200 LOCATE 16,10 :PRINT CHR$(235);"          ";
4210 INPUT "",DLT
4220 LOCATE 17,10
4230 IF ABS(DLT) 1! THEN PRINT "RAcr      "; :INPUT "",RACRS
4240 IF ABS(DLT) =1! THEN PRINT "RA       "; :INPUT "",RAS
4250 '
4260 A  = A2 /2!
4270 CDF= 1.5 *L *KGD /(WAVE *R)
4280 '
4290 DDLT = DLT *PI /180!
4300 IF ABS(DLT) 1! THEN 4560
4310 C  = G*SIN(DDLT)*A2*A2*A2          'for DLT 1
4320 RACRO= 0!
4330 T10  = TI
4340 T1   = TI +30!
4350 RACROO= RACRO                      'start of loop
4360  T100 = T10
4370  T10  = T1
4380  TBO  = .5*(T10 +T2)
4390   TF  = .5*(TBO +TI) +273.15
4400   GOSUB 7300
4410  RACRO= C *(T10 -T2)/TF *PR /(VNU*VNU)
4420 T1    = T10 +(T100 -T10) *(RACRS -RACRO) /(RACROO -RACRO)
4430 IF ABS(T1-T10) .1 OR ABS(T1-T100) .1 THEN 4350
4440 TB = .5*(T1 +T2)
4450  TF    = .5*(TB +TI) +273.15
4460  GOSUB 7300
4470 RACR   = C *(T1-T2)/TF *PR /(VNU*VNU)
4480 CDF    = CDF *P
4490 DF1 = CDF *(1!/(TI+273.15) -1!/(T1+273.15))
4500 DF2 = CDF *(1!/(TI+273.15) -1!/(T2+273.15))
4510 DT1 = T1 -TI
4520 DT2 = T2 -TI
4530 RATIO= TAN(DDLT) *(T1-T2) /(TB-TI) *8! *L /A
4540 RA   = RACR /RATIO
4550 GOTO 4820
4560 '
4570 C   = G*COS(DDLT)*A*A*A*A /L       'for DLT 1
4580 RA0 = 0!
4590 T10 = TI
4600 T1  = TI +30!
4610 RA00= RA0                          'start of loop
4620  T100 = T10
```

```
4630  T10  = T1
4640  TBO  = .5*(T10 +T2)
4650   TF  = .5*(TBO +TI) +273.15
4660   GOSUB 7300
4670  RAO  = C *(TBO -TI)/TF *PR /(VNU*VNU)
4680 T1    = T10 +(T100 -T10) *(RACRS -RACRO) /(RACRO -RACRO)
4690 IF ABS(T1-T10) .1 OR ABS(T1-T100) .1 THEN 4350
4700 TB  = .5*(T1 +T2)
4710  TF = .5*(TB +TI) +273.15
4720  GOSUB 7300
4730 RA  = C *(TB-TI)/TF *PR /(VNU*VNU)
4740 CDF = CDF *P
4750 DF1 = CDF *(1!/(TI+273.15) -1!/(T1+273.15))
4760 DF2 = CDF *(1!/(TI+273.15) -1!/(T2+273.15))
4770 DT1 = T1 -TI
4780 DT2 = T2 -TI
4790 RATIO= TAN(DDLT) *(T1-T2) /(TB-TI) *8! *L /A
4800 RACR = RA *RATIO
4810 '
4820 FOR I=10 TO 19 :LOCATE I,1 :PRINT CLR$;CLR$; :NEXT I
4830 LOCATE 10,10 :PRINT "T";CHR$(236);"   ="; :PRINT USING "###.##";TI;
4840 PRINT TAB(35);"PO   = "; :PRINT USING "####.#";PO;
4850 PRINT TAB(60);"A    = "; :PRINT USING "#.######";A
4860 PRINT TAB(10);CHR$(233);"    = "; :PRINT USING "##.#";THETA;
4870 PRINT TAB(35);"P    = "; :PRINT USING "#######.#";P;
4880 PRINT TAB(60);"2A   = "; :PRINT USING "#.######";A2 :PRINT
4890 PRINT TAB(10);CHR$(235);"    = "; :PRINT USING "##.#";DLT
4900 PRINT TAB(10);"RA   = "; :PRINT USING "####.##";RA
4910 PRINT TAB(10);"RAcr = "; :PRINT USING "######.#";RACR
4920 IF ABS(DLT) 1! THEN PRINT :GOTO 4940
4930 PRINT TAB(10);"Ratio= "; :PRINT USING "######.#";RATIO
4940 PRINT TAB(10);"T1   = "; :PRINT USING "###.##";T1;
4950 PRINT TAB(35);CHR$(235);"T1   = "; :PRINT USING "###.##";DT1;
4960 PRINT TAB(60);CHR$(235);"F1   = "; :PRINT USING "###.##";DF1
4970 PRINT TAB(10);"T2   = "; :PRINT USING "###.##";T2;
4980 PRINT TAB(35);CHR$(235);"T2   = "; :PRINT USING "###.##";DT2;
4990 PRINT TAB(60);CHR$(235);"F2   = "; :PRINT USING "###.##";DF2
5000 '
5010 FOR I=21 TO 24 :LOCATE I,1 :PRINT CLR$;CLR$; :NEXT I
5020 LOCATE 22,10 :PRINT "New parameters (y/n)";
5030 ADHS2$=INKEY$ :IF ADHS2$="" THEN 5030
5040 IF ADHS2$="Y" OR ADHS2$="y" THEN 4030
5050 IF ADHS2$="Q" OR ADHS2$="q" OR ADHS2$="E" OR ADHS2$="e" THEN 1730
5060 GOTO 2990
5070 END
5080 '++++++++++++++++++++++++++++++++++++++++++++++++++++++++++++++++++++++
5090 '    This subroutine examines the inclined isothermal square duct.
5100 '
5110 '
5120 FOR I=21 TO 24 :LOCATE I,1 :PRINT CLR$;CLR$; :NEXT I
5130 FOR I=5  TO 19 :LOCATE I,1 :PRINT CLR$;CLR$; :NEXT I
5140 FOR I=1  TO  3 :LOCATE I,1 :PRINT CLR$;CLR$; :NEXT I
```

```
5150 COLOR 1,0
5160 LOCATE 2,10 :PRINT "INCLINED ISOTHERMAL SQUARE DUCT"
5170 LOCATE 7,10 :PRINT "Select option (1 or 2)"
5180 COLOR 2,0
5190 LOCATE  9,6
5200 PRINT "1) Calculate duct width with ";CHR$(235);"T specified."
5210 LOCATE 10,6
5220 PRINT "2) Calculate ";CHR$(235);"T for a given duct."
5230  LOCATE 22,6 :PRINT "Select geometry again :type. space bar "
5240 LOCATE 12,20
5250 AIID$=INKEY$ :IF AIID$="" THEN 5250
5260  IF AIID$="1" THEN 5320
5270  IF AIID$="2" THEN 5930
5280  IF AIID$=" " THEN 1330
5290 IF AIID$="Q" OR AIID$="q" OR AIID$="E" OR AIID$="e" THEN 1730
5300 GOTO 1730
5310 END
5320 '++++++++++
5330 '          Subroutine
5340 '          Inclined isothermal square duct.
5350 '          2A with dT specified
5360 '
5370 FOR I=21 TO 24 :LOCATE I,1 :PRINT CLR$;CLR$; :NEXT I
5380 FOR I=5  TO 19 :LOCATE I,1 :PRINT CLR$;CLR$; :NEXT I
5390 LOCATE 7,10  :PRINT "Duct widths with ";CHR$(235);"T and RA specified."
5400 LOCATE 10,10 :PRINT "Enter these values:"
5410 LOCATE 12,10 :PRINT "T";CHR$(236);" ";CHR$(248);"C     ";
5420 INPUT "",TI
5430 LOCATE 13,10 :PRINT "Ts ";CHR$(248);"C     ";
5440 INPUT "",TS
5450 LOCATE 14,10 :PRINT "P (mm Hg) ";
5460 INPUT "",PO
5470 '
5480 DT=TS-TI
5490 TF = .5*(TS+TI) +273.15
5500 GOSUB 7300                    'Air properties.
5510 CDF= 1.5 *L *P *KGD /(WAVE *R)
5520 DF = CDF *(1!/(TI+273.15) -1!/(TS+273.15))
5530 FOR I=10 TO 15 :LOCATE I,1 :PRINT CLR$;CLR$; :NEXT I
5540 LOCATE 10,1
5550 PRINT "     TI= "; :PRINT USING "##.##";TI
5560 PRINT "     Ts= "; :PRINT USING "##.##";TS
5570 PRINT "     DT= "; :PRINT USING "##.##";DT
5580 PRINT "     PO= "; :PRINT USING "###.#";PO
5590 PRINT "     P = "; :PRINT USING "######.#";P
5600 PRINT "     DF= "; :PRINT USING "##.##";DF
5610 FOR I=16 TO 19 :LOCATE I,1 :PRINT CLR$;CLR$; :NEXT I
5620 FOR I=21 TO 24 :LOCATE I,1 :PRINT CLR$;CLR$; :NEXT I
5630 LOCATE 22,10
5640 PRINT "Enter ";CHR$(235);" -angle in inclination (degrees) ";
5650 INPUT "";DLT
5660 LOCATE 22,1 :PRINT CLR$;CLR$;
```

```
5670 LOCATE 10,35 :PRINT CHR$(235);" =";
5680 PRINT USING "###.#";DLT; :PRINT CHR$(248)
5690 LOCATE 11,25 :PRINT "  A        2A         RA       RAcr     Ratio"
5700 DDLT = DLT *3.141592654# /180!
5710 C  = G *COS(DDLT) *DT /TF *PR /(VNU*VNU *L)
5720 RA = 10!
5730 NO=5 :FACT=SQR(10!)
5740 FOR I=1 TO NO
5750  A = (RA /C) .25
5760  A2= A *2!
5770 RATIO= TAN(DDLT) *8!*L /A
5780 RACR = RA *RATIO
5790 LOCATE I+12,25 :PRINT USING "#.######";A
5800 LOCATE I+12,34 :PRINT USING "#.######";A2
5810 LOCATE I+12,44 :PRINT USING "####.#";RA
5820 LOCATE I+12,53 :PRINT USING "######.#";RACR
5830 LOCATE I+12,62 :PRINT USING "#####.##";RATIO
5840  RA = RA *FACT
5850 NEXT I
5860 LOCATE 22,1 :PRINT CLR$;CLR$;
5870 LOCATE 22,10 :PRINT "Another angle  (y/n) ";
5880 AIID2$=INKEY$ :IF AIID2$="" THEN 5880
5890 IF AIID2$="Y" OR AIID2$="y" THEN 5620
5900 IF AIID2$="Q" OR AIID2$="q" OR AIID2$="E" OR AIID2$="e" THEN 1730
5910 GOTO 5080
5920 END
5930 '++++++++++
5940 '          Subroutine
5950 '          Inclined isothermal square duct
5960 '          dT with 2A and RA specified
5970 '
5980 FOR I=21 TO 24 :LOCATE I,1 :PRINT CLR$;CLR$; :NEXT I
5990 FOR I=5  TO 19 :LOCATE I,1 :PRINT CLR$;CLR$; :NEXT I
6000 LOCATE 7,10 :PRINT CHR$(235);"T with duct width and RA specified."
6010 LOCATE 10,10 :PRINT "Enter these values:"
6020 LOCATE 12,10 :PRINT "T";CHR$(236);" (";CHR$(248);"C)    ";
6030 INPUT "",TI
6040 LOCATE 13,10 :PRINT "P (mm Hg)  ";
6050 INPUT "",PO
6060 LOCATE 14,10 :PRINT "2A (m)     ";
6070 INPUT "",A2
6080 LOCATE 15,10 :PRINT CHR$(235);"          ";
6090 INPUT "",DLT
6100 LOCATE 16,10 :PRINT "RA         ";
6110 INPUT "",RAS
6120 '
6130 A  = A2 /2!
6140 CDF= 1.5 *L *KGD /(WAVE *R)
6150 DDLT= DLT *PI /180!
6160 C  = G*COS(DDLT)*A*A*A*A /L
6170 RAO= 0!
6180 TSO  = TI
```

```
6190 TS    = TI +30!
6200 RA00= RA0                              'start of loop
6210  TS00 = TS0
6220  TS0  = TS
6230   TF  = .5*(TS0 +TI) +273.15
6240   GOSUB 7300
6250  RA0= C *(TS0 -TI)/TF *PR /(VNU*VNU)
6260 TS    = TS0 +(TS00 -TS0) *(RAS -RA0) /(RA00 -RA0)
6270 IF ABS(TS-TS0) .1 OR ABS(TS-TS00) .1 THEN 6200
6280  TF    = .5*(TS +TI) +273.15
6290  GOSUB 7300
6300 RA    = C *(TS-TI)/TF *PR /(VNU*VNU)
6310 CDF    = CDF *P
6320 DF  = CDF *(1!/(TI+273.15) -1!/(TS+273.15))
6330 DT  = TS -TI
6340 RATIO= TAN(DDLT) *8! *L /A
6350 RACR = RA *RATIO
6360 '
6370 FOR I=10 TO 19 :LOCATE I,1 :PRINT CLR$;CLR$; :NEXT I
6380 LOCATE 10,10 :PRINT "T";CHR$(236);"   ="; :PRINT USING "###.##";TI;
6390 PRINT TAB(35);"P0   = "; :PRINT USING "####.#";P0;
6400 PRINT,TAB(60);"A    = "; :PRINT USING "#.######";A
6410 PRINT TAB(35);"P    = "; :PRINT USING "#######.#";P;
6420 PRINT TAB(60);"2A   = "; :PRINT USING "#.######";A2
6430 PRINT TAB(10);CHR$(235);"    = "; :PRINT USING "##.#";DLT
6440 PRINT TAB(10);"RA   = "; :PRINT USING "####.##";RA
6450 PRINT TAB(10);"RAcr = "; :PRINT USING "######.#";RACR
6460 PRINT TAB(10);"Ratio= "; :PRINT USING "######.#";RATIO
6470 PRINT TAB(10);"Ts   = "; :PRINT USING "###.##";TS
6480 PRINT TAB(10);CHR$(235);"T   = "; :PRINT USING "###.##";DT
6490 PRINT TAB(10);CHR$(235);"F   = "; :PRINT USING "###.##";DF
6500 FOR I=21 TO 24 :LOCATE I,1 :PRINT CLR$;CLR$; :NEXT I
6510 LOCATE 22,10 :PRINT "New parameters  (y/n)";
6520 AIID2$=INKEY$ :IF AIID2$="" THEN 6520
6530 IF AIID2$="Y" OR AIID2$="y" THEN 5930
6540 IF AIID2$="Q" OR AIID2$="q" OR AIID2$="E" OR AIID2$="e" THEN 1730
6550 GOTO 5080
6560 END
6570 '+++++++++++++++++++++++++++++++++++++++++++++++++++++++++++++++++++++
6580 '    This subroutine examines the inclined isothermal tube.
6590 '
6600 '
6610 FOR I=21 TO 24 :LOCATE I,1 :PRINT CLR$;CLR$; :NEXT I
6620 FOR I=5  TO 19 :LOCATE I,1 :PRINT CLR$;CLR$; :NEXT I
6630 FOR I=1  TO  3 :LOCATE I,1 :PRINT CLR$;CLR$; :NEXT I
6640 COLOR 1,0
6650 LOCATE 2,10 :PRINT "INCLINED ISOTHERMAL TUBE"
6660 COLOR 2,0
6670 '
6680 '          Inclined isothermal tube
6690 '          dT with L and RA specified
6700 '
```

```
6710 FOR I=21 TO 24 :LOCATE I,1 :PRINT CLR$;CLR$; :NEXT I
6720 FOR I=5  TO 19 :LOCATE I,1 :PRINT CLR$;CLR$; :NEXT I
6730 LOCATE 7,10 :PRINT CHR$(235);"T with tube length and RA specified."
6740 LOCATE 10,10 :PRINT "Enter these values:"
6750 LOCATE 12,10 :PRINT "T";CHR$(236);" (";CHR$(248);"C)    ";
6760 INPUT "",TI
6770 LOCATE 13,10 :PRINT "P (mm Hg)  ";
6780 INPUT "",PO
6790 LOCATE 14,10 :PRINT "L (m)      ";
6800 INPUT "",LTUBE
6810 LOCATE 15,10 :PRINT CHR$(235);"          ";
6820 INPUT "",DLT
6830 LOCATE 16,10 :PRINT "RA          ";
6840 INPUT "",RAS
6850 '
6860 A2 = .0251028
6870 A  = A2 /2!
6880 CDF= 1.5 *LTUBE *KGD /(WAVE *R)
6890 DDLT= DLT *PI /180!
6900 C  = G*COS(DDLT)*A*A*A*A /LTUBE
6910 RA0= 0!
6920 TS0  = TI
6930 TS   = TI +30!
6940 RA00= RA0                          'start of loop
6950  TS00 = TS0
6960  TS0  = TS
6970   TF   = .5*(TS0 +TI) +273.15
6980   GOSUB 7300
6990  RA0= C *(TS0 -TI)/TF *PR /(VNU*VNU)
7000 TS    = TS0 +(TS00 -TS0) *(RAS -RA0) /(RA00 -RA0)
7010 IF ABS(TS-TS0) .1 OR ABS(TS-TS00) .1 THEN 6940
7020  TF    =.5*(TS +TI) +273.15
7030  GOSUB 7300
7040 RA   = C *(TS-TI)/TF *PR /(VNU*VNU)
7050 CDF  = CDF *P
7060 DF   = CDF *(1!/(TI+273.15) -1!/(TS+273.15))
7070 DT   = TS -TI
7080 RATIO= TAN(DDLT) *8! *LTUBE /A
7090 RACR = RA *RATIO
7100 '
7110 FOR I=10 TO 19 :LOCATE I,1 :PRINT CLR$;CLR$; :NEXT I
7120 LOCATE 10,10 :PRINT "T";CHR$(236);"   ="; :PRINT USING "###.##";TI;
7130 PRINT TAB(35);"PO   = "; :PRINT USING "####.#";PO;
7140 PRINT,TAB(60);"L    = "; :PRINT USING "#.###";LTUBE
7150 PRINT TAB(35);"P    = "; :PRINT USING "######.#";P;
7160 PRINT TAB(60);"2A   = "; :PRINT USING "#.######";A2
7170 PRINT TAB(10);CHR$(235);"   = "; :PRINT USING "##.#";DLT
7180 PRINT TAB(10);"RA   = "; :PRINT USING "####.##";RA
7190 PRINT TAB(10);"RAcr = "; :PRINT USING "######.#";RACR
7200 PRINT TAB(10);"Ratio= "; :PRINT USING "######.#";RATIO
7210 PRINT TAB(10);"Ts   = "; :PRINT USING "###.##";TS
7220 PRINT TAB(10);CHR$(235);"T   = "; :PRINT USING "###.##";DT
```

```
7230 PRINT TAB(10);CHR$(235);"F    = "; :PRINT USING "###.##";DF
7240 LOCATE 22,10 :PRINT "New parameters  (y/n)";
7250 AIIT2$=INKEY$ :IF AIIT2$="" THEN 7250
7260 IF AIIT2$="Y" OR AIIT2$="y" THEN 6710
7270 IF AIIT$="Q" OR AIIT$="q" OR AIIT$="E" OR AIIT$="e" THEN 1730
7280 GOTO 1330
7290 END
7300 '++++++++++++++++++++++++++++++++++++++++++++++++++++++++++++++++++++++
7310 '              This subroutine PROP interpolates
7320 '              for the air properties.
7330 '
7340 '
7350 '
7360                                        'interpolate.
7370 G    = 9.806
7380 P = P0 /1000! *9.80665*(13598.571# -2.54286*TI)
7390 FOR IG=27 TO 39
7400  I=IG-26
7410  T = IG*10
7420  TP= T+10!
7430  IF TF =T THEN 7490
7440  IF TF TP THEN 7490
7450   F    = (TF-T)/(TP-T)
7460   VMU = (TVMU(I) +F*(TVMU(I+1)-TVMU(I)))*.00001
7470   VNU = VMU *R *TF /P
7480   K    = TK(I) +F*(TK(I+1)-TK(I))
7490 NEXT IG
7500 FOR IG=13 TO 19
7510  I  =IG-12
7520  T =IG*20
7530  TP=T+20!
7540  IF TF =T THEN 7580
7550  IF TF TP THEN 7580
7560   F = (TF-T)/(TP-T)
7570   PR= TPR(I) +F*(TPR(I+1)-TPR(I))
7580 NEXT IG
7590 '
7600 RETURN
7610 '++++++++++++++++++++++++++++++++++++++++++++++++++++++++++++++++++++++
```

APPENDIX C

ANALYSIS OF INCLINED ISOTHERMAL DUCT INTERFEROGRAMS

The following program, IID.BAS, accepts the data from the fringe location measurements interactively, and calculates and plots the fringe shift and heat transfer profiles. This program was written in BASIC on a Tandy 2000 personal computer. The resolution of the monitor was 640x400 pixels. If this program were to be run on another computer with a different resolution, the graphics statements would have to be rewritten to be compatible.

```
1010 '
1020 '      This program IID.BAS reads in and analyses the fringe
1030 '      locations for the inclined isothermal square duct.
1040 '
1050 '          by Michael Papple
1060 '             87 02 13
1070 '
1080 '
1090 '      Set up defaults.
1100 '
1110 DEFINT I,J,M
1120 '
1130 KEY OFF
1140 WIDTH 80
1150 SCREEN 4
1160 LINE (  1,  1)-(638,398),1,BF
1170 LINE ( 11, 21)-(628,378),0,BF
1180 '
1190 LOCATE  6,10 :PRINT "              ++++++++++++++++++++++      "
1200 LOCATE  7,10 :PRINT "              +++       IID     +++      "
1210 LOCATE  8,10 :PRINT "              ++++++++++++++++++++++      "
1220 '
1230 '
1240 LOCATE 11,10
      :PRINT "This program reads in and analyses the fringe locations "
1250 LOCATE 12,10
      :PRINT "for inclined isothermal square ducts and shows the"
1260 LOCATE 13,10 :PRINT "fringe shift profiles and the Nusselt numbers."
1270 '
1280 '
1290 LOCATE 16,10 :PRINT "                    by Michael Papple "
1300 LOCATE 17,10 :PRINT "                       87 02 13       "
1310 '
1320 FOR I=1 TO 2000 :NEXT I              'pause for title page.
1330 CLS
1340 '
1350 DIM X(6),XR(6),FR(6),F(6)            'initialize variables.
1360 DIM TVMU(14),TK(14),TPR(8)
1370 READ KGD,WAVE,R,L,PI
1380 DATA 1.504E-04,6.328E-07,287.0987,0.600,3.141592654
1390                                      'initialize tables.
1400 FOR J=1 TO 14 :READ TVMU(J) :NEXT J
1410 DATA 1.707,1.757,1.805,1.853,1.900,1.946,1.992
1420 DATA 2.037,2.081,2.125,2.168,2.211,2.252,2.294
1430 '
1440 FOR J=1 TO 14 :READ TK(J) :NEXT J
1450 DATA 0.02384,0.02461,0.02538,0.02614,0.02687,0.02759,0.02830
1460 DATA 0.02900,0.02970,0.03039,0.03107,0.03173,0.03239,0.03305
1470 '
1480 FOR J=1 TO 8 :READ TPR(J) :NEXT J
1490 DATA 0.719,0.713,0.708,0.703,0.699,0.695,0.691,0.689
1500 '
```

```
1510 AANU3=0! :AANU4=0! :AANU5=0!
1520 '
1530 FOR ISURF=1 TO 4
1540 LINE (  1,  1)-(638,398),1,BF
1550 LINE (  4,283)-(325,395),0,BF
1560 LINE (340,283)-(635,395),0,BF
1570 '                                          preliminary info.
1580 LOCATE 19,8  :PRINT " COMMAND SECTION"
1590 LOCATE 19,44 :PRINT " PRELIMINARY INFO."
1600 LINE (1,301)-(638,301),1
1610 '
1620 IF ISURF  1 THEN IF ANSI$="Y" OR ANSI$="y" THEN 5450 ELSE 2280
1630 LOCATE 22,2 :PRINT "Read in old information?  (y/n) ";
1640 ANSI$=INKEY$ :IF ANSI$="" THEN 1640
1650 LINE (4,302)-(325,395),0,BF
1660 IF ANSI$="Y" OR ANSI$="y" THEN 5270
1670 '
1680 DT$=MID$(DATE$,9,2)+MID$(DATE$,1,2)+MID$(DATE$,4,2)
                        +" " +MID$(TIME$,1,5)
1690 LOCATE 20,2  :PRINT "Enter date and time of photograph"
1700 LOCATE 22,2  :PRINT "eg.  ";DT$
1710 LOCATE 23,2  :INPUT "     ",DTTM$ :IF DTTM$="" THEN DTTM$=DT$
1720 LINE (4,302)-(325,395),0,BF
1730 LOCATE 19,67 :PRINT DTTM$
1740 LINE (1,301)-(638,301),1
1750 '
1760 LOCATE 20,44 :PRINT " T";CHR$(236);" ="
1770 LOCATE 21,44 :PRINT " Ts ="
1780 LOCATE 22,44 :PRINT " PO ="
1790 LOCATE 23,44 :PRINT " P ="
1800 LOCATE 24,44 :PRINT " 2a=            ";CHR$(235);"  =";
1810 LOCATE 25,44 :PRINT " Ra=           Racr=";
1820 LINE (340,396)-(635,398),1,BF
1830 '
1840 LOCATE 20,2  :PRINT "Room and surface temperatures (";CHR$(248);"C)"
1850 LOCATE 22,2  :PRINT "enter T";CHR$(236); :INPUT "  ",TI
1860 LOCATE 23,2  :INPUT "enter TS  ",TS
1870 LINE (4,302)-(325,395),0,BF
1880 LOCATE 20,50 :PRINT USING "###.##";TI
1890 LOCATE 21,50 :PRINT USING "###.##";TS
1900 '
1910 LOCATE 20,2  :PRINT "room pressure (mm Hg)"
1920 LOCATE 22,2  :INPUT "enter PO  ",PO
1930 LINE (4,302)-(325,395),0,BF
1940 GOSUB 3180                          'evaluate air properties.
1950 LOCATE 22,50 :PRINT PO :LOCATE 23,50 :PRINT USING "######.#";P
1960 '
1970 LOCATE 20,2  :PRINT "duct width (m)"
1980 LOCATE 22,2  :INPUT "enter 2a  ",A2
1990 LINE (  4,302)-(325,395),0,BF
2000 LOCATE 24,50 :PRINT A2;
2010 A = A2 /2!
```

```
2020 '
2030 LOCATE 20,2  :PRINT "angle of inclination (degrees)"
2040 LOCATE 22,2  :PRINT "enter ";CHR$(235); :INPUT "  ",DELTA
2050 LINE (  4,302)-(325,395),0,BF
2060 LOCATE 24,67 :PRINT USING "###.#";DELTA;
2070 BETA = 1! /TF                          'calculate Rayleigh numbers.
2080 RA    = G*COS(DELTA*PI/180!)*BETA*(TS-TI)*A*A*A*A*PR /(VNU*VNU*L)
2090 RACR = G*SIN(DELTA*PI/180!)*BETA*(TS-TI)*A2*A2*A2*PR /(VNU*VNU)
2100 LOCATE 25,50 :PRINT USING "####.##";RA;
2110 LOCATE 25,67 :PRINT USING "######.##";RACR;
2120 LINE (340,396)-(635,398),1,BF
2130 '
2140 LOCATE 22,2 :PRINT "Enter preliminary info again?  (y/n) ";
2150 ANSP$=INKEY$ :IF ANSP$="" THEN 2150
2160 IF ANSP$="Y" OR ANSP$="y" THEN 1500
2170 LINE (  4,302)-(325,395),0,BF
2180 LINE (340,302)-(635,395),0,BF
2190 '
2200 IF ISURF  1 THEN 2270
2210 LINE (490,  4)-(635,279),0,BF
2220  GOSUB 6310
2230  LOCATE 21,2 :PRINT "Place interferogram under microscope,"
2240  LOCATE 22,2 :PRINT "Press  space bar  when ready."
2250  ANSG$=INKEY$ :IF ANSG$="" THEN 2250
2260 LINE (4,302)-(325,395),0,BF
2270 '
2280 LOCATE 20,62 :PRINT "WW1=           "
2290 LOCATE 21,62 :PRINT "WW2=           "
2300 LOCATE 22,62 :PRINT "W1 =           "
2310 LOCATE 23,62 :PRINT "W2 =           "
2320 '
2330 LOCATE 20,2  :PRINT "top and bottom wall locations (m)"
2340 LOCATE 22,2  :INPUT "enter WW1 ",WW1
2350 LOCATE 23,2  :INPUT "enter WW2 ",WW2
2360 LINE (4,302)-(325,395),0,BF
2370 LOCATE 20,67 :PRINT WW1 :LOCATE 21,67 :PRINT WW2
2380 '
2390 LOCATE 20,2  :PRINT "Near and far wall locations (m)"
2400 LOCATE 22,2  :INPUT "enter W1  ",W1
2410 LOCATE 23,2  :INPUT "enter W2  ",W2
2420 LINE (4,302)-(325,395),0,BF
2430 LOCATE 22,67 :PRINT W1 :LOCATE 23,67 :PRINT W2
2440 '
2450 LOCATE 22,2 :INPUT "Enter no. of scans  ";ISCAN
2460 LINE (4,302)-(325,395),0,BF
2470 '
2480 '
2490 GOSUB 4390                             'printing preliminary info.
2500 '
2510 ANU3=0! :ANU4=0! :ANU5=0!              'loop for scans.
2520 SCAN = 0! :ISC = 0
2530 SCAN = SCAN +.1 :ISC = ISC +1
```

```
2540 '                                          'inputing fringes.
2550 IF ANSI$="Y" OR ANSI$="y" THEN GOSUB 5770 ELSE GOSUB 3520
2560 GOSUB 3750                                 'calculate fringe shift profile.
2570 GOSUB 4090                                 'calculate Nusselt numbers.
2580 GOSUB 4740                                 'plot fringe shift profile.
2590 '
2600 IF ANSI$="Y" OR ANSI$="y" THEN 2660
2610 LINE (4,302)-(325,395),0,BF
2620 LOCATE 22,2 :PRINT "Enter fringe locations again?  (y/n) .";
2630 ANSF$=INKEY$ :IF ANSF$="" THEN 2630
2640 IF ANSF$="Y" OR ANSF$="y" THEN 2540
2650 '
2660 ANU3=ANU3 +NU3 :ANU4=ANU4 +NU4 :ANU5=ANU5 +NU5
2670 GOSUB 4620                                 'print results of scan.
2680 '
2690 LINE (4,302)-(325,395),0,BF
2700 LOCATE 21,2 :PRINT "Y / 2A = "; :PRINT USING "#.##";SCAN
2710 SLOC = WW1 +SCAN*(WW2 -WW1)
2720 LOCATE 22,2  :PRINT "scanning location on wall is ";
2730 PRINT USING "##.###";SLOC
2740 LOCATE 24,2
2750 IF ISC=ISCAN THEN PRINT "Press  space bar  or  cr  to continue"; ELSE
                       PRINT "Another scanning location?  (y/n) ";
2760 ANSC$=INKEY$
2770  IF ISC=ISCAN  AND ANSC$=" "       THEN 2850
2780  IF ISC=ISCAN  AND ANSC$=CHR$(13) THEN 2850
2790  IF ISC  ISCAN AND ANSC$="Y"       THEN 2530
2800  IF ISC  ISCAN AND ANSC$="y"       THEN 2530
2810  IF ISC  ISCAN AND ANSC$="N"       THEN 2850
2820  IF ISC  ISCAN AND ANSC$="n"       THEN 2850
2830  IF ANSC$="E" OR ANSC$="e" OR ANSC$="Q" OR ANSC$="q" THEN 3140
2840 GOTO 2760
2850 '
2860 LINE (  4,  4)-(635,279),0,BF
2870 LOCATE 19,44 :PRINT " Ave. Nusselt No.   "
2880 LINE (340,302)-(635,395),0,BF
2890 LINE (  1,301)-(638,301),1
2900 ANU3=ANU3/(ISC+1) :ANU4=ANU4/(ISC+1) :ANU5=ANU5/(ISC+1)
2910 LOCATE 21,44 :PRINT " RA    ="; :PRINT USING "####.##";RA
2920 LOCATE 22,44 :PRINT " "CHR$(235);"    ="; :PRINT USING "###.#";DELTA
2930 LOCATE 23,44 :PRINT " RAcr ="; :PRINT USING "######.#";RACR
2940 LOCATE 21,63 :PRINT " Nu(3) ="; :PRINT USING "##.###";ANU3
2950 LOCATE 22,63 :PRINT " Nu(4) ="; :PRINT USING "##.###";ANU4
2960 LOCATE 23,63 :PRINT " Nu(5) ="; :PRINT USING "##.###";ANU5;
2970 LOCATE 25,44 :PRINT " Surface";ISURF;
2980 LINE (340,396)-(635,398),1,BF
2990 PRINT#2,USING "###.###";ANU3;ANU4;ANU5;
    :PRINT#2,TAB(60);"ANU3 ANU4 ANU5"
3000 '
3010 AANU3=AANU3 +ANU3/4! :AANU4=AANU4 +ANU4/4! :AANU5=AANU5 +ANU5/4!
3020 '
3030 LINE (  4,  4)-(635,279),0,BF
```

```
3040 LINE (4,302)-(325,395),0,BF
3050 IF ISURF 4 THEN GOSUB 6100
        :LOCATE 21,2 :PRINT "Rotate negative 90 degrees clockwise,"
        :LOCATE 22,2 :PRINT "Press  space bar  when ready."
3060 IF ISURF 4 THEN LOCATE 25,2 :PRINT "Press (E/e/Q/q) to quit";
                ELSE LOCATE 25,2 :PRINT "Press  space bar  to end";
3070 LINE (  4,396)-(325,398),1,BF
3080 ANS$ = INKEY$
3090  IF ANS$=" " OR ANS$=CHR$(13) THEN 3100 ELSE
      IF ANS$="E" OR ANS$="e" OR ANS$="Q" OR ANS$="q" THEN 3140 ELSE 3080
3100 NEXT ISURF
3110 '
3120 PRINT#2,USING "###.###";AANU3;AANU4;AANU5;
   :PRINT#2,TAB(60);"AANU3 AANU4 AANU5"
3130                                    'ending program.
3140 CLOSE
3150 SCREEN 0
3160 KEY ON
3170 END
3180 '+++++++++++++++++++++++++++++++++++++++++++++++++++++++++++++++++++++++
3190 '              This subroutine PROP interpolates
3200 '              for the air properties.
3210 '
3220 '
3230 '
3240 '
3250                                    'interpolate.
3260 G    = 9.806
3270 '    Convert P (mm Hg to N/m.m)
3280 P = P0/1000! *9.80665*(13598.571# -2.54286*TI)
3290 TF = .5*(TS +TI) +273.15
3300 FOR IG=27 TO 39
3310  I=IG-26
3320  T = IG*10
3330  TP= T+10!
3340 IF TF =T THEN 3400
3350  IF TF TP THEN 3400
3360   F    = (TF-T)/(TP-T)
3370   VMU = (TVMU(I) +F*(TVMU(I+1)-TVMU(I)))*.00001
3380   VNU = VMU *R *TF /P
3390   K    = TK(I) +F*(TK(I+1)-TK(I))
3400 NEXT IG
3410 FOR IG=13 TO 19
3420  I  =IG-12
3430  T =IG*20
3440  TP=T+20!
3450  IF TF =T THEN 3490
3460  IF TF TP THEN 3490
3470   F = (TF-T)/(TP-T)
3480   PR= TPR(I) +F*(TPR(I+1)-TPR(I))
3490 NEXT IG
3500 '
```

```
3510 RETURN
3520 '++++++++++++++++++++++++++++++++++++++++++++++++++++++++++++++++++++++++
3530 '
3540 '     subroutine for inputing fringes.
3550 '
3560 LINE (4,302)-(325,395),0,BF
3570 LOCATE 21,2 :PRINT "Y / 2A = "; :PRINT USING "#.##";SCAN
3580 SLOC = WW1 +SCAN*(WW2 -WW1)
3590 LOCATE 22,2  :PRINT "scanning location on wall is ";
3600 PRINT USING "##.###";SLOC
3610 LINE (  1,  1)-(638,283),1,BF
3620 LINE (  4,  4)-(635,279),0,BF
3630 GOSUB 5920
3640 '
3650 LOCATE 2,3 :PRINT "Input wall and first five fringe locations."
3660 '
3670 LOCATE 6,3  :INPUT "WALL ",XR(1)
3680 LOCATE 7,3  :INPUT "f1   ",XR(2)
3690 LOCATE 8,3  :INPUT "f2   ",XR(3)
3700 LOCATE 9,3  :INPUT "f3   ",XR(4)
3710 LOCATE 10,3 :INPUT "f4   ",XR(5)
3720 LOCATE 11,3 :INPUT "f5   ",XR(6)
3730 '
3740 RETURN
3750 '++++++++++++++++++++++++++++++++++++++++++++++++++++++++++++++++++++++++
3760 '
3770 '     subroutine for calculating fringe shifts.
3780 '
3790 DF1=-ABS( (XR(2)-XR(1))/(XR(3)-XR(2)) )
3800 FR(1) = 0!
3810 FR(2) = DF1
3820 FOR I=3 TO 6 :FR(I)= FR(I-1) -1! :NEXT I
3830 '
3840 TSA = TS +273.15
3850 C  = 1.5 *P *GD *L *(TS-TI) /(R *WAVE *TSA *TSA)
3860 FOR I=1 TO 6
3870  X(I) = ABS( (XR(I) -XR(1)) *A2 /(W1-W2) )
3880  F(I) = FR(I) /C
3890 NEXT I
3900 '
3910 LINE (  4,  4)-(635,279),0,BF
3920 LOCATE 2,3 :PRINT TAB(3);"Fringe shift profiles."
3930 LOCATE 4,9  :PRINT "raw X"
3940 LOCATE 4,20 :PRINT "X"
3950 LOCATE 4,31 :PRINT "raw ";CHR$(238)
3960 LOCATE 4,44 :PRINT CHR$(238)
3970 LOCATE 6,3  :PRINT "WALL "; :PRINT USING "#.######";XR(1)
3980 LOCATE 7,3  :PRINT "f1   "; :PRINT USING "#.######";XR(2)
3990 LOCATE 8,3  :PRINT "f2   "; :PRINT USING "#.######";XR(3)
4000 LOCATE 9,3  :PRINT "f3   "; :PRINT USING "#.######";XR(4)
4010 LOCATE 10,3 :PRINT "f4   "; :PRINT USING "#.######";XR(5)
4020 LOCATE 11,3 :PRINT "f5   "; :PRINT USING "#.######";XR(6)
```

```
4030 '
4040 FOR I=1 TO 6
4050 LOCATE I+5,17 :PRINT USING "#.######";X(I)
4060 LOCATE I+5,30 :PRINT USING "##.###";FR(I)
4070 LOCATE I+5,41 :PRINT USING "##.###";F(I) :NEXT I
4080 RETURN
4090 '+++++++++++++++++++++++++++++++++++++++++++++++++++++++++++++++++++++++
4100 '                This subroutine calculates the Nusselt numbers.
4110 '
4120 '
4130  SX = 0! :SXX = 0! : SF = 0! : SXF = 0!
4140 FOR I=2 TO 4
4150  SX = SX  +X(I)
4160  SXX= SXX +X(I)*X(I)
4170  SF = SF  +F(I)
4180  SXF= SXF +X(I)*F(I)
4190 NEXT I
4200 NU3 = ABS( (3!*SXF -SX*SF) /(3!*SXX -SX*SX) ) *A
4210  SX = SX  +X(I)
4220  SXX= SXX +X(I)*X(I)
4230  SF = SF  +F(I)
4240  SXF= SXF +X(I)*F(I)
4250 NU4 = ABS( (4!*SXF -SX*SF) /(4!*SXX -SX*SX) ) *A
4260  SX = SX  +X(I)
4270  SXX= SXX +X(I)*X(I)
4280  SF = SF  +F(I)
4290  SXF= SXF +X(I)*F(I)
4300 NU5 = ABS( (5!*SXF -SX*SF) /(5!*SXX -SX*SX) ) *A
4310 '
4320 '
4330 LOCATE 14,7 :PRINT "Nusselt numbers."
4340 LOCATE 15,7 :PRINT USING "###.###";NU3; :PRINT "  (3)"
4350 LOCATE 16,7 :PRINT USING "###.###";NU4; :PRINT "  (4)"
4360 LOCATE 17,7 :PRINT USING "###.###";NU5; :PRINT "  (5)"
4370 RETURN
4380 END
4390 '+++++++++++++++++++++++++++++++++++++++++++++++++++++++++++++++++++++++
4400 '
4410 '   Printing preliminary info.
4420 IF ISURF  1 THEN 4580
4430 LOCATE 22,2 :INPUT "Enter name of output file ",FOUT$
4440 LINE (4,302)-(325,395),0,BF
4450 IF FOUT$="" THEN FOUT$="OUT.DAT"
4460 OPEN "O",#2,FOUT$
4470 PRINT#2," ";DTTM$;TAB(20);FOUT$;TAB(45);
          "Inclined isothermal square duct"
4480 PRINT#2,USING "####.##";TS;TI;     :PRINT#2,TAB(50);"Ts    Ti"
4490 PRINT#2,USING "##.######";A2;      :PRINT#2,TAB(50);"2A"
4500 PRINT#2,USING "####.##";PO;
4510 PRINT#2,USING "######.#";P;        :PRINT#2,TAB(50);"PO    P"
4520 PRINT#2,USING "##.####";PR;
4530 PRINT#2,USING "##.####";VNU;
```

```
4540 PRINT#2,USING "##.######";K;       :PRINT#2,TAB(50);"PR    VNU    K"
4550 PRINT#2,USING "####.###";RA;
4560 PRINT#2,USING "###.#";DELTA;
4570 PRINT#2,USING "######.##";RACR;
    :PRINT#2,TAB(50);"RA    DELTA  RAcr"
4580 PRINT#2,USING "##.######";WW1;WW2; :PRINT#2,TAB(50);"WW1   WW2"
4590 PRINT#2,USING "##.######";W1;W2;   ;PRINT#2,TAB(50);"W1    W2"
4600 PRINT#2,ISCAN;TAB(50);"No. of scans  (normally 9)"
4610 RETURN
4620 '+++++++++++++++++++++++++++++++++++++++++++++++++++++++++++++++++++++++
4630 '              This subroutine prints out scan results.
4640 '
4650  PRINT#2,USING "##.###";SCAN;SLOC;
     :PRINT#2,TAB(60);"Y /2A     SLOC"
4660  PRINT#2,USING "##.######";XR(1);X(1);
4670  PRINT#2,USING "###.###";FR(1);F(1);
     :PRINT#2,TAB(60);"XR   X    FR   F"
4680 FOR I=2 TO 6
4690  PRINT#2,USING "##.######";XR(I);X(I);
4700  PRINT#2,USING "###.###";FR(I);F(I)
4710 NEXT I
4720  PRINT#2,USING "###.###";NU3;NU4;NU5;
     :PRINT#2,TAB(60);"NU3  NU4  NU5"
4730 RETURN
4740 '+++++++++++++++++++++++++++++++++++++++++++++++++++++++++++++++++++++++
4750 '
4760 '
4770 '      subroutine for plotting fringe shift profiles.
4780 '
4790 '
4800 XO%=530 :YO%=60 :YC%=400 :PI=3.141593
4810 IF RA 110! THEN XC%=200 :ITICNX=5 ELSE XC%=400 :ITICNX=2
4820 LINE (487,  1)-(638,282),1,BF
4830 LINE (490,  4)-(635,279),0,BF
4840 '
4850 IF RA 110! THEN LINE (XO%,YO%)-(XO%+ .5*XC%,YO%),1 ELSE
                   LINE (XO%,YO%)-(XO%+.25*XC%,YO%),1
4860 LINE (XO%,YO%)-(XO%,YO%-.25*YC%),1
4870 '
4880 TICI=.1 :TICL=.015
4890 FOR I=0 TO ITICNX
4900 LINE (XO% +I*TICI*XC%,YO%)-(XO% +I*TICI*XC%,YO% +TICL*YC%),1
4910 NEXT I
4920 FOR I=0 TO 2
4930 LINE (XO%,YO% -I*TICI*YC%)-(XO% -TICL*XC%,YO% -I*TICI*YC%),1
4940 NEXT I
4950 '
4960 TICI=.1 :TICL=.01
4970 FOR I=0 TO ITICNX-1
4980 LINE (XO% +.5*TICI*XC% +I*TICI*XC%,YO%)-(XO% +.5*TICI*XC%
          +I*TICI*XC%,YO% +TICL*YC%),1
4990 NEXT I
```

```
5000 FOR I=0 TO 2
5010 LINE (XO%,YO% -.5*TICI*YC% -I*TICI*YC%)-(XO% -TICL*XC%,YO%
          -.5*TICI*YC% -I*TICI*YC%),1
5020 NEXT I
5030 '
5040 CIRCLE (514,110),8,1,.55*PI,1.45*PI,8!/7!
5050 LINE   (514,110)-(507,110),1
5060 '
5070 PSET (XO%,YO%)
5080 FOR I=2 TO 6
5090 LINE          -(XO% +X(I)/A*XC%,YO% +F(I)*YC%),1
5100 CIRCLE STEP (0,0),2,1
5110 NEXT I
5120 '
5130 PHI = ATN(NU3)
5140 DY% =-.23*YC%*SIN(PHI)
5150 DX% = .23*XC%*COS(PHI)
5160 PSET (XO% +DX%,YO% +DY%)
5170 PHI = ATN(NU4)
5180 DY% =-.24*YC%*SIN(PHI)
5190 DX% = .24*XC%*COS(PHI)
5200 PSET (XO% +DX%,YO% +DY%)
5210 PHI = ATN(NU5)
5220 DY% =-.25*YC%*SIN(PHI)
5230 DX% = .25*XC%*COS(PHI)
5240 PSET (XO% +DX%,YO% +DY%)
5250 GOSUB 5920
5260 RETURN
5270 '++++++++++++++++++++++++++++++++++++++++++++++++++++++++++++++++++++++++
5280 '
5290 '
5300 '      subroutine for reading in old preliminary information.
5310 '
5320 '
5330 LOCATE 22,2 :INPUT "Enter name of input file ",FIN$
5340 LINE (4,302)-(325,395),0,BF
5350 IF FIN$="" THEN FIN$="IN.DAT"
5360 OPEN "I",#1,FIN$
5370 '
5380 DTTM$= INPUT$(13,1)                    :INPUT#1,DUM$
5390 DTTM$= RIGHT$(DTTM$,12)
5400 INPUT#1,TS,TI                          :INPUT#1,DUM$
5410 INPUT#1,A2                             :INPUT#1,DUM$
5420 INPUT#1,PO,P                           :INPUT#1,DUM$
5430 INPUT#1,PR,VNU,K                       :INPUT#1,DUM$
5440 INPUT#1,RA,DELTA,RACR                  :INPUT#1,DUM$
5450 '
5460 INPUT#1,WW1,WW2                        :INPUT#1,DUM$
5470 INPUT#1,W1,W2                          :INPUT#1,DUM$
5480 INPUT#1,ISCAN                          :INPUT#1,DUM$
5490 '
5500 GOSUB 3180                              'evaluate air properties.
```

```
5510 BETA = 1! /TF                          'calculate Rayleigh number.
5520 A    = A2 /2!
5530 RA   = G*COS(DELTA*PI/180!)*BETA*(TS-TI)*A*A*A*A*PR /(VNU*VNU*L)
5540 RACR = G*SIN(DELTA*PI/180!)*BETA*(TS-TI)*A2*A2*A2*PR /(VNU*VNU)
5550 '
5560 LOCATE 19,67 :PRINT DTTM$
5570 LINE (1,301)-(638,301),1
5580 LOCATE 20,44 :PRINT " T";CHR$(236);" =              WW1="
5590 LOCATE 21,44 :PRINT " Ts =             WW2="
5600 LOCATE 22,44 :PRINT " PO =             W1 ="
5610 LOCATE 23,44 :PRINT " P =              W2 ="
5620 LOCATE 24,44 :PRINT " 2a=              ";CHR$(235);"  =";
5630 LOCATE 25,44 :PRINT " Ra=             Racr=";
5640 LINE (340,396)-(635,398),1,BF
5650 LOCATE 20,50 :PRINT USING "###.##";TI
5660 LOCATE 21,50 :PRINT USING "###.##";TS
5670 LOCATE 22,50 :PRINT PO :LOCATE 23,50 :PRINT USING "######.#";P
5680 LOCATE 20,67 :PRINT WW1 :LOCATE 21,67 :PRINT WW2
5690 LOCATE 22,67 :PRINT W1 :LOCATE 23,67 :PRINT W2
5700 LOCATE 24,50 :PRINT A2;
5710 LOCATE 24,67 :PRINT USING "###.#";DELTA;
5720 LOCATE 25,50 :PRINT USING "####.##";RA;
5730 LOCATE 25,67 :PRINT USING "######.##";RACR;
5740 LINE (340,396)-(635,398),1,BF
5750 GOTO 2470
5760 '
5770 '++++++++++++++++++++++++++++++++++++++++++++++++++++++++++++++++++++++++
5780 '
5790 '
5800 '       subroutine for reading in old fringe locations.
5810 '
5820 '
5830 INPUT#1,DUMM,DUMM                  :INPUT#1,DUM$
5840 INPUT#1,XR(1),DUMM,DUMM,DUMM       :INPUT#1,DUM$
5850 FOR I=2 TO 6
5860  INPUT#1,XR(I),DUMM,DUMM,DUMM
5870 NEXT I
5880 INPUT#1,DUMM,DUMM,DUMM             :INPUT#1,DUM$
5890  IF ISC=ISCAN THEN INPUT#1,DUMM,DUMM,DUMM        :INPUT#1,DUM$
5900 '
5910 RETURN
5920 '++++++++++++++++++++++++++++++++++++++++++++++++++++++++++++++++++++++++
5930 '
5940 '
5950 '       subroutine for plotting duct schematic.
5960 '
5970 '
5980 XO%=533 :YO%=195
5990 LINE (XO%,YO%)-(XO%+60,YO%+50),1,B
6000 LINE (XO%-5,YO%+ISC*5)-(XO%+5,YO%+ISC*5),1
6010 '
6020 FOR I=1 TO ISCAN
```

```
6030  PRESET (XO%,YO%+50-I*5) :PRESET (XO%+60,YO%+50-I*5)
6040  PRESET (XO%+I*6,   YO%) :PRESET (XO%+I*6,   YO%+50)
6050 NEXT I
6060 '
6070 LOCATE 17,67 :PRINT "Surface";ISURF;
6080 '
6090 RETURN
6100 '++++++++++++++++++++++++++++++++++++++++++++++++++++++++++++++++++++++++
6110 '
6120 '
6130 '      subroutine for plotting duct schematic before rotating..
6140 '
6150 '
6160 XO%=533 :YO%=195
6170 LINE (XO%,YO%)-(XO%+60,YO%+50),1,BF
6180 LINE (XO%-5,YO%+5)-(XO%  ,YO%+5),1
6190 LINE (XO%  ,YO%+5)-(XO%+5,YO%+5),0
6200 '
6210 FOR I=1 TO ISCAN
6220  PRESET (XO%,YO%+50-I*5) :PRESET (XO%+60,YO%+50-I*5)
6230  PRESET (XO%+I*6,   YO%) :PRESET (XO%+I*6,   YO%+50)
6240 NEXT I
6250 '
6260 CIRCLE (XO%+30,YO%+25),15,0,PI,PI*.5,5!/6!
6270 LINE (XO%+15,YO%+25)-(XO%+18,YO%+34),0
6280 LINE (XO%+15,YO%+25)-(XO%+12,YO%+34),0
6290 '
6300 RETURN
6310 '++++++++++++++++++++++++++++++++++++++++++++++++++++++++++++++++++++++++
6320 '
6330 '
6340 '      subroutine for plotting duct schematic before viewing.
6350 '
6360 '
6370 XO%=533 :YO%=195
6380 LINE (XO%,YO%)-(XO%+60,YO%+50),1,BF
6390 '
6400 FOR I=1 TO ISCAN
6410  PRESET (XO%,YO%+50-I*5) :PRESET (XO%+60,YO%+50-I*5)
6420  PRESET (XO%+I*6,   YO%) :PRESET (XO%+I*6,   YO%+50)
6430 NEXT I
6440 '
6450 LOCATE 12,71 :PRINT "T"
6460 LOCATE 17,71 :PRINT "B"
6470 '
6480 RETURN
```

APPENDIX D

INTERFEROGRAM ANALYSIS SAMPLE OUTPUT

The following file, IID5.DAT, contains the raw data of the fringe location measurements, as well as the calculated fringe shift and heat transfer profiles. This output file is for the particular experiment where Ra=10 and δ=45°.

This file can be used both as an output file and an input file for the program IID given in appendix C. When the fringe locations are entered interactively, as is the case when the fringe locations are first read from the interferogram, this file is the output file. This file can also be used as an input file to display the results of a previously read interferogram graphically.

```
870319 19:17        IID5.DAT          Inclined isothermal square duct
 85.34  23.30                            Ts    Ti
0.013903                                 2A
744.10 98798.2                           PO    P
0.7015 1.8845E-05 0.028120               PR    VNU    K
 10.099 45.0  6973.28                    RA    DELTA  RAcr
5.149000 5.360000                        WW1   WW2
0.031457 0.036871                        W1    W2
9                                        No. of scans  (normally 9)
0.100 5.170                                       Y /2A      SLOC
0.031572 0.000000  0.000  0.000                   XR   X     FR   F
0.031830 0.000663 -0.518 -0.015
0.032328 0.001941 -1.518 -0.043
0.033024 0.003729 -2.518 -0.071
0.033973 0.006166 -3.518 -0.099
0.034675 0.007968 -4.518 -0.127
 0.126  0.105  0.102                          NU3  NU4  NU5
0.200 5.191                                       Y /2A      SLOC
0.031550 0.000000  0.000  0.000                   XR   X     FR   F
0.031642 0.000236 -0.364 -0.010
0.031895 0.000886 -1.364 -0.038
0.032158 0.001561 -2.364 -0.067
0.032452 0.002316 -3.364 -0.095
0.032842 0.003318 -4.364 -0.123
 0.295  0.283  0.281                          NU3  NU4  NU5
0.300 5.212                                       Y /2A      SLOC
0.031465 0.000000  0.000  0.000                   XR   X     FR   F
0.031568 0.000264 -0.579 -0.016
0.031746 0.000722 -1.579 -0.044
0.031938 0.001215 -2.579 -0.073
0.032122 0.001687 -3.579 -0.101
0.032326 0.002211 -4.579 -0.129
 0.412  0.411  0.411                          NU3  NU4  NU5
0.400 5.233                                       Y /2A      SLOC
0.031534 0.000000  0.000  0.000                   XR   X     FR   F
0.031654 0.000308 -0.779 -0.022
0.031808 0.000704 -1.779 -0.050
0.031951 0.001071 -2.779 -0.078
0.032097 0.001446 -3.779 -0.106
0.032259 0.001862 -4.779 -0.134
 0.513  0.517  0.518                          NU3  NU4  NU5
0.500 5.255                                       Y /2A      SLOC
0.031511 0.000000  0.000  0.000                   XR   X     FR   F
0.031611 0.000257 -0.806 -0.023
0.031735 0.000575 -1.806 -0.051
0.031863 0.000904 -2.806 -0.079
0.031988 0.001225 -3.806 -0.107
0.032117 0.001556 -4.806 -0.135
 0.605  0.605  0.605                          NU3  NU4  NU5
0.600 5.276                                       Y /2A      SLOC
0.031490 0.000000  0.000  0.000                   XR   X     FR   F
0.031581 0.000234 -0.728 -0.020
```

```
0.031706 0.000555 -1.728 -0.049
0.031823 0.000855 -2.728 -0.077
0.031944 0.001166 -3.728 -0.105
0.032060 0.001464 -4.728 -0.133
 0.629  0.632  0.632                          NU3  NU4  NU5
0.700 5.297                                   Y /2A     SLOC
0.031488 0.000000  0.000  0.000               XR   X    FR   F
0.031582 0.000241 -0.777 -0.022
0.031703 0.000552 -1.777 -0.050
0.031830 0.000878 -2.777 -0.078
0.031949 0.001184 -3.777 -0.106
0.032078 0.001515 -4.777 -0.134
 0.614  0.620  0.621                          NU3  NU4  NU5
0.800 5.318                                   Y /2A     SLOC
0.031487 0.000000  0.000  0.000               XR   X    FR   F
0.031601 0.000293 -0.736 -0.021
0.031756 0.000691 -1.736 -0.049
0.031903 0.001068 -2.736 -0.077
0.032054 0.001456 -3.736 -0.105
0.032204 0.001841 -4.736 -0.133
 0.504  0.506  0.506                          NU3  NU4  NU5
0.900 5.339                                   Y /2A     SLOC
0.031503 0.000000  0.000  0.000               XR   X    FR   F
0.031685 0.000470 -0.715 -0.020
0.031942 0.001127 -1.715 -0.048
0.032188 0.001759 -2.715 -0.076
0.032457 0.002450 -3.715 -0.105
0.032748 0.003197 -4.715 -0.133
 0.303  0.298  0.297                          NU3  NU4  NU5
 0.400  0.398  0.397                          ANU3 ANU4 ANU5
```

```
5.147000 5.358000                          WW1   WW2
0.029281 0.034728                          W1    W2
9                                          No. of scans  (normally 9)
0.100 5.168                                          Y /2A      SLOC
0.029312 0.000000  0.000  0.000                      XR   X     FR   F
0.029447 0.000345 -0.502 -0.014
0.029716 0.001031 -1.502 -0.042
0.030007 0.001774 -2.502 -0.070
0.030379 0.002723 -3.502 -0.099
0.030995 0.004296 -4.502 -0.127
 0.274  0.247  0.243                                NU3  NU4  NU5
0.200 5.189                                          Y /2A      SLOC
0.029266 0.000000  0.000  0.000                      XR   X     FR   F
0.029311 0.000115 -0.308 -0.009
0.029457 0.000488 -1.308 -0.037
0.029599 0.000850 -2.308 -0.065
0.029744 0.001220 -3.308 -0.093
0.029894 0.001603 -4.308 -0.121
 0.532  0.532  0.532                                NU3  NU4  NU5
0.300 5.210                                          Y /2A      SLOC
0.029280 0.000000  0.000  0.000                      XR   X     FR   F
0.029373 0.000237 -0.939 -0.026
0.029472 0.000490 -1.939 -0.055
0.029576 0.000756 -2.939 -0.083
0.029684 0.001031 -3.939 -0.111
0.029792 0.001307 -4.939 -0.139
 0.755  0.739  0.736                                NU3  NU4  NU5
0.400 5.231                                          Y /2A      SLOC
0.029266 0.000000  0.000  0.000                      XR   X     FR   F
0.029334 0.000174 -0.791 -0.022
0.029420 0.000393 -1.791 -0.050
0.029510 0.000623 -2.791 -0.079
0.029597 0.000845 -3.791 -0.107
0.029687 0.001075 -4.791 -0.135
 0.871  0.872  0.872                                NU3  NU4  NU5
0.500 5.252                                          Y /2A      SLOC
0.029251 0.000000  0.000  0.000                      XR   X     FR   F
0.029325 0.000189 -0.871 -0.024
0.029410 0.000406 -1.871 -0.053
0.029493 0.000618 -2.871 -0.081
0.029578 0.000835 -3.871 -0.109
0.029664 0.001054 -4.871 -0.137
 0.912  0.910  0.910                                NU3  NU4  NU5
0.600 5.274                                          Y /2A      SLOC
0.029258 0.000000  0.000  0.000                      XR   X     FR   F
0.029336 0.000199 -0.848 -0.024
0.029428 0.000434 -1.848 -0.052
0.029518 0.000664 -2.848 -0.080
0.029607 0.000891 -3.848 -0.108
0.029701 0.001131 -4.848 -0.136
 0.847  0.849  0.850                                NU3  NU4  NU5
```

```
0.700 5.295                                          Y /2A      SLOC
0.029286 0.000000  0.000  0.000                     XR    X    FR    F
0.029377 0.000232 -0.867 -0.024
0.029482 0.000500 -1.867 -0.052
0.029588 0.000771 -2.867 -0.081
0.029698 0.001052 -3.867 -0.109
0.029809 0.001335 -4.867 -0.137
 0.726  0.717  0.715                                NU3  NU4  NU5
0.800 5.316                                          Y /2A      SLOC
0.029247 0.000000  0.000  0.000                     XR    X    FR    F
0.029333 0.000220 -0.581 -0.016
0.029481 0.000597 -1.581 -0.044
0.029635 0.000990 -2.581 -0.073
0.029798 0.001406 -3.581 -0.101
0.029966 0.001835 -4.581 -0.129
 0.507  0.495  0.492                                NU3  NU4  NU5
0.900 5.337                                          Y /2A      SLOC
0.029274 0.000000  0.000  0.000                     XR    X    FR    F
0.029458 0.000470 -0.605 -0.017
0.029762 0.001246 -1.605 -0.045
0.030116 0.002149 -2.605 -0.073
0.030716 0.003681 -3.605 -0.101
0.031321 0.005225 -4.605 -0.130
 0.233  0.181  0.175                                NU3  NU4  NU5
 0.565  0.554  0.553                                ANU3 ANU4 ANU5
```

```
5.054000 5.267000                                   WW1   WW2
0.029357 0.034698                                   W1    W2
9                                                   No. of scans  (normally 9)
0.100 5.075                                                Y /2A      SLOC
0.029347 0.000000  0.000  0.000                            XR   X     FR    F
0.029596 0.000648 -0.877 -0.025
0.029880 0.001387 -1.877 -0.053
0.030178 0.002163 -2.877 -0.081
0.030452 0.002876 -3.877 -0.109
0.030758 0.003673 -4.877 -0.137
 0.258  0.262  0.263                                        NU3   NU4   NU5
0.200 5.097                                                Y /2A      SLOC
0.029323 0.000000  0.000  0.000                            XR   X     FR    F
0.029452 0.000336 -0.777 -0.022
0.029618 0.000768 -1.777 -0.050
0.029776 0.001179 -2.777 -0.078
0.029938 0.001601 -3.777 -0.106
0.030095 0.002010 -4.777 -0.134
 0.464  0.465  0.465                                        NU3   NU4   NU5
0.300 5.118                                                Y /2A      SLOC
0.029322 0.000000  0.000  0.000                            XR   X     FR    F
0.029421 0.000258 -0.744 -0.021
0.029554 0.000604 -1.744 -0.049
0.029681 0.000935 -2.744 -0.077
0.029812 0.001276 -3.744 -0.105
0.029941 0.001611 -4.744 -0.134
 0.578  0.578  0.578                                        NU3   NU4   NU5
0.400 5.139                                                Y /2A      SLOC
0.029320 0.000000  0.000  0.000                            XR   X     FR    F
0.029417 0.000253 -0.795 -0.022
0.029539 0.000570 -1.795 -0.051
0.029663 0.000893 -2.795 -0.079
0.029788 0.001218 -3.795 -0.107
0.029906 0.001525 -4.795 -0.135
 0.611  0.608  0.607                                        NU3   NU4   NU5
0.500 5.161                                                Y /2A      SLOC
0.029329 0.000000  0.000  0.000                            XR   X     FR    F
0.029431 0.000266 -0.785 -0.022
0.029561 0.000604 -1.785 -0.050
0.029688 0.000935 -2.785 -0.078
0.029814 0.001262 -3.785 -0.107
0.029948 0.001611 -4.785 -0.135
 0.585  0.589  0.590                                        NU3   NU4   NU5
0.600 5.182                                                Y /2A      SLOC
0.029247 0.000000  0.000  0.000                            XR   X     FR    F
0.029335 0.000229 -0.633 -0.018
0.029474 0.000591 -1.633 -0.046
0.029608 0.000940 -2.633 -0.074
0.029757 0.001328 -3.633 -0.102
0.029905 0.001713 -4.633 -0.130
 0.550  0.537  0.534                                        NU3   NU4   NU5
```

```
0.700 5.203                                          Y /2A      SLOC
0.029252 0.000000  0.000  0.000                     XR   X     FR   F
0.029381 0.000336 -0.750 -0.021
0.029553 0.000784 -1.750 -0.049
0.029731 0.001247 -2.750 -0.077
0.029913 0.001721 -3.750 -0.106
0.030112 0.002239 -4.750 -0.134
 0.429  0.424  0.423                                NU3  NU4  NU5
0.800 5.224                                          Y /2A      SLOC
0.029295 0.000000  0.000  0.000                     XR   X     FR   F
0.029441 0.000380 -0.591 -0.017
0.029688 0.001023 -1.591 -0.045
0.029944 0.001689 -2.591 -0.073
0.030259 0.002509 -3.591 -0.101
0.030695 0.003644 -4.591 -0.129
 0.299  0.276  0.273                                NU3  NU4  NU5
0.900 5.246                                          Y /2A      SLOC
0.029334 0.000000  0.000  0.000                     XR   X     FR   F
0.029629 0.000768 -0.560 -0.016
0.030156 0.002140 -1.560 -0.044
0.030894 0.004061 -2.560 -0.072
0.031485 0.005599 -3.560 -0.100
0.032183 0.007416 -4.560 -0.128
 0.118  0.119  0.119                                NU3  NU4  NU5
 0.389  0.386  0.385                                ANU3 ANU4 ANU5
```

```
5.056000 5.269000
0.031655 0.037036
9.
0.1[illegible]7
0.031670 0.000000  0.000  0.000
0.031932 0.000677 -0.639 -0.018
0.032342 0.001736 -1.639 -0.046
0.032725 0.002726 -2.639 -0.074
0.033118 0.003741 -3.639 -0.102
0.033570 0.004909 -4.639 -0.131
 0.191  0.192  0.192
0.200 5.099
0.031631 0.000000  0.000  0.000
0.031807 0.000455 -0.638 -0.018
0.032083 0.001168 -1.638 -0.046
0.032355 0.001871 -2.638 -0.074
0.032619 0.002553 -3.638 -0.102
0.032890 0.003253 -4.638 -0.131
 0.276  0.280  0.280
0.300 5.12[illegible]
0.031623 0.000000  0.000  0.000
0.031768 0.000375 -0.681 -0.019
0.031981 0.000925 -1.681 -0.047
0.032195 0.001478 -2.681 -0.075
0.032413 0.002041 -3.681 -0.104
0.032633 0.002610 -4.681 -0.132
 0.355  0.352  0.352
0.400 5.141
0.031614 0.000000  0.000  0.000
0.031746 0.000341 -0.691 -0.019
0.031937 0.000835 -1.691 -0.048
0.032135 0.001346 -2.691 -0.076
0.032328 0.001845 -3.691 -0.104
0.032535 0.002380 -4.691 -0.132
 0.389  0.389  0.389
0.500 5.163
0.031617 0.000000  0.000  0.000
0.031745 0.000331 -0.703 -0.020
0.031927 0.000801 -1.703 -0.048
0.032118 0.001294 -2.703 -0.076
0.032306 0.001780 -3.703 -0.104
0.032509 0.002305 -4.703 -0.132
 0.406  0.404  0.404
0.600 5.184
0.031617 0.000000  0.000  0.000
0.031765 0.000382 -0.818 -0.023
0.031946 0.000850 -1.818 -0.051
0.032136 0.001341 -2.818 -0.079
0.032327 0.001834 -3.818 -0.107
0.032526 0.002349 -4.818 -0.136
 0.408  0.404  0.403
```

```
WW1   WW2
W1    W2
No. of scans (normally 9)
          Y /2A      SLOC
          XR   X     FR   F

          NU3  NU4   NU5
          Y /2A      SLOC
          XR   X     FR   F

          NU3  NU4   NU5
          Y /2A      SLOC
          XR   X     FR   F

          NU3  NU4   NU5
          Y /2A      SLOC
          XR   X     FR   F

          NU3  NU4   NU5
          Y /2A      SLOC
          XR   X     FR   F

          NU3  NU4   NU5
          Y /2A      SLOC
          XR   X     FR   F

          NU3  NU4   NU5
```

```
0.700 5.205                                          Y /2A      SLOG
0.031627 0.000000  0.000  0.000                     XR   X     FR   F
0.031780 0.000395 -0.750 -0.021
0.031984 0.000922 -1.750 -0.049
0.032186 0.001444 -2.750 -0.077
0.032395 0.001984 -3.750 -0.106
0.032604 0.002524 -4.750 -0.134
 0.373  0.370  0.369                                NU3  NU4  NU5
0.800 5.226                                          Y /2A      SLOC
0.031631 0.000000  0.000  0.000                     XR   X     FR   F
0.031834 0.000524 -0.790 -0.022
0.032091 0.001189 -1.790 -0.050
0.032351 0.001860 -2.790 -0.079
0.032612 0.002535 -3.790 -0.107
0.032895 0.003266 -4.790 -0.135
 0.293  0.292  0.292                                NU3  NU4  NU5
0.900 5.248                                          Y /2A      SLOC
0.031642 0.000000  0.000  0.000                     XR   X     FR   F
0.031978 0.000868 -0.730 -0.021
0.032438 0.002057 -1.730 -0.049
0.032918 0.003297 -2.730 -0.077
0.033456 0.004687 -3.730 -0.105
0.034226 0.006676 -4.730 -0.133
 0.161  0.154  0.153                                NU3  NU4  NU5
 0.285  0.284  0.283                                ANU3 ANU4 ANU5
 0.410  0.405  0.405                                AANU3 AANU4 AANU5
```

REFERENCES

1. Franke, M.E. "Interferometer Measurements in Free Convection on a Vertical Plate with Temperature Variation in Light Beam Direction" paper NC1.2 presented at the Fourth International Heat Transfer Conference, Paris 1970.

2. Yousef, W.W. and J.D. Tarasuk "An Interferometric Study of Combined Free and Forced Convection in a Horizontal Isothermal Tube" J. of Heat Transfer v.103 pp249-256 May 1981.

3. Yousef, W.W. and J.D. Tarasuk "Free Convection Effects on Laminar Forced Convective Heat Transfer in a Horizontal Isothermal Tube" J. of Heat Transfer v.104 pp145-152 Feb 1982.

4. Yousef, W.W. "Convective Heat Transfer in an Isothermal Horizontal Tube" Ph.D thesis, The University of Western Ontario, London, Ontario, Canada. July 1980.

5. McKeen, W.J. "An Interferometric Study of Combined Forced and Free Convection Heat Transfer in the Entrance Region of Horizontal Concentric Annuli" Ph.D thesis, The University of Western Ontario, London, Ontario, Canada. Dec 1981.

6. Elenbass, W. "The Dissipation of Heat Transfer by Free Convection, The Inner Surface of Vertical Tubes of Different Shapes of Cross-Sections" Physics (Utrecht) v9 pp865-873 1942.

7. Dyer, J.R. "The Development of Natural Convection in a Vertical Circular Duct" Mechanical and Chemical Engineering Transactions, The Institution of Engineers, Australia. May 1968 pp78-86.

8. Davis, L.P. and J.J. Perona "Development of Free Convection Flow of a Gas in a Heated Vertical Open Tube" Int. J. Heat Mass Transfer v14 pp889-903 1971.

9. Pollard, A. and P.H. Oosthuizen "Free Convection Through Open-Ended Pipes" ASME paper no. 83-HT-68 1983.

10. Aihara, T., S. Maruyama and J.S. Choi "Laminar Free Convection with Variable Fluid Properties in Vertical Ducts of Different Cross-Sectional Shapes" Proceedings, 8th International Heat Transfer Conference Hemisphere Publishing Corp. Washington D.C. v4 1986 pp1581-1586.

11. Meric, R.A. "An Analytical Study of Natural Convection in a Vertical Open Tube" Int. J. Heat Mass Transfer v20 1977 pp429-431.

12. Churchill, S.W. "A Comprehensive Correlating Equation for Buoyancy-Induced Flow in Channels" Letters in Heat and Mass Transfer v4 1977 pp193-199.

13. Aihara, T. "Natural Convection Air Cooling" invited paper at the International Symposium on Cooling Technology for Electronic Equipment 1987 in Honolulu.

14. Ramakrishna, K.; S.G. Rubin and P.K. Khosla "Laminar Natural Convection along Vertical Square Ducts" Numerical Heat Transfer v5 pp59-79 1982.

15. Ramakrishna, K. "Laminar Natural Convection along Vertical Corners and Rectangular Ducts" PhD thesis, Polytechnic Institute of New York, 1980.

16. Iqbal, M. "Natural Convection Heat Transfer Inside Inclined Tubes with Uniform Heat Flux" Brace Experimental Station of McGill University, Barbados Technical Report No. 9, Sept. 1962.

17. Schlichting, H. "Boundary-Layer Theory" 7th ed. McGraw-Hill Book Company, New York, N.Y. 1979. pp271-272.

18. Cook, A.E. and M. Rahman " Temperature and Velocity Distributions in a Square Duct" Applied Math. Modelling, v10 June 1986. pp221-223.

19. Spalding, D.B. "A Novel Finite Difference Formulation for Differential Expressions Involving Both First and Second Derivatives" Int. J. for Numerical Methods in Engineering, v4 1972 pp551-559.

20. Dennis, S.C.R. and J.D. Hudson "A Difference Method for Solving the Navier-Stokes Equations" from "Numerical Methods in Laminar and Turbulent Flow", Proceedings of the First International Conference held at University College Swansea, Swansea SA2 8PP, U.K. July 17-21, 1978.

21. Wilkes, J.O. and S.W. Churchill, "The Finite-Difference Computation of Natural Convection in a Rectangular Enclosure", A.I.Ch.E. Journal, v.12, No.1, Jan. 1966, pp161-166.

22. Patankar, S.V. "Numerical Heat Transfer and Fluid Flow", Hemisphere Publishing Corporation, New York, 1980.

23. Patankar, S.V. "A Calculation Procedure for Two-Dimensional Elliptic Situations", Numerical Heat Transfer, v.4, pp.409-425, 1981.

24. de Vahl Davis, G. and I.P. Jones "Natural Convection in a Square Cavity: A Comparison Exercise" International Journal for Numerical Methods in Fluids, v.3, 1983, pp.227-248.

25. de Vahl Davis, G. "Natural Convection of Air in a Square Cavity: A Bench Mark Numerical Solution" International Journal for Numerical Methods in Fluids, v.3 1983 pp.227-248.

26. Thomas, R.W. and G. de Vahl Davis "Natural Convection in Annular and Rectangular Cavities -A Numerical Study" Heat Transfer 1970, 4th Int. Heat Transfer Conf, Paris 1970. v.4 paper NC 2.4

27. de Vahl Davis, G. "Laminar Natural Convection in an Enclosed Rectangular Cavity", Int. J. Heat Mass Transfer, v.11, 1968 pp.1675-1693.

28. MacGregor, R.K. and A.F. Emery "Free Convection Through Vertical Plane Layers -Moderate and High Prandtl Number Fluids" J. of Heat Transfer, August 1969. pp.391-403.

29. Kublbeck, K., G.P. Merker and J. Straub "Advanced Numerical Computation of Two-Dimensional Time-Dependent Free Convection in Cavities" Int. J. Heat Mass Transfer, v.23, pp.203-217, 1980.

30. Markatos, N.C. and Pericleous, K.A. "Laminar and Turbulent Natural Convection in an Enclosed Cavity", Int. J. Heat Mass Transfer, v.27, no.5, pp.755-772, 1984.

31. Hauf, W. and U. Grigull "Optical Methods in Heat Transfer", in Harnett, J.P. and Irvine, T.F. (editors), "Advances in Heat Transfer" Academic Press, New York, v.6 pp283-293 1970.

32. Goldstein, R.J. and T.Y. Chu "Thermal Convection in a Horizontal Layer of Air" in "Progress in Heat and Mass Transfer" edited by T.F. Irvine et. al. Pergamon Press, New York. v.2 pp55-75 1970.

33. Chu, T.Y, and Goldstein, R.J. "Turbulent Convection in a Horizontal Layer of Water" J. Fluid Mechanics v.60 1973. pp141-159.

34. M.L.C. Papple and J.D. Tarasuk "Fully Developed Natural Convective Flow in Inclined Square Ducts" Presented at CANCAM conference Edmonton, Alberta. June 1987.

35. M.L.C. Papple and J.D. Tarasuk "An Interferometric Study of Developing Natural Convective Flow in Inclined Isothermal Ducts" AIAA paper no. 87-1589 Presented at AIAA Thermophysics conference Hawaii. June 1987.